

2-22-2022 9:00 AM

Role of the epithelial-to-mesenchymal transition (EMT) on circulating tumor cell (CTC) and metastasis biology in prostate cancer

Jenna M. Kitz, *The University of Western Ontario*

Supervisor: Alison, Allan L., *The University of Western Ontario*

A thesis submitted in partial fulfillment of the requirements for the Doctor of Philosophy degree in Anatomy and Cell Biology

© Jenna M. Kitz 2022

Follow this and additional works at: <https://ir.lib.uwo.ca/etd>



Part of the [Cells Commons](#)

Recommended Citation

Kitz, Jenna M., "Role of the epithelial-to-mesenchymal transition (EMT) on circulating tumor cell (CTC) and metastasis biology in prostate cancer" (2022). *Electronic Thesis and Dissertation Repository*. 8418.
<https://ir.lib.uwo.ca/etd/8418>

This Dissertation/Thesis is brought to you for free and open access by Scholarship@Western. It has been accepted for inclusion in Electronic Thesis and Dissertation Repository by an authorized administrator of Scholarship@Western. For more information, please contact wlsadmin@uwo.ca.

Abstract

Prostate cancer is the second leading cause of cancer-related deaths in American men. Most of these deaths occur as the result of metastasis, which is associated with an epithelial-to-mesenchymal transition (EMT). EMT leads to greater migratory/invasive capacity and resistance to therapy. During metastasis and associated EMT, cancer cells shed from the primary tumor and disseminate throughout the body as circulating tumor cells (CTCs) in the bloodstream. CTCs have been correlated with increased metastatic disease, reduced survival, and therapy response/resistance. Assessing CTCs presents an opportunity to study cancer progression/treatment effectiveness from a blood test. However, outstanding questions regarding CTCs and EMT has resulted in hesitation in the clinical adoption of CTCs. This thesis aimed to gain a greater understanding of the functional role of EMT in CTC generation, detection, and metastatic behavior in prostate cancer. We converged available CTC isolation technologies to develop protocols for EMT-independent isolation and molecular analysis of CTCs in pre-clinical mouse and human samples. We compared the effectiveness of CellSearch® and Parsortix® for analyzing CTCs in prostate cancer patients and observed that both technologies were equally effective at enumerating CTCs across the clinical spectrum of prostate cancer metastasis. This resulted in identification of 24 genes whose altered expression in patient CTCs may be influencing disease progression, including several related to EMT. We then investigated how EMT affects cell morphology, phenotype, and marker expression by knockdown of the EMT-inducing transcription factor Zeb1 in mesenchymal prostate cancer cells using shRNA (Zeb1^{KD} cells). We observed an aggressive partial (p-EMT) phenotype in Zeb1^{KD} cells compared to controls, which was mitigated by treatment with the demethylating drug 5-azacytidine. Lastly, we identify a unique panel of p-EMT markers for aggressive disease using methylation chip analysis. This research provides the groundwork for increasing future accessibility of CTC liquid biopsies for prostate cancer patients of any disease stage and/or EMT status, thus allowing a greater number of patients to benefit from a personalized medicine approach to combating disease progression and improving outcomes.

Keywords

Circulating tumor cells (CTCs), prostate cancer, epithelial-to-mesenchymal transition (EMT), CellSearch®, Parsortix®, VyCap, HyCEAD, partial-EMT, Zeb1, DNA methylation

Summary for Lay Audience

Prostate cancer is the second leading cause of cancer-related deaths among American men. Most of these deaths occur because of the spread of cancer from the prostate to distant organs in the body such as bone, which is very difficult to treat. Cancer cells spread by escaping from the original prostate tumor and entering into the bloodstream, where they become circulating tumor cells (CTCs). Capturing and studying CTCs in the bloodstream is an opportunity for early detection of disease progression and the use of more aggressive treatments which may ultimately extend patient lives. In this thesis we addressed 3 scientific questions based on the current challenges of capturing CTCs from the blood. Question 1: How can we capture every CTC from the blood in mouse and human samples? Question 2: How can we identify CTCs in prostate cancer patients in order to better identify aggressive cancer? Question 3: What are the biological changes that make cancer cells more likely to enter the blood and spread, and how can these changes be identified and targeted? One of the major challenges with capturing CTCs is that each CTC has different characteristics. Therefore, to answer Question 1 we assessed how current CTC technologies work and developed new ways to capture every CTC in blood samples from mouse models and humans. This formed the basis for answering Question 2, where we assessed how CTCs could be effectively detected at different stages of prostate cancer and identified gene signatures that were altered in patient CTCs. Finally, in Question 3 we mimicked the biological changes that prostate cancer cells undergo as they enter the bloodstream and become more aggressive and demonstrated ways of identifying and targeting these changes that could be applied clinically in the future to benefit patients. Together, this knowledge lays the groundwork for more effective capture of CTCs from the blood in order to help prostate cancer patients use a personalized medicine approach to combat disease progression and improve outcomes.

Co-Authorship Statement (where applicable)

All chapters in this thesis were written by Jenna Kitz and edited by Alison L. Allan. Jenna Kitz performed or oversaw all experiments and data analysis in this thesis.

Chapter 1 has been previously published as: Jenna Kitz, Lori E. Lowes, David Goodale and Alison L. Allan. Circulating Tumor Cell Analysis in Preclinical Mouse Models of Metastasis. *Diagnostics*. 2018; 8(2):1-19.

Chapter 2 has been previously published as: Jenna Kitz, David Goodale, Carl Postenka, Lori E. Lowes, and Alison L. Allan. EMT-independent detection of circulating tumor cells in human blood samples and pre-clinical mouse models of metastasis. *Clin. Exp. Metastasis*. 2021; 38:97-108. Lori E. Lowes assisted with data acquisition and analysis. David Goodale assisted with performing *in vivo* experiments. Carl Postenka assisted with histology of *in vivo* samples.

In Chapter 3, prostate cancer patients were accrued and consented with the help of Kes Sebborn from the Cancer Clinical Trials Unit and radiation/medical oncologists on the genitourinary (GU) cancer multidisciplinary disease site team at the London Regional Cancer Program (LRCP). The HyCEAD analysis was carried out by Kelly Seto and Pinki Nandi through a collaboration between the Allan Lab and Angle PLC.

Chapter 4 has been previously published as: Kitz, J.; Lefebvre, C.; Carlos, J.; Lowes, L.E.; Allan, A.L. Reduced *Zeb1* Expression in Prostate Cancer Cells Leads to an Aggressive Partial-EMT Phenotype Associated with Altered Global Methylation Patterns. *Int. J. Mol. Sci.* 2021, 22, 12840. Lori E. Lowes and Joselia Carlos assisted with data acquisition and analysis. Cory Lefebvre assisted with data analysis of methylation chip data. Additionally, Carl Postenka assisted in the histological analysis of pre-clinical mouse samples and the methylation chip analysis was performed on a fee-for-service basis by Nathan Cawte from the Clinical Research Laboratory and Biobank (CRLB) and the Genetic and Molecular Epidemiology Laboratory (GMEL) at McMaster University.

Acknowledgments

I would first like to thank my supervisor, Dr. Alison Allan for her continued mentorship, guidance, and friendship over the past six years. Having started as a (naïve) incoming graduate student I could have never guessed how this project would challenge me, change, and grow over six years, and how Alison would continue to mentor my progress, and assist me through every obstacle along the way. Her guidance and openness in allowing me to try new experiences has helped me to develop and flourish during my time as a graduate student. She unwaveringly supported me in every one of my extracurricular endeavors and helped to guide my future career. Alison has never made me feel like doors were closed rather, that every door and opportunity was always open for me. Finally, I would like to thank Alison for her friendship. Thank you for always allowing me to be a genuine version of myself. For supporting me on my good days, and bad days, and being there for me no matter what. I feel extremely lucky to have found myself under your supervision for my graduate degree and think of you as far more than just a supervisor.

I would also like to thank the members of the Allan Lab, past and present who have helped to shape and mold me into who I am today. Firstly, those who have taken their time to mentor me. Dr. Lori Lowes for your guidance and mentorship throughout the entirety of this project. Without you, this project would not exist, but more importantly, I would not be the scientist I am today. Dr. Ying Xia, for your patience in teaching me many of the laboratory techniques that made this thesis possible. David Goodale, for your support and organization of everything that is “the Allan Lab”, without which we would achieve hardly anything. Carl Postenka for your expertise, your can-do attitude, and our friendly conversations, which have always made my days better. Secondly, my lab mates, who have always been there to support me: on days when things worked, and days when things don’t. You have been there to talk through every problem, and never think twice to offer your help. Importantly, you have become my friends: Dr. Cory Levebre, Dr. Vasudeva Bhat, Sierra Pellizzari, Penny Haloulos, and Gabby Schoettle.

I would like to thank the members of my advisory committee: Dr. Trevor Shepherd, Dr. Paul Walton, and Dr. John Ronald. You have continued to support my journey; your help and guidance has helped to mold this thesis into what it is today. Thank you for always making me feel heard and respected.

Lastly, I would like to thank my family. My parents, Shirley Young, Tony Kitz, Trisha Kitz, and Perry Young for their never-ending love and support. For making me feel like I can accomplish anything, and that the world is opened to me. To my siblings, Emma Young, Miranda Kitz, and Mitchell Kitz, blood makes us family, but hearts make us friends. I cannot thank you enough for being my best friends, for listening to me when I complain, and for celebrating with me through my accomplishments. I am so proud to know you and to have you in my life, I can't wait to see where the future takes you.

This thesis is dedicated to Olga Kitz. Baba, thank you for making me feel like the most special person to ever exist, when, in fact, that person was always you. You helped me to become the empowered, strong woman I am today, and I will continue to model myself in your grace. I miss you every day and am so lucky to have had you in my life. Love you, Jenna xo.

Table of Contents

Abstract	ii
Summary for Lay Audience	iii
Co-Authorship Statement (where applicable)	iv
Acknowledgments	v
Table of Contents	vii
List of Tables.....	xii
List of Figures	xiii
List of Supplemental Tables.....	xv
List of Supplemental Figures	xvi
List of Appendices.....	xvii
Chapter 1	1
1 Introduction	1
1.1 Cancer.....	1
1.2 Prostate Cancer.....	1
1.2.1 Prostate Cancer Diagnosis.....	2
1.2.2 Prostate Cancer Grading.....	3
1.2.3 Prostate Cancer Staging.....	4
1.3 Metastasis	6
1.4 Epithelial-to-Mesenchymal Transition.....	8
1.5 Circulating Tumor Cells.....	10
1.5.1 CTC Enrichment Techniques	11
1.5.2 CTC Detection/Characterization Techniques.....	14
1.5.3 Additional CTC Analysis Approaches	16
1.6 Pre-Clinical Models of Metastasis and CTC Generation	17

1.7 Summary and Thesis Rationale	19
1.8 Overall Hypothesis and Thesis Objectives	20
1.9 References	21
Chapter 2	1
2 EMT- independent detection of circulating tumor cells in human blood samples and pre-clinical mouse models of metastasis.....	26
2.1 Introduction	26
2.2 Materials and methods.....	28
2.2.1 Cell Culture and Labeling	28
2.2.2 Blood Collection and Tumor Cell Spiking.....	29
2.2.3 CTC Analysis	29
2.2.4 <i>In Vivo</i> Metastasis Studies.....	30
2.2.5 CTC Characterization.....	31
2.2.6 Statistical Analysis	31
2.3 Results	33
2.3.1 The Parsortix® and CellSearch® platforms provide similar recovery of epithelial CTCs in human blood samples, but Parsortix® is superior for recovering mesenchymal CTCs.....	33
2.3.2 The VyCap CTC platform provides enhanced recovery of epithelial and mesenchymal CTCs in mouse blood samples compared to CellSearch®.	36
2.3.3 The VyCap CTC platform provides enhanced recovery of mesenchymal CTCs from <i>in vivo</i> mouse models of prostate cancer metastasis	39
2.3.4 CTCs can be harvested from the VyCap and Parsortix® for downstream molecular characterization	39
2.4 Discussion	41
2.5 Supplemental Data – Chapter 2.....	46
2.6 References	48
Chapter 3	51

3	Comparison of EMT dependent and independent circulating tumor cell enumeration and downstream molecular characterization in metastatic prostate cancer patients	51
3.1	Introduction	52
3.2	Materials and Methods	54
3.2.1	Patient Population and Study Eligibility	54
3.2.2	Clinical Data Collection	55
3.2.3	Blood Collection and CTC Enumeration	56
3.2.4	CTC Harvest, RNA Isolation and HyCEAD Analysis.....	56
3.2.5	TCGA Analysis	57
3.2.6	Statistical Data Analysis.....	57
3.3	Results	57
3.3.1	Patient characteristics	57
3.3.2	CTC enumeration in metastatic prostate cancer patients is similar between CellSearch® and Parsortix®	58
3.3.3	CellSearch® identifies the presence of increased CTCs in HV-mHSPC versus LV-mHSPC prostate cancer patients	60
3.3.4	HyCEAD chip analysis identified increased expression of 119 genes including 14 biologically relevant genes which may contribute to prostate cancer progression.....	60
3.4	Discussion	64
3.5	Supplemental Data – Chapter 3.....	73
3.6	References	77
Chapter 4	51
4	Reduced Zeb1 Expression in Prostate Cancer Cells Leads to an Aggressive Partial-EMT Phenotype Associated with Altered Global Methylation Patterns	84
4.1	Introduction	85
4.2	Materials and Methods	86
4.2.1	Cell Culture	86
4.2.2	Cell Transductions.....	86

4.2.3	Immunoblotting	87
4.2.4	Quantitative Real-Time PCR.....	87
4.2.5	Transwell Migration and Invasion Assays	87
4.2.6	Physical Barrier Wound Healing Assay	88
4.2.7	Spheroid Invasion Assay	88
4.2.8	BrdU Proliferation Assay	88
4.2.9	Cell Morphology Assay.....	89
4.2.10	<i>In Vivo</i> Studies.....	89
4.2.11	DNA Extraction and Dot-Blot DNA Analysis	90
4.2.12	DNA Methylation Chip Analysis	91
4.2.13	Patient Sample Analysis	91
4.2.14	Statistical Analysis	92
4.3	Results	92
4.3.1	Inducible Knockdown of Zeb1 in PC-3 Human Prostate Cancer Cells Results in Enhanced Expression of Epithelial Proteins	92
4.3.2	Knockdown of Zeb1 in PC-3 Prostate Cancer Cells Increases Migration and Invasion but Does Not Alter Proliferation	94
4.3.3	Knockdown of Zeb1 in PC-3 Prostate Cancer Cells Does Not Alter <i>In Vivo</i> CTC Generation or Macrometastases.....	94
4.3.4	Knockdown of Zeb1 in PC-3 Prostate Cancer Cells Leads to a Partial EMT Phenotype at the Cellular and Molecular Level	94
4.3.5	Treatment of PC-3 Zeb1 ^{KD} Prostate Cancer Cells with the Global Demethylating Agent 5-Azacitadine Results in Decreased DNA Methylation, Migration, and Invasion	98
4.3.6	Methylation Chip Analysis of Zeb1 ^{KD} PC-3 Prostate Cancer Cells Identified 10 Genes Associated with a p-EMT Phenotype.....	98
4.3.7	MAN1A1, EPB41, HSD17B13 and MYOM2 Are Altered in Prostate Cancer Patients	101
4.4	Discussion	105
4.5	Conclusions	107

4.6 Supplemental Data – Chapter 4.....	108
4.7 References	114
Chapter 5	118
5 Overall Discussion.....	118
5.1 Summary of Key Experimental Findings.....	118
5.2 Implications of Experimental Findings	119
5.2.1 Parsortix® and VyCap technologies are valuable for EMT-independent capture, enumeration and analysis of CTCs in clinical and pre-clinical blood samples	119
5.2.2 Use of Parsortix® and HyCEAD for analysis of CTCs in prostate cancer patients.....	121
5.2.3 Reduced Zeb1 expression in prostate cancer cells leads to an aggressive partial-EMT phenotype associated with altered global methylation patterns	122
5.3 Possible Limitations of the Thesis Work	123
5.4 Future Directions	127
5.5 Final Conclusions.....	129
5.6 References	130
Appendices	137
Curriculum Vitae.....	140

List of Tables

Table 1-1. Comparison of protein-based and nucleic acid-based approaches for circulating tumor cell characterization.	15
Table 2-1. Forward and reverse primers used for RT-qPCR analysis.....	32
Table 2-2. CTC recovery in spiked human blood samples using Parsortix® versus CellSearch®	35
Table 2-3. CTC recovery in spiked mouse blood samples using VyCap versus CellSearch® ..	38
Table 2-4. Advantages and disadvantages of CellSearch®, Parsortix® and VyCap CTC analysis platforms.....	45
Table 3-1. Patient Characteristics.....	59
Table 3-2. Individual patient CTC recovery for each cohort using the CellSearch® and Parsortix®	63
Table 3-3. Expression and functional relevance of HyCEAD-identified genes that lose expression in CTCs with advancing prostate cancer disease progression.....	67
Table 3-4. Expression and functional relevance of HyCEAD-identified genes that gain expression in CTCs with advancing prostate cancer disease progression.....	67
Table 4-1. Functional relevance of genes identified in DNA methylation chip analysis.....	103

List of Figures

Figure 1.1. Stages of prostate cancer progression.....	5
Figure 1.2. An overview of the metastatic process.	7
Figure 1.3. Epithelial-to-mesenchymal plasticity.....	9
Figure 1.4. An overview of circulating tumor cell enrichment techniques.....	12
Figure 2.1. The Parsortix® and CellSearch® CTC platforms provide equivalent recovery of epithelial CTCs in human blood samples, but Parsortix® is superior for recovery of mesenchymal CTCs.....	34
Figure 2.2. The VyCap CTC platform provides enhanced recovery of spiked-in epithelial and mesenchymal CTCs in mouse blood samples compared to the CellSearch®.....	37
Figure 2.3. The VyCap CTC platform provides enhanced recovery of mesenchymal CTCs from <i>in vivo</i> mouse models of prostate cancer metastasis.	40
Figure 2.4. CTCs can be harvested from the VyCap and Parsortix systems for downstream molecular characterization.	42
Figure 3.1. CTC recovery in metastatic prostate cancer patients is similar between CellSearch® and Parsortix®.....	61
Figure 3.2. CellSearch® identifies the presence of increased CTCs in HV-mHSPC versus LV-mHSPC prostate cancer patients.	62
Figure 3.3. HyCEAD prostate cancer (PC) chip analysis identified 49 genes with increased expression in the three prostate cancer patient cohorts.	65
Figure 3.4. HyCEAD high expression chip analysis identified 70 genes with increased expression in the three prostate cancer patient cohorts.	66

Figure 3.5. TCGA analysis reveals that FAM107A, GNMT, ADAMTS9, HOXB13, and FERMT2 have lower expression in prostate cancer patients with primary and/or metastatic disease. 69

Figure 3.6. TCGA analysis reveals that BMP6, TOP2A, BRCA1, CLDN3, BIRC5, ITGBL1, ZNF217, ST14, and TBP have higher expression in prostate cancer patients with primary and/or metastatic disease. 70

Figure 4-1. Inducible knockdown of Zeb1 in PC-3 human prostate cancer cells results in enhanced expression of epithelial proteins..... 93

Figure 4-2. Knockdown of Zeb1 in PC-3 prostate cancer cells increases cell migration. 95

Figure 4-3. Knockdown of Zeb1 in PC-3 prostate cancer cells increases cell invasion. 96

Figure 4-4. Knockdown of Zeb1 in PC-3 prostate cancer cells does not alter *in vivo* CTC generation or macrometastases..... 97

Figure 4-5. Knockdown of Zeb1 in PC-3 prostate cancer cells leads to a partial-EMT phenotype at the cellular and molecular level..... 99

Figure 4-6. Treatment of PC-3 Zeb1KD prostate cancer cells with the global demethylating agent 5-azacitadine (5-aza) results in decreased DNA methylation, migration and invasion. 100

Figure 4-7. DNA methylation chip analysis of Zeb1^{KD} PC-3 prostate cancer cells identified 10 genes associated with a p-EMT phenotype. 102

Figure 4-8. MAN1A1, EPB41, HSD17B13 and MYOM2 are altered in prostate cancer patients. 104

List of Supplemental Tables

Supplemental Table 3-1. HyCEAD gene expression panels used to analyze prostate cancer CTC samples.	73
Supplemental Table 3-2. Summary of HyCEAD Prostate Cancer (PC) chip gene expression analysis ^a	74
Supplemental Table 3-3. Summary of HyCEAD High Expression (HE) chip gene expression analysis	75
Supplemental Table 4-1. Antibodies for Immunoblotting.	108
Supplemental Table 4-2. Forward and Reverse Primers used for RT-qPCR.	109

List of Supplemental Figures

Supplemental Figure 2-1. Representative images of positive CTCs isolated from human blood using CellSearch® and Parsortix®.....	46
Supplemental Figure 2-2. Representative images of positive CTCs isolated from mouse blood using CellSearch® and VyCap.....	47
Supplemental Figure 3-1. Percent of upregulated genes in each cohort.....	76
Supplemental Figure 4-1. Cell morphology assay calculations.....	110
Supplemental Figure 4-2. Schematic of <i>in vivo</i> experimental design.....	111
Supplemental Figure 4-3. Zeb1 RNA can be inducibly knocked down in PC-3 human prostate cancer cells.....	112
Supplemental Figure 4-4. Knockdown of Zeb1 in PC-3 prostate cancer cells does not alter cell proliferation.....	113

List of Appendices

Appendix 1. Research Ethics Board approval for project ID: 109759 “Dynamic influence of the epithelial-to-mesenchymal transition (EMT) on circulating tumor cell (CTC) generation, phenotype, and disease progression in prostate cancer”.	137
Appendix 2. Animal Care Committee Approval for 2020-124 “Circulating tumor cells (CTCs) in prostate cancer”.	138

Chapter 1

1 Introduction

A version of this chapter has been published as a review paper:

Jenna Kitz, Lori E. Lowes, David Goodale and Alison L. Allan. Circulating Tumor Cell Analysis in Preclinical Mouse Models of Metastasis. *Diagnostics*. 2018; 8 (2) 30:1-19.

1.1 Cancer

Cancer is currently one of the leading causes of death worldwide, with the projected number of cases expected to increase fifty percent from 2012 to 2030¹. Cancer is a subset of diseases characterized by atypical cell growth and proliferation. Oncogenes may become activated through gain-of-function mutations, which enables proliferative signaling, allowing the cell to grow uncontrollably as it evades growth suppressors². Tumor suppressor genes can be negative regulators of cell growth and can be inactivated through loss-of-function mutations, again leading to an increase in cell proliferation³. A non-cancerous tumor is termed benign, while a cancerous tumor is classified as malignant. Benign tumors typically are non-life threatening because of their localization to the primary tumor site, however, malignant tumors have the ability to leave the primary tumor site and invade and travel to a secondary region of the body, a process called metastasis, is the most common contributor to cancer-related mortality⁴.

1.2 Prostate Cancer

The prostate is located inferior to the urinary bladder and its primary function is to contribute to seminal fluid, which nourishes and transports sperm^{5,6}. In adults, the prostate is a homogenous structure which has three anatomical zones: the peripheral zone (65%), the transition zone (10%), and the central zone (25%), the anatomical boundaries of which are relatively subtle in the absence of disease⁶. Prostate cancer is unique in that not every prostate cancer tumor is a serious threat, and some men die before their prostate cancer ever progresses past an initial benign tumor⁶. The main risk factors for prostate cancer include a western-type lifestyle and an increasingly aged society which is progressively more susceptible to disease⁶. Other risk factors include ethnicity, family history, sexually transmitted diseases (STDs), obesity, smoking, alcohol consumption, vasectomies, and diet⁷. Together this has led to an increase in the incidence and death rate from

prostate cancer⁶. The 5-year survival rate for non-metastatic prostate cancer in the United States is nearly 100%^{8,9}. However, as the cancer progresses cells may escape from the primary tumor and spread to distant organs in the body, a deadly process termed metastasis¹⁰. Approximately 90% of prostate cancer-related deaths occur as a result of metastasis¹¹. Correspondingly, 5-year survival rates for metastatic prostate cancer drops to approximately 30%^{12,9}. Recurrence is also seen in 30-40% of patients after successful treatment of a primary tumor, of which 50% is a recurrence of metastatic disease^{10,13}. The current challenge in prostate cancer is therefore to distinguish potentially dangerous lesions from the slow-growing, well-differentiated cancers which are unlikely to progress into aggressive disease⁶.

Nodules of benign prostatic tissue usually originate within and expand the transition zone, which typically distorts and compresses the adjacent peripheral zone⁶. Although malignancy can occur in all three zones, the majority of cancers are believed to originate in the glands of the peripheral zone⁶. This is hypothesized to be due to the proximity of the peripheral zone to the neurovascular bundles which may facilitate spread and enhance metastatic potential⁶. About one third of American men greater than 50 have histological evidence of prostate cancer, but most of these cases remain “silent”, and many genetic changes are necessary for aggressive cancer to develop¹⁴. Patients with localized prostate cancer often undergo “watchful waiting/active surveillance” whereby the disease is monitored by PSA (prostate-specific antigen) tests, rectal exams, and symptom changes at regular intervals. If the prostate cancer begins to become symptomatic, which includes urinary issues or enlarged prostate glands, it is recommended that the prostate be surgically removed¹⁵. The entire prostate is usually removed via radical prostatectomy, and the patient may undergo adjuvant radiation, chemotherapy, and/or hormone therapy¹⁵. In prostate cancer, hormone therapy aims to reduce the levels of androgens including testosterone and dihydrotestosterone (DHT) which stimulate prostate cancer cells to grow¹⁶. However, over time the cancer will develop mechanisms that allow it to become resistant to hormones (termed castrate resistant), and progress to castrate resistant metastatic prostate cancer (mCRPC), for which there is currently no cure¹⁴.

1.2.1 Prostate Cancer Diagnosis

Prostate cancer can be diagnosed in various ways, including digital rectal examinations (DRE), serum PSA (prostate specific antigen) tests, and/or transrectal ultrasounds, with confirmation by

biopsy¹⁷. However, the most accepted screening for prostate cancer is with PSA and DRE¹⁷. Prostate specific antigen (PSA) is a protein released by prostate tissue¹⁸. PSA levels are detected by a blood test and may be used as an early indicator of prostate cancer as levels rise when abnormal activity is present in the prostate¹⁸. This abnormal activity can be an indicator of prostate cancer, but it can also occur in the presence of prostate inflammation and benign prostatic hyperplasia (an enlarged prostate gland)¹⁸. Therefore, changes in PSA levels are not only an indicator of prostate cancer, and this can lead to over-diagnosis of prostate cancer based on PSA levels¹⁹. In addition, PSA levels vary between individuals so only changes in PSA levels within an individual may give an indication of abnormal prostate activity, making PSA levels imperfect for diagnosing prostate cancer¹⁸.

After a radical prostatectomy, PSA levels typically become undetectable. However, although it is generally accepted that a rise in PSA levels after prostatectomy is a good measure of recurrence after an initial diagnosis²⁰, this too is imperfect. This is because not all prostate cancers release PSA. *In vivo* mouse experiments have compared PSA levels in mice that were orthotopically injected with one of two prostate cancer cell lines (LNCaP or PC-3M), which vary in their molecular characteristics²¹. Although all the mice had large primary tumors, only LNCaP mice had detectable levels of PSA in the serum²¹. These mice also had detectable levels of PSA in prostate cancer tissue via immunohistochemistry analysis²¹. Importantly, mice with PC-3M prostate cancer tumors did not have detectable levels of PSA in the serum regardless of tumor size and did not have detectable tissue PSA expression²¹. This experimental model highlights that different prostate cancers can release varying levels of PSA, making it an imperfect marker for detecting prostate cancer recurrence even after a prostatectomy.

1.2.2 Prostate Cancer Grading

Following a prostate biopsy or prostatectomy, prostate cancer tissues are analyzed and assigned a Gleason score, which is based on how the cancer looks under a microscope and helps determine the grade of the tumour²². The Gleason score, in addition to the stage of the cancer (described below), is used to help create a treatment plan for prostate cancer patients²². A score of 1-5 is assigned based on how healthy or differentiated the cells look²². More differentiated cells are typically associated with less aggressive tumors and are given a low score, while more aggressive-looking, less differentiated cells are assigned a higher score²². Gleason patterns 1-2 consist of

circumscribed nodules and packed glands²³. These glands are uniform in size and shape, with slightly more variation in pattern 2 than in pattern 1²³. Gleason pattern 3 consists of variable sized individual glands that are well formed²³. Gleason pattern 4 is designated as fused glands, irregular cribriform glands and hypernephroma pattern, or ill-defined glands with poorly formed glandular lamina²³. Gleason pattern 5 consists of sheets of tumor, individual cells, and cords of cells. Gleason pattern 5 is commonly under-graded on needle biopsy²³. Two areas of the tumor section or biopsy are used to create the Gleason score; one area where the cancer is most obvious, and a second area which exhibits a less common pattern of growth²². Both scores are added together to give an overall score from 2-10²². Gleason scores from 2-4 are not typically assigned as cancerous by needle biopsy due to poor reproducibility, poor correlation with radical prostatectomy, and the potential for overdiagnosis of prostate cancer²³. Consequently, most low-grade prostate cancer diagnosis by needle biopsies occurs at or above Gleason scores of 5 and 6²³, where a score of 5-6 is associated with low-grade cancer, 7 is medium-grade cancer, and 8-10 is high grade cancer²². The higher the grade, the more likely the cancer is to spread²². However, Gleason scores are again imperfect for creating a treatment plan for prostate cancer patients, even when used in conjunction with PSA levels. This is because 1) the portion of the specimen that is analyzed may not be an accurate representation of the cancer as a whole, 2) a Gleason score of 7 does not differentiate between mostly well-differentiated cancer (Gleason 3+4=7) or mostly poorly differentiated cancer (Gleason 4+3=7) which are prognostically different, and 3) in practice, the lowest score assigned is a 6 (although the scale is 2-10) which leads to fear of cancer diagnosis in patients leading to an expectation of unnecessary treatments^{24,25}.

1.2.3 Prostate Cancer Staging

Staging is a description of where the cancer is located, and if metastasis has occurred. Staging allows clinicians to create a treatment plan and helps to assess a patient's prognosis. In prostate cancer, clinical staging is determined based on PSA levels, Gleason score, and from pathological observations related to biopsies or surgical specimens²² (**Figure 1.1**). In stage I prostate cancer, malignant cells are found only in the prostate, and they are generally slow growing. Stage II describes a tumor that is larger but has not spread outside of the prostate gland to the lymph tissue or to distant organs. These cells are usually abnormal and can grow quickly. In stage III, cancer has spread beyond the prostate into nearby tissues and perhaps to the seminal vesicles. Lastly,

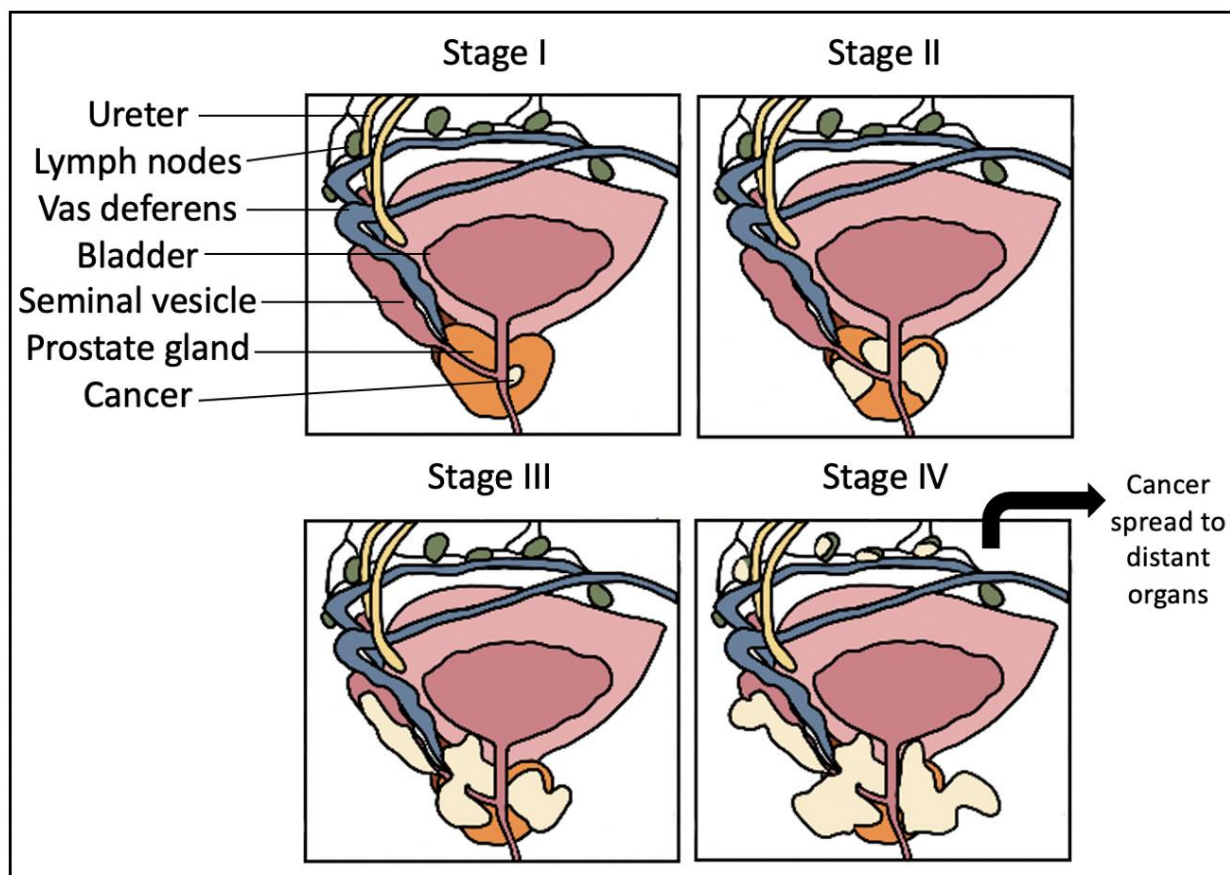


Figure 1.1. Stages of prostate cancer progression. Stage I prostate cancer is associated with malignant cells contained entirely within one lobe of the prostate. Stage II prostate cancer is associated with a larger tumor, contained entirely within one or more lobes of the prostate. In stage III the prostate cancer has spread beyond the prostate into nearby tissues and/or the seminal vesicles. Stage IV prostate cancer represents a tumor that has metastasized to create secondary tumors throughout the body or the lymph nodes.

stage IV represents a tumor that has metastasized to create secondary tumors throughout the body, a process that ultimately ends up causing more than 90% of prostate cancer deaths²² (**Figure 1.1**).

1.3 Metastasis

Metastasis is the spread of cancer from the primary tumor to a secondary location within the body²⁶. Development of prostate cancer at the primary site is typically a slow process, sometimes taking decades to form a palpable mass and disseminate to a secondary site²⁷. Metastasis is a multistep process (**Figure 1.2**) that begins with the local infiltration of tumor cells from the primary tumor into adjacent tissues²⁸. For prostate cancer to metastasize, multicellular changes occur that switch normal slow-growing cells to rapidly proliferating cells with unchecked growth²⁷. Specifically, mutations in the phosphatase PTEN/MMAC1 or CDK inhibitor p27 have been shown to be correlated with progression to metastatic disease²⁷. Additionally, angiogenesis, the growth of a vascular network formed from pre-existing vessels, is an important step in tumor invasion by providing nutrients and oxygen to aid in tumor growth²⁹. For example, IL-8 expression has been shown to regulate angiogenesis in orthotopic human prostate cancer cells in athymic nude mice²⁷. Once the tumor is vascularized, tumor cells may intravasate in order to move into the bloodstream²⁸. Once in the bloodstream, cells that survive in the circulatory system may disseminate, or spread, throughout the body²⁸. These cells can then extravasate to move out of the bloodstream in order to proliferate and colonize to form another tumor at a secondary organ site²⁸ (**Figure 1.2**). It has been suggested that individual tumor cells have specific affinity for their target organs which support growth of the secondary tumor. This is known as the seed and soil hypothesis³⁰. According to the seed and soil hypothesis, each cancer type will most commonly spread to and grow in specific organs³⁰. For prostate cancer, the most common metastatic site is bone²⁷. One possible explanation for the propensity of prostate cancer to metastasize to bone is the abundance of growth factors in the bone including transferrin, which promotes prostate cancer formation and metastases²⁷. These growth factors are either absent, or are suppressed by inhibitory molecules at the primary site²⁷. Because tumor metastasis involves many steps, prostate cancer cells often transition from non-invasive to invasive phenotypes through an epithelial-to-mesenchymal transition (EMT), resulting in altered cell-substrate attachments, decreased cell-cell adhesion, and increased cell motility and invasive abilities²⁷.

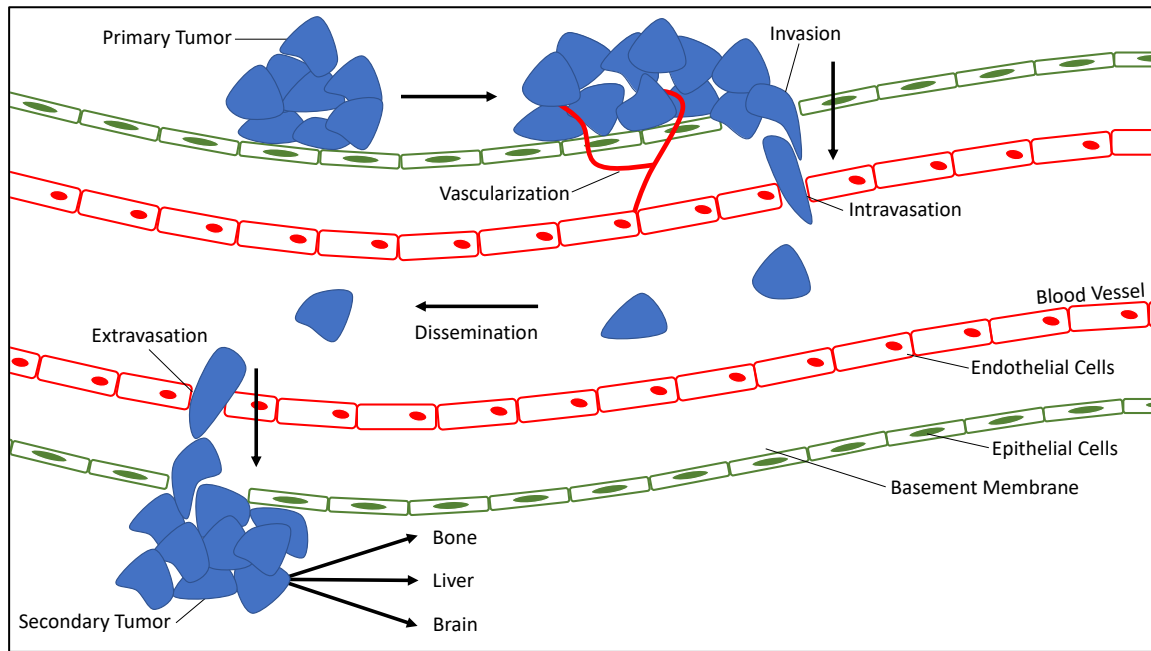


Figure 1.2. An overview of the metastatic process. Metastasis is a multi-step process that involves primary tumor vascularization, invasion into neighboring tissues, intravasation into the bloodstream, dissemination throughout the body, extravasation out of the bloodstream, and secondary tumor formation at various organ sites within the body.

1.4 Epithelial-to-Mesenchymal Transition

Epithelial-to-mesenchymal transition (EMT) is a process by which a polarized epithelial cell undergoes molecular changes that enable it to gain a mesenchymal phenotype³¹. Cells with this phenotype have greater migratory capacity, increased invasiveness, and elevated resistance to apoptosis³¹. EMT is categorized into three types; type 1 EMT is associated with development and is a mechanism for dispersing cells in embryos, type 2 is associated with tissue repair and pathological stress, and type 3 occurs in neoplastic cells, or cells with abnormal growth as is the case for cancer cells³¹. In prostate cancer, EMT involves molecular changes resulting in increased cellular motility, increased invasive properties, altered cell-substrate attachment, and decreased cell-cell adhesions²⁷ (**Figure 1.3**). The acquisition of these properties results in a transition from non-invasive to an invasive phenotype which is critical for prostate cancer progression²⁷. Activation of transcription factors is one of the many processes that can initiate EMT³¹. These transcription factors include Snail, Slug, Zeb1, Zeb2, Twist1 and Twist2, each of which can mediate downstream events to initiate the EMT program by disrupting cell-cell junctions and the cell-matrix adhesions mediated by integrins³¹. Specifically, Zeb1 is a pivotal EMT transcription factor which facilitates silencing of E-cadherin to promote the loss of epithelial properties and induce phenotypic and cellular plasticity^{32,33}. Many studies have established a connection between loss of E-Cadherin expression by cancer cells that have undergone EMT³¹. Additionally, Zeb1 has been shown to promote multidrug resistance, proliferation, and metastasis and its expression is indicative of worse clinical prognosis in prostate cancer^{32,33}.

The reverse process, mesenchymal-to-epithelial transition (MET) involves the conversion of mesenchymal cells to epithelial analogs³⁴ (**Figure 1.3**). This occurs at metastatic sites and is postulated to be an integral part of metastatic tumor formation³⁴. One of the main hallmarks of MET is the re-expression of E-cadherin and its role in enabling metastatic colonization^{34,35}. However, re-emergence of the epithelial phenotype is often only partial or incomplete³⁴. Partial conversion from epithelial-to-mesenchymal (p-EMT) involves cells maintaining attributes from both epithelial and mesenchymal cells^{31,36} (**Figure 1.3**). Often this p-EMT phenotype is associated with co-expression of both epithelial and mesenchymal markers and enhanced ability for migration, stemness, and tumor progression^{35,37}. Due to the enhanced properties of p-EMT cells

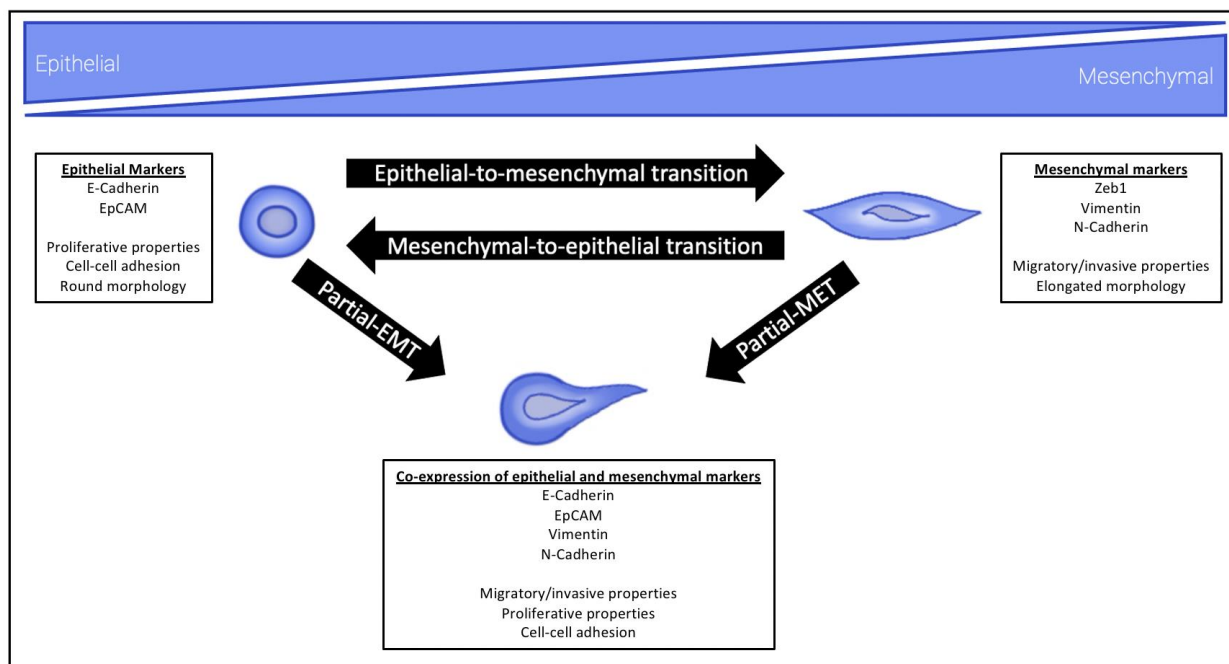


Figure 1.3. Epithelial-to-mesenchymal plasticity. EMT results in mesenchymal cells with increased expression of mesenchymal markers, increased migration and invasive properties and an elongated morphology. The reverse process of MET results in epithelial cells with increased expression of epithelial markers, proliferative properties, cell-cell adhesion, and round morphology. Partial EMT (p-EMT) or partial-MET results in co-expression of epithelial and mesenchymal and concomitant presence of epithelial and mesenchymal properties including migratory and invasive properties, proliferative capabilities, and cell-cell adhesion.

and their high tumorigenic potential, these cells have been associated with poorer patient prognosis compared to cells with complete EMT or MET³⁷. There are still many unknowns about the EMT, MET and p-EMT processes as they relate to the development and movement of cancer cells³¹. Relevant to this thesis, EMT has been shown to be associated with increased generation of circulating tumor cells (CTCs; described further below), leading to increased disease aggressiveness and metastasis³⁸.

1.5 Circulating Tumor Cells

Despite advances in clinical imaging technologies, challenges remain for accurate detection and tracking of metastasis in prostate cancer patients, particularly at earlier stages of the metastatic process^{38,39}. Emerging alternative approaches may help address these challenges in both the clinical and pre-clinical settings and involve blood- and urine-based detection and tracking of metastatic disease^{38,39}. Recent advances have identified urinary biomarkers which have the potential to be used for prostate cancer screening, diagnosis, prognosis, and prediction³⁹. These include traditional prostate cancer markers such as PSA (described above), and approximately 40 others which may be used in conjunction to create prostate cancer screening panels in the future³⁹. Additionally, the detection of disseminated cells in the bloodstream, called circulating tumor cells (CTCs) presents an opportunity to monitor disease progression much less invasively than metastatic tissue biopsy. CTCs present a unique opportunity to analyze rare metastatic events and early stage metastatic cancer by capturing and characterizing cells collected from patient blood samples^{38,40}. CTCs can provide important insight into patients' individual disease and offer an opportunity for single or rare cell analyses in the form of a minimally-invasive, "liquid-biopsy" for monitoring disease progression and treatment responses⁴¹. These CTCs can be used for real-time monitoring in patients for early metastasis, disease progression, and/or treatment responses⁴². In prostate cancer, CTCs in the blood are correlated with metastatic disease, poor prognosis and reduced survival rates⁴³, and changes in CTC number throughout treatment have been observed to be reflective of therapy response⁴⁴. The presence of increased numbers of CTCs is associated with significantly poorer treatment responses in the clinical setting⁴⁵, and CTCs can also be used as predictive markers for therapy to dramatically increase treatment efficacy⁴⁶. The use of CTCs as a clinical biomarker has the potential to reduce healthcare costs and could eventually be a leading prognostic and/or predictive tool in personalized treatment based on genetic and molecular

information from patients' own tumors⁴⁷⁻⁴⁹. However, highly sensitive technologies are required for accurate CTC detection and analysis due to the extremely rare frequency of these cells in the blood (1 CTC per 10^6 leukocytes)^{38,40,50}. Because of this, most CTC assays use a combination of enrichment and detection/characterization techniques as summarized in **Figure 1.4**.

1.5.1 CTC Enrichment Techniques

1.5.1.1 Density-Based Enrichment

Density-based isolation of CTCs takes advantage of the differences in density between CTCs (<1.077 g/ml) and blood cells (>1.077 g/ml)⁵¹. Ficoll-Paque® (Sigma-Aldrich, St. Louis, MO), OncoQuick® (Greiner Bio-One, Monroe, NC), and RosetteSep™ (StemCell Technologies, Vancouver, BC) are all technologies that use density-based differences to separate CTCs from the blood. These approaches use density gradient medium to collect mononuclear cells (including CTCs) from blood samples⁵² (**Figure 1.4a**). Similar to size-based enrichment techniques, collecting CTCs by density gradient allows for capture of both epithelial and mesenchymal CTCs and these techniques are also relatively easy and inexpensive to perform⁵¹. However, some shortcomings of density-based techniques include low specificity (because of the lack of specific selection for CTCs within the mononuclear fraction) combined with the opportunity for cross-contamination of CTCs with other cell types in the blood due to movement of these cells into the plasma layer, or due to the presence of clotting/aggregates⁵¹.

1.5.1.2 Size-based enrichment

Sized-based isolation of CTC capitalizes on the differences in size between CTCs ($>8\mu\text{m}$) compared to leukocytes ($<8\mu\text{m}$)^{52,53}. Parsortix® (Angle PLC; Surrey, UK), ScreenCell® (Westford, MA), and ISET® (Rarecells, Paris, FR) are examples of CTC technologies that use size-based techniques, in conjunction with other methods, to isolate the cells from blood samples. Typically, whole blood is passed through a filtration device with different pores or channels (typically 6-10 μm) or different filter-based approaches, with the common goal of allowing isolation of CTCs from other blood components and retrieval of CTCs for further experimentation, including multiplexed imaging, genetic analysis, or culturing⁵²⁻⁵⁴ (**Figure 1.4b**). The advantages of sized-based enrichment techniques include the straightforward and relatively inexpensive

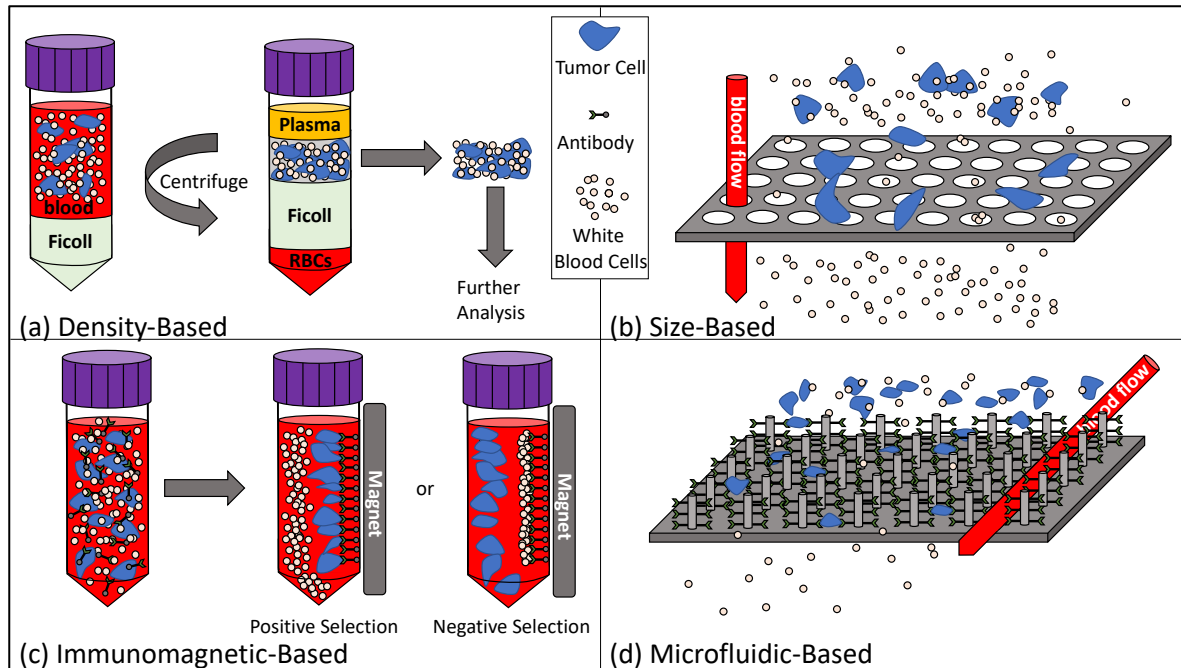


Figure 1.4. An overview of circulating tumor cell enrichment techniques. (a) Density-based CTC enrichment combines whole blood with Ficoll to separate based on cell density. Mononucleated cells can then be recovered for further analysis. (b) Size-based CTC enrichment allows the small blood cells to pass through the pore, while larger tumor cells remain stuck behind. (c) Immunomagnetic-based CTC enrichment either selects positively (for CTCs) or negatively (for white blood cells) using iron labeled target antibodies. (d) Microfluidic-based CTC enrichment passes blood through either chip-based devices or antibody-coated microposts (depicted) to enumerate CTCs from whole blood.

nature of these assays, as well as the ability to identify both epithelial and mesenchymal CTCs⁵¹. However, size-based assays can be prone to clogging within the pores/channels, and the low specificity of these assays sometimes causes small CTCs to be lost during the enrichment process⁵¹.

1.5.1.3 Immunomagnetic-based enrichment

The most widely used CTC enrichment/isolation technique is immunomagnetic-based selection of CTCs⁵⁴. Immunomagnetic separation uses magnetic, bead-based separation technology⁵¹. CTCs are enriched from blood samples using antibodies conjugated to magnetic beads, which are designed to either positively select for CTCs by targeting various epithelial or tumor-specific antigens expressed by tumor cells, or negatively select for CTCs by targeting contaminating blood cell antigens such as CD45^{51,52} (**Figure 1.4c**). AdnaTest (QIAGEN Hannover GmbH, Langenhagen, Germany), MACS® (Miltenyi Biotec, Auburn, CA), IsoFlux™ (Fluxion Biosciences, Alameda, CA), and CellSearch® (Menarini Silicon Biosystems Inc, San Diego, CA) all use immunomagnetic approaches for CTC enrichment. The various immunomagnetic technologies have different advantages, i.e. MACS maintains cell integrity, while AdnaTest uses defined markers and allows for downstream analysis of CTCs, with the possibility of characterization of epithelial/mesenchymal phenotype⁵¹. Through customizable IgG beads, Isoflux allows users to mix the antibodies of their choice when enumerating CTCs, allowing for very high customization⁵⁵. Lastly, CellSearch® is an FDA and Health Canada approved, semi-automated technology that uses positive CTC enrichment via EpCAM (epithelial cell adhesion molecule) combined with image analysis⁵¹. However, each of these technologies also has drawbacks, including false positive/false negative isolation of CTCs (MACS®, AdnaTest) and limited flexibility in assay design or marker choice (AdnaTest, CellSearch®)⁵¹. In addition, CellSearch® only allows for capture of epithelial CTCs and has very limited capacity for downstream analysis of CTCs once they are identified⁵¹. The greatest limitation with regards to immunomagnetic separation of CTCs from blood samples is the lack of a reliable “universal marker” that can be used independently of both the tumor type and the stage of disease progression⁵¹.

1.5.1.4 Microfluidic-based enrichment

To enrich for CTCs using microfluidic-based techniques, whole blood is passed through small channels, often using chip-based devices designed with micro-channels etched or molded into surfaces such as glass, silicon or polymers⁵². Similar to immunomagnetic-based techniques, CTCs can be captured by antibody-coated microposts, or by size/deformability⁵² (**Figure 1.4d**). Parsortix®, CTC-Chip/iChip, IsoFlux™ (Fluxion Biosciences, Alameda, CA), and GILUPI CellCollector™ (NanoMedizin Potsdam, DE), are all techniques that use microfluidics as a basis to enrich for and capture CTCs. Microfluidic-based techniques generally have high enrichment percentages and allow for the release of intact CTCs after enrichment to allow for downstream analysis. However, similar to immunomagnetic enrichment techniques, these assays lack a “universal marker” targeting all cancer subtypes including cancers of advanced metastatic disease.

1.5.2 CTC Detection/Characterization Techniques

Once CTCs have been enriched from the blood, detection, enumeration and/or molecular characterization can be carried out using a variety of protein-based and nucleic acid-based approaches⁵¹ (**Table 1.1**).

1.5.2.1 Protein-based detection and characterization

Protein-based detection and characterization of CTCs can be carried out using different techniques such as immunofluorescence, flow cytometry, CellSearch®, and the CTC-Chip/iChip⁵³. Typically this is done through use of fluorescent-conjugated antibodies targeting epithelial antigens such as CK-19 and EpCAM on CTCs and identification via laser-based and/or image-based detection systems^{52,53}. These approaches allow for analysis of large sample volumes with high specificity⁵¹. However, some image-based characterization techniques such as manual microscopy-based analysis of stained CTCs can be very slow and labour-intensive, while other techniques such as flow cytometry have low sensitivity and can be technically challenging⁵¹⁻⁵³.

1.5.2.2 Nucleic acid-based detection and characterization

Frequently used nucleic acid-based detection and characterization of CTCs include reverse transcription (RT) and quantitative polymerase chain reaction (qPCR) to identify CTCs

Table 1-1. Comparison of protein-based and nucleic acid-based approaches for circulating tumor cell characterization.

		Sample Size Analysis	Ability for CTC Quantification	High Specificity	High Sensitivity	Labour-Intensive/Challenging	Down-Stream Analysis
Protein-Based	Immunofluorescence	Small (<100 μ L)	Yes	Yes	No	Yes	Yes
	Flow Cytometry	Large (>300 μ L)	Yes	Yes	No	Yes	Yes
	CellSearch®	Large (7.5 mL)	Yes	Yes	Yes	No	No
	CTC-Chip/iChip	Large (8 mL)	Yes	Yes	Yes	Yes	Yes
Nucleic Acid-Based	RT-PCR	Small (1 μ L)	No	No	Yes	No	No
	RT-qPCR	Small (1 μ L)	No	No	Yes	No	No
	Next-Gen Sequencing	Small (<50 μ L)	No	Yes	Yes	Yes	Yes

based on expression of specific genes of interest⁵³. In addition, more sophisticated methods such as next generation sequencing and genomic analysis (including at the single-cell level) are emerging as valuable (albeit technically challenging) tools for detailed CTC characterization as it relates to molecular disease features. The high sensitivity of nucleic acid-based techniques allows for analysis of small numbers of CTCs, although the amplification basis of PCR can lead to false positive results and/or low specificity of CTC detection⁵³. In addition, these approaches cannot accurately quantify/enumerate the number of CTCs in a sample, don't allow for visualization of CTCs, and do not allow for recovery and further analysis of CTCs⁵¹.

1.5.3 Additional CTC Analysis Approaches

1.5.3.1 Dielectrophoresis

Approaches such as DEPArray™ (Silicon Biosystems, Bologna, IT) involve an electrophoretic-based cell-sorting and isolation platform for single-cell purification and analysis of live or fixed cells. DEPArray™ digitally sorts 100% pure subpopulations of cells from samples using a chip-based microfluidic cartridge and automated microscope image-based analysis^{56,57}. This system does require that cells are already enriched from whole blood samples using one of the techniques described above⁴². Labeled cells are loaded into the DEPArray™ cartridge, where electrodes are activated to form DEP cages, trapping the labeled cells. The cartridge is scanned in each desired fluorescence channel to identify target cells which are moved into a designated area. Individual cells are then dispensed into a collection tube for further analysis with Silicon Biosystems CellBrowser™ software^{56,57}. This allows for differential analysis and characterization of tumor cell populations using next-generation sequencing⁵⁸. The DEPArray™ is suited for small sample sizes (<10,000 cells) because the assay has the ability for single-cell recovery, and is ideal for further molecular characterization of small pure CTC samples^{42,56,57}.

1.5.3.2 Direct cellular imaging

The Epic Sciences CTC platform was designed for detection and molecular characterization of CTCs regardless of epithelial status⁵⁹. To enumerate cells, and for protein biomarker analysis, the EPIC Sciences platform first consists of slide prep, where whole blood is lysed and nucleated cells are deposited onto slides and frozen^{59,60}. Slides are then immunofluorescently stained and scanned by Epic's rapid scanning method^{59,60}. By assessing protein expression and morphology, Epic can

differentiate between white blood cells and CTCs, which can then be characterized into traditional CTCs, CTC clusters, CK-negative CTCs, and apoptotic CTCs^{59,60}. Studies have shown that the Epic Science platform has high CTC recovery, high specificity, and high repeatability for CTC detection⁵⁹.

Overall, there are a number of promising technologies being developed for tracking and characterizing metastasis and treatment response using CTCs. However, several challenges remain, and further work is needed to understand the biology of CTCs in the context of metastatic progression in order to optimize their widespread use as clinical biomarkers. In order to do this, analysis of CTCs using *in vivo* pre-clinical animal models of metastasis provides an important opportunity to study CTCs and to develop and/or optimize CTC assays in controlled experimental metastasis studies. The next section describes different approaches that can be used to study metastatic progression and CTCs in the pre-clinical setting, including details of each of the various available CTC assays and a summary of the current advances and challenges of pre-clinical CTC analysis.

1.6 Pre-Clinical Models of Metastasis and CTC Generation

The presence of CTCs in the blood has been correlated with disease progression towards metastasis³⁸. Thus, in order to study CTCs in a pre-clinical setting, we must generate metastatic disease in animal models. There are many different pre-clinical animal models of metastasis, including spontaneous, experimental, genetically engineered mouse, and patient-derived xenograft metastasis models. Each of these models have their own specific advantages and disadvantages which largely differ in many facets, including time to metastasis, experimental costs, and patient specificity. For the purposes of the current thesis we will focus on spontaneous metastasis models of prostate cancer, which involve injection of cancer cells into their orthotopic site of origin, the prostate gland^{61,62} followed by monitoring of disease progression over time. The advantage of spontaneous metastasis models is the ability to recapitulate and analyze all steps of disease progression including the growth of the primary tumor and eventual spontaneous metastasis to distant organs⁶¹. This allows for natural development and monitoring of disease as it progresses in a biological setting, and thus is an optimal model to assess morphology, growth, and developmental characteristics of clinical disease. In the pre-clinical setting, CTC analysis can

provide a means for tracking metastasis and understanding its biology, and several studies by our lab and others (described below) have contributed valuable knowledge in this area.

To address whether CTCs are present concurrently with metastatic disease, our lab performed *in vivo* experiments showing that prostate cancer cell lines with increasingly mesenchymal phenotypes shed greater numbers of CTCs more quickly and with greater metastatic capacity than prostate cancer cell lines with an epithelial phenotype³⁸. To assess whether CTCs are present but not detected by CellSearch®, our lab observed that the CellSearch®-based assay failed to detect 40-50% of mesenchymal CTCs. Furthermore, the CellSearch®-based assay captured most of the CTCs shed during early-stage disease *in vivo*, and only after the establishment of metastasis were significant numbers of undetectable CTCs present, with CTCs acquiring more mesenchymal phenotypes during disease progression³⁸. In the current thesis, we aim to build on these studies to determine the functional impact of EMT on CTC biology and detection.

A preclinical study conducted by Baccelli et al (2013)⁶³ demonstrated that CTCs isolated from breast cancer patient samples contained transplantable metastasis-initiating cells which gave rise to metastatic disease in mice. Co-expression of CD44v6 and c-MET was observed to be particularly important for metastasis initiation, where interaction with hepatocyte growth factor (HGF) in breast cancer metastases enhanced MET-kinase signaling⁶³. Another study by Vishnoi and colleagues (2015)⁶⁴ used patient samples to culture CTC-derived 3D tumorspheres that allowed assessment of biomarker profiling and biological characteristics. Using multiparametric flow cytometry they revealed that enriched CTC populations from breast tumors had unique gene signatures. They also observed that fluorescence-activated cell sorting (FACS)-sorted CTC populations, which expanded into 3D CTC tumorspheres in non-adherent stem cell conditions, had suggestive metastatic competency and cellular protrusions. Through their findings they elucidated mechanisms for the generation of tumor-associated vesicles (oncosomes) and their related role in mediating intracellular signaling. Lastly, they were able to characterize the 3D CTC tumorspheres as non-hematopoietic, tumorigenic, and possessing stem-cell properties⁶⁴. In a report from Zhang et al (2013)⁶⁵, CTCs isolated from patients with breast cancer were characterized and used to create multiple cell lines for subsequent *in vitro* and *in vivo* work. This study identified a potential signature for breast cancer brain metastasis and analyzed these cells for invasiveness and metastatic competency. With the development of brain metastatic breast cancer CTC cell lines,

this group is now exploring potential protein signatures and mechanisms of brain cancer metastasis in the pre-clinical setting⁶⁵. Finally, a review by Kang and Pantel (2013)⁶⁶ nicely summarizes how animal models of CTCs mimic the complexity of patient cancers in the clinic and how pre-clinical studies have identified many important mechanisms of metastasis; including pathways, inhibitors, and gene signatures that are accelerating the identification and implementation of clinically relevant CTC information.

1.7 Summary and Thesis Rationale

Traditionally, translational research progresses using a “bench-to-bedside” model, where techniques are created and perfected in a laboratory setting before being implemented for clinical use. CTC research is quite unique in this regard, as it has evolved using a “bedside-to-bench” approach. This has allowed CTC technology to enter quickly into the clinical setting, by way of CellSearch® and other emerging technologies. Clinical and pre-clinical CTC analysis studies to date have provided insights into mechanisms of prostate cancer metastasis, into the transition between epithelial-to-mesenchymal phenotypes, and into potential new biomarkers. Technological advances in single-cell CTC analysis have also elucidated potential gene expression profiles and cell mutations which influence cell aggressiveness. However, outstanding questions have resulted in clinicians’ hesitance in the adoption of CTCs as a biomarker for directing patient care³⁸. Previously, our lab has demonstrated that CTC dissemination occurs relatively early in the metastatic cascade, and that both primary tumors and metastases are able to generate CTCs^{61,67,68}. However, currently there is very little known about the functional role of EMT in CTC generation, detection and metastasis. This is particularly apparent when looking at CTC capture by the CellSearch® as it relates to EMT of prostate cancer. Further investigation of this biological and clinical question is the focus of this PhD thesis. By converging pre-clinical and clinical CTC studies, we will continue to develop the intellectual framework of the metastasis field, which has many unresolved questions to be addressed in future studies to improve cancer therapies. In particular, the ability to increase accessibility of liquid CTC biopsies for prostate cancer patients of any disease stage and/or EMT status will allow for a greater number of patients to benefit from a personalized medicine approach to combating disease progression and improving outcomes.

1.8 Overall Hypothesis and Thesis Objectives

The *overall hypothesis* of this thesis is that dynamic EMT processes enhance CTC generation and metastasis in prostate cancer, yet reduce the effectiveness of epithelial-based CTC technologies.

In order to test this hypothesis, the specific objectives of this thesis are:

1. Optimize and validate EMT-independent approaches for CTC analysis of blood samples from humans and pre-clinical mouse models.
2. Investigate the value of a clinically relevant, EMT-independent CTC analysis platform in prostate cancer patients at different disease progression stages.
3. Modify EMT phenotype of prostate cancer cells and determine the functional impact on metastasis biology.

1.9 References

1. Institute NC. Cancer Statistics. <https://www.cancer.gov/about-cancer/understanding/statistics>. Published 2017. Accessed February 7, 2018.
2. Hanahan D, Weinberg RA. Review Hallmarks of Cancer : The Next Generation. *Cell*. 2011;144(5):646-674. doi:10.1016/j.cell.2011.02.013
3. Macleod K. Tumor suppressor genes. *Curr Opin Genet Dev*. 2000;10(1):81-93. doi:10.1016/S0959-437X(99)00041-6
4. National Cancer Institute. <https://www.cancer.gov>. Accessed June 17, 2019.
5. Marieb, Wilhelm, Mallatt. *Human Anatomy Eighth Edition*. Pearson; 2017.
6. Kirby R, Christmas T, Brawer M. *Prostate Cancer Second Edition.*; 2001.
7. Perdana NR, Mochtar CA, Umbas R, Hamid ARA. The Risk Factors of Prostate Cancer and Its Prevention: A Literature Review. *Acta Med Indones*. 2016;48(3):228-238.
8. Siegel RL, Miller KD, Jemal A. Cancer statistics, 2020. *CA Cancer J Clin*. 2020. doi:10.3322/caac.21590
9. Society AC. Breast Cancer Survival Rates. <https://www.cancer.org/cancer/breast-cancer/understanding-a-breast-cancer-diagnosis/breast-cancer-survival-rates.html>. Published 2017. Accessed February 7, 2018.
10. Chambers AF, Groom AC, MacDonald IC. Dissemination and growth of cancer cells in metastatic sites. *Nat Rev Cancer*. 2002;2(8):563-572. doi:10.1038/nrc865
11. Mehlen P, Puisieux A. Metastasis: A question of life or death. *Nat Rev Cancer*. 2006;6(6):449-458. doi:10.1038/nrc1886
12. Society AC. Survival Rates for Prostate Cancer. <https://www.cancer.org/cancer/prostate-cancer/detection-diagnosis-staging/survival-rates.html>. Published 2017. Accessed February 7, 2018.
13. Poulsen MH, Petersen H, Høilund-Carlsen PF, et al. Spine metastases in prostate cancer: Comparison of technetium-99m-MDP whole-body bone scintigraphy, [18F]choline positron emission tomography(PET)/computed tomography (CT) and [18F]NaF PET/CT. *BJU Int*. 2014;114(6):818-823. doi:10.1111/bju.12599
14. Crawford ED. Understanding the Epidemiology, Natural History, and Key Pathways Involved in Prostate Cancer. *Urology*. 2009;73(5 SUPPL.):S4. doi:10.1016/j.urology.2009.03.001
15. Staff MC. Prostatectomy.

16. Society AC. Hormone Therapy for Prostate Cancer.
17. Tewari A, Whelan P, Graham J. *Prostate Cancer: Diagnosis and Clinical Management*. John Wiley & Sons, Ltd.; 2014.
18. Cancer.Net. Prostate Cancer: Diagnosis. www.cancer.net. Accessed June 17, 2019.
19. Clinic M. PSA Test.
20. Beer TM, Lemmon D, Lowe BA, Henner WD. High-dose weekly oral calcitriol in patients with a rising PSA after prostatectomy or radiation for prostate carcinoma. *Cancer*. 2003;97(5):1217-1224. doi:10.1002/cncr.11179
21. Stephenson RA, Dinney CP, Gohji K, Ordóñez NG, Killion JJ, Fidler IJ. Metastatic model for human prostate cancer using orthotopic implantation in nude mice. *J Natl Cancer Inst*. 1992;84(12):951-957. doi:10.1093/jnci/84.12.951
22. Cancer.Net. Prostate Cancer: Stages and Grades.
23. Epstein J. *The Gleason Grading System [Electronic Resource] : A Complete Guide for Pathologists and Clinicians*. Ovid Technologies, Inc.; 2013.
24. Epstein JI, Zelefsky MJ, Sjoberg DD, et al. A Contemporary Prostate Cancer Grading System: A Validated Alternative to the Gleason Score. *Eur Urol*. 2016;69(3):428-435. doi:10.1016/j.eururo.2015.06.046
25. Alchin DR, Murphy D, Lawrentschuk N. What are the predictive factors for gleason score upgrade following RP? *Urol Int*. 2016;96(1):1-4. doi:10.1159/000439139
26. Mazzocca A, Carloni V. The metastatic process: methodological advances and pharmacological challenges. *Curr Med Chem*. 2009;16(14):1704-1717. doi:http://dx.doi.org/10.2174/092986709788186192
27. Cancer P. *Ablin, R. J. & Mason, M. D. in Metastasis of Prostate Cancer (Mason, 1) 1-405 (Springer Netherlands, 2007)*. <http://link.springer.com/10.1007/978-1-4020-5847-9>.
28. Van Zijl F, Krupitza G, Mikulits W. Initial steps of metastasis: Cell invasion and endothelial transmigration. *Mutat Res - Rev Mutat Res*. 2011;728(1-2):23-34. doi:10.1016/j.mrrev.2011.05.002
29. Albanese C, Rodriguez OC, VanMeter J, et al. Preclinical magnetic resonance imaging and systems biology in cancer research: current applications and challenges. *Am J Pathol*. 2013;182(2):312-318. doi:10.1016/j.ajpath.2012.09.024
30. Auerbach R. Patterns of tumor metastasis: organ selectivity in the spread of cancer cells. *Lab Invest*. 1988;58(4):361-364. <http://www.ncbi.nlm.nih.gov/pubmed/3282122>.
31. Kalluri R, Weinberg RA. The basics of epithelial-mesenchymal transition. *J Clin Invest*.

- 2009;119(6):1420-1428. doi:10.1172/JCI39104
32. Zhang Y, Xu L, Li A, Han X. The roles of ZEB1 in tumorigenic progression and epigenetic modifications. *Biomed Pharmacother.* 2019;110(November 2018):400-408. doi:10.1016/j.biopha.2018.11.112
 33. Bery F, Figiel S, Kouba S, et al. Hypoxia promotes prostate cancer aggressiveness by upregulating EMT-activator Zeb1 and SK3 channel expression. *Int J Mol Sci.* 2020;21(13):1-10. doi:10.3390/ijms21134786
 34. Yao D, Dai C, Peng S. Mechanism of the Mesenchymal-Epithelial Transition and Its Relationship with Metastatic Tumor Formation. *Mol Cancer Res.* 2011. doi:10.1158/1541-7786.mcr-10-0568
 35. Chao Y, Wu Q, Acquafondata M, Dhir R, Wells A. Partial mesenchymal to epithelial reverting transition in breast and prostate cancer metastases. *Cancer Microenviron.* 2012;5(1):19-28. doi:10.1007/s12307-011-0085-4
 36. Saitoh M. JB special review-cellular plasticity in epithelial homeostasis and diseases: Involvement of partial EMT in cancer progression. *J Biochem.* 2018;164(4):257-264. doi:10.1093/jb/mvy047
 37. Sinha D, Saha P, Samanta A, Bishayee A. Emerging concepts of hybrid epithelial-to-mesenchymal transition in cancer progression. *Biomolecules.* 2020;10(11):1-22. doi:10.3390/biom10111561
 38. Lowes LE, Goodale D, Xia Y, et al. Epithelial-to-mesenchymal transition leads to disease-stage differences in circulating tumor cell detection and metastasis in pre-clinical models of prostate cancer. *Oncotarget.* 2016. doi:10.18632/oncotarget.12682
 39. Rigau M, Oliván M, Garcia M, et al. The present and future of prostate cancer urine biomarkers. *Int J Mol Sci.* 2013;14(6):12620-12649. doi:10.3390/ijms140612620
 40. Andree KC, van Dalum G, Terstappen LWMM. Challenges in circulating tumor cell detection by the CellSearch system. *Mol Oncol.* 2016;10(3):395-407. doi:10.1016/j.molonc.2015.12.002
 41. Huang X, Gao P, Song Y, et al. Meta-analysis of the prognostic value of circulating tumor cells detected with the CellSearch System in colorectal cancer. *BMC Cancer.* 2015;15(1). doi:10.1186/s12885-015-1218-9
 42. Mu Z, Benali-Furet N, Uzan G, et al. Detection and characterization of circulating tumor associated cells in metastatic breast cancer. *Int J Mol Sci.* 2016;17(10). doi:10.3390/ijms17101665
 43. de Bono JS, Scher HI, Montgomery RB, et al. Circulating tumor cells predict survival benefit from treatment in metastatic castration-resistant prostate cancer. *Clin Cancer Res.* 2008;14(19):6302-6309. doi:10.1158/1078-0432.CCR-08-0872

44. Goldkorn A, Ely B, Quinn DI, et al. Circulating tumor cell counts are prognostic of overall survival in SWOG S0421: A phase III trial of docetaxel with or without atrasentan for metastatic castration-resistant prostate cancer. *J Clin Oncol*. 2014;32(11):1136-1142. doi:10.1200/JCO.2013.51.7417
45. Lee SJ, Lee J, Kim ST, et al. Circulating tumor cells are predictive of poor response to chemotherapy in metastatic gastric cancer. *Int J Biol Markers*. 2015;30(4):e382-e386. doi:10.5301/jbm.5000151
46. Qiao Y-Y, Lin K-X, Zhang Z, et al. Monitoring disease progression and treatment efficacy with circulating tumor cells in esophageal squamous cell carcinoma: A case report. *World J Gastroenterol*. 2015;21(25):7921-7928. doi:10.3748/wjg.v21.i25.7921
47. Bredemeier M, Edimiris P, Mach P, et al. Gene expression signatures in circulating tumor cells correlate with response to therapy in metastatic breast cancer. *Clin Chem*. 2017;63(10):1585-1593. doi:10.1373/clinchem.2016.269605
48. Görner K, Bachmann J, Holzhauer C, et al. Genetic analysis of circulating tumor cells in pancreatic cancer patients: A pilot study. *Genomics*. 2015;106(1):7-14. doi:10.1016/j.ygeno.2015.02.003
49. Williams S. Not all tumor cells are equal: Study reveals genetic diversity in cells shed by tumors.
50. Allan AL, Keeney M. Circulating tumor cell analysis: Technical and statistical considerations for application to the clinic. *J Oncol*. 2010;2010. doi:10.1155/2010/426218
51. Alunni-Fabbroni M, Sandri MT. Circulating tumour cells in clinical practice: Methods of detection and possible characterization. *Methods*. 2010;50(4):289-297. doi:10.1016/j.ymeth.2010.01.027
52. Lowes LE, Allan AL. Recent advances in the molecular characterization of circulating tumor cells. *Cancers (Basel)*. 2014;6(1):595-624. doi:10.3390/cancers6010595
53. Lianidou ES, Markou A. Circulating tumor cells in breast cancer: Detection systems, molecular characterization, and future challenges. *Clin Chem*. 2011;57(9):1242-1255. doi:10.1373/clinchem.2011.165068
54. Yu M, Stott S, Toner M, Maheswaran S, Haber DA. Circulating tumor cells: Approaches to isolation and characterization. *J Cell Biol*. 2011;192(3):373-382. doi:10.1083/jcb.201010021
55. Biosciences F. IsoFlux CTC Enrichment and Analysis Kit.
56. Peeters DJE, De Laere B, Van Den Eynden GG, et al. Semiautomated isolation and molecular characterisation of single or highly purified tumour cells from CellSearch enriched blood samples using dielectrophoretic cell sorting. *Br J Cancer*. 2013;108(6):1358-1367. doi:10.1038/bjc.2013.92

57. Abonnenc M, Manaresi N, Borgatti M, et al. Programmable interactions of functionalized single bioparticles in a dielectrophoresis-based microarray chip. *Anal Chem.* 2013;85(17):8219-8224. doi:10.1021/ac401296m
58. Luca F De, Rotunno G, Salvianti F, et al. Mutational analysis of single circulating tumor cells by next generation sequencing in metastatic breast cancer. *Oncotarget.* 2016;7(18):26107-26119. doi:10.18632/oncotarget.8431
59. Werner SL, Graf RP, Landers M, et al. Analytical Validation and Capabilities of the Epic CTC Platform: Enrichment-Free Circulating Tumour Cell Detection and Characterization. *J Circ Biomarkers.* 2015;1. doi:10.5772/60725
60. Sciences E. CTC Detection and Characterization Platform. <https://www.epicsciences.com/platform/ctc-detection-characterization>. Published 2018. Accessed March 29, 2018.
61. Goodale D, Phay C, Postenka CO, Keeney M, Allan AL. Characterization of tumor cell dissemination patterns in preclinical models of cancer metastasis using flow cytometry and laser scanning cytometry. *Cytom Part A.* 2009;75A(4):344-355. doi:10.1002/cyto.a.20657
62. Fan ZC, Yan J, Liu G Da, et al. Real-time monitoring of rare circulating hepatocellular carcinoma cells in an orthotopic model by in vivo flow cytometry assesses resection on metastasis. *Cancer Res.* 2012;72(10):2683-2691. doi:10.1158/0008-5472.CAN-11-3733
63. Baccelli I, Schneeweiss A, Riethdorf S, et al. Identification of a population of blood circulating tumor cells from breast cancer patients that initiates metastasis in a xenograft assay. *Nat Biotechnol.* 2013;31(6):539-544. doi:10.1038/nbt.2576
64. Vishnoi M, Peddibhotla S, Yin W, et al. The isolation and characterization of CTC subsets related to breast cancer dormancy. *Sci Rep.* 2015;5. doi:10.1038/srep17533
65. Zhang L, Ridgway LD, Wetzel MD, et al. The identification and characterization of breast cancer CTCs competent for brain metastasis. *Sci Transl Med.* 2013;5(180). doi:10.1126/scitranslmed.3005109
66. Kang Y, Pantel K. Tumor Cell Dissemination: Emerging Biological Insights from Animal Models and Cancer Patients. *Cancer Cell.* 2013;23(5):573-581. doi:10.1016/j.ccr.2013.04.017
67. Allan AL, Vantuyghem S a, Tuck AB, Chambers AF, Chin-Yee IH, Keeney M. Detection and quantification of circulating tumor cells in mouse models of human breast cancer using immunomagnetic enrichment and multiparameter flow cytometry. *Cytometry A.* 2005;65(1):4-14. doi:10.1002/cyto.a.20132
68. Lowes LE, Goodale D, Keeney M, Allan AL. *Image Cytometry Analysis of Circulating Tumor Cells.* Vol 102.; 2011. doi:10.1016/B978-0-12-374912-3.00010-9

Chapter 2

2 EMT- independent detection of circulating tumor cells in human blood samples and pre-clinical mouse models of metastasis

A version of this chapter has been published:

Jenna Kitz, David Goodale, Carl Postenka, Lori E. Lowes, and Alison L. Allan. EMT-independent detection of circulating tumor cells in human blood samples and pre-clinical mouse models of metastasis. *Clin. Exp. Metastasis*. 2021; 38:97-108.

Abstract

Circulating tumor cells (CTCs) present an opportunity to detect/monitor metastasis throughout disease progression. The CellSearch® is currently the only FDA-approved technology for CTC detection in patients. The main limitation of this system is its reliance on epithelial markers for CTC isolation/enumeration, which reduces its ability to detect more aggressive mesenchymal CTCs that are generated during metastasis via epithelial-to-mesenchymal transition (EMT). This Technical Note describes and validates two EMT-independent CTC analysis protocols; one for human samples using Parsortix® and one for mouse samples using VyCap. Parsortix® identifies significantly more mesenchymal human CTCs compared to the clinical CellSearch® test, and VyCap identifies significantly more CTCs compared to our mouse CellSearch® protocol regardless of EMT status. Recovery and downstream molecular characterization of CTCs is highly feasible using both Parsortix® and VyCap. The described CTC protocols can be used by investigators to study CTC generation, EMT and metastasis in both pre-clinical models and clinical samples.

2.1 Introduction

Cancer is the second leading cause of death in the United States; with over 600,000 Americans dying from this disease in 2020¹. It is estimated that up to 90% of cancer-related deaths are due to metastasis, the spread of disease to other sites in the body². This is because current therapies are non-curative against these aggressive cancers. The process of metastasis has been shown to be associated with an epithelial-to-mesenchymal transition (EMT)³. During the EMT process, a polarized epithelial cell undergoes morphological and molecular changes that enable it to gain a mesenchymal phenotype⁴; characterized by a greater migratory capacity, increased invasiveness, and elevated resistance to apoptosis⁵. During metastasis and associated EMT, tumor cells can shed

from the primary tumor and disseminate throughout the body as circulating tumor cells (CTCs) in the bloodstream⁶. The presence and molecular characteristics of CTCs in patients have been correlated with increased metastatic disease, reduced survival, and therapy response/resistance⁷⁻¹⁰.

Although EMT has been shown to be associated with increased metastasis and CTC generation, many technologies used to detect CTCs rely on epithelial characteristics¹¹. For example, CellSearch® (Menarini Silicon Biosystems) is currently the only CTC assay approved by the U.S. Food and Drug Administration for clinical CTC analysis^{7,8,12}. CellSearch® distinguishes CTCs from leukocytes through immunomagnetic selection of cells with an EpCAM⁺ (epithelial cell adhesion molecule) phenotype followed by differential fluorescent staining for cytokeratins (CK) 8/18/19, CD45 (leukocyte marker), and DNA (4',6-diamidino-2-phenylindole [DAPI]). Despite being considered the “gold standard” clinical CTC platform^{7,8,12}, previous studies have shown that in some diseases such as prostate cancer, CTCs are undetectable in ~30% of patients despite the presence of widespread metastatic disease¹³. While it is possible that CTCs are truly not present in one third of prostate cancer patients with metastasis, it is more likely that CTCs are present but not detected by the CellSearch® system. This may be because they do not meet the standard CTC definition (EpCAM⁺/CK⁺/DAPI⁺/CD45⁻) due to EMT and associated downregulation of epithelial markers^{14,15}.

Importantly, several studies have demonstrated that CTCs with a purely mesenchymal phenotype are undetectable by CellSearch®, but that the presence of mesenchymal marker expression on CTCs with a hybrid epithelial-mesenchymal phenotype is indicative of poor prognosis¹⁵⁻¹⁹. We have previously described the use of this epithelial-based system in capturing both human and mouse CTCs^{20,21} and demonstrated that a CellSearch®-based assay failed to detect a significant number (~40-50%) of mesenchymal CTCs. Notably, the CellSearch®-based assay captured the majority of CTCs shed during early-stage disease *in vivo*, and only after the establishment of metastases were a significant number of undetectable CTCs present¹¹. Taken together, this suggests that current clinical assays may be limiting our ability to capitalize on the full potential of CTCs, and that additional technologies that do not rely on epithelial characteristics should be explored.

The Parsortix® system (Angle PLC) is a sized-based microfluidics platform that allows for recovery of relatively pure populations of CTCs for downstream molecular analysis based on CTC size and deformability, and is thus independent of EMT status²². Whole blood is processed through a filtration cartridge etched with microchannels that are 6.5-10µm wide²⁰. Using microfluidics, CTCs (>8µm) are isolated within the cartridge and stained with immunofluorescent antibodies²⁰. The VyCap system (VyCap B.V.) is a sized-based CTC isolation and enumeration platform which uses a pump unit to process whole blood through a disposable filter cartridge^{23,24}. CTCs are captured on top of the microsieve which has 160,000 pores; each 5µm in diameter^{23,24}. The VyCap allows for recovery of CTCs based on CTC size rather than epithelial cell characteristics²⁴ and is thus similar to the Parsortix® in providing the potential for an EMT-independent approach to CTC capture and analysis.

The purpose of this Technical Note is to describe and validate two EMT-independent CTC isolation/enumeration protocols that we have developed for unbiased analysis of CTCs in human blood samples (using Parsortix®) and pre-clinical mouse models of metastasis (using VyCap). We also provide a summary of advantages/disadvantages and technical considerations that metastasis researchers may find valuable for application of these methods to studies in the areas of CTCs, EMT, and cancer progression.

2.2 Materials and methods

2.2.1 Cell Culture and Labeling

Epithelial human MDA-MB-468²⁵ breast cancer cells (American Type Culture Collection [ATCC], Manassas, VA) were cultured in minimum essential medium (MEM)- α + 10% fetal bovine serum (FBS). Mesenchymal human PC-3²⁶ prostate cancer cells (ATCC) were cultured in F12-K media + 10% FBS. Cell lines were authenticated via third-party testing (IDEXX, Columbia, MO). Media and reagents were obtained from Life Technologies (Carlsbad, CA), and FBS from Sigma (St. Louis, MO). For baseline recovery experiments, MDA-MB-468 cells were stained with the CellTrace™ carboxyfluorescein succinimidyl ester (CFSE) Cell Proliferation Kit (Invitrogen, Waltham, MA). Dimethyl sulfoxide (DMSO; 18µL) was added to one CellTrace™ tube. Dissolved CellTrace™ was added directly to cells suspended in phosphate-buffered saline (PBS) at a concentration of 1:1000. Cells + CellTrace™ were incubated for 20 min at 37°C, 5% CO₂. After

incubation, an equal amount of cell culture media was added to the mixture to stop the staining reaction and cells were incubated for a further 5 min. Cells were centrifuged, supernatant was discarded, and cells were resuspended in PBS for counting and spiking into whole blood as described below.

2.2.2 Blood Collection and Tumor Cell Spiking

For human subjects, 2 x 10mL of whole blood was collected in CellSave preservation tubes (Menarini Silicon Biosystems, Huntingdon Valley, PA). For mice, whole blood (150 μ L) was drawn from male athymic nude mice (Harlan Sprague- Dawley, Indianapolis, IN) via cardiac puncture at endpoint as previously described¹¹. Blood was collected into ethylenediaminetetraacetic acid (EDTA) microtubes (Becton Dickinson, Mississauga, ON) and separated into two aliquots of 50 μ L to be analyzed by each CTC assay. For cell spiking and recovery experiments, unlabeled or prelabeled PC-3 and MDA-MB-468 cells were grown to approximately 80% confluence and harvested using either 0.25% Trypsin/EDTA or 0.25% Trypsin (ThermoFisher Scientific, Waltham, MA) respectively. Cells were counted by hemocytometer and serially diluted using PBS to concentrations of 1000, 100, 10, or 5 cells/10 μ L prior to spiking into matched whole blood samples (7.5mL human; 50 μ L mouse).

2.2.3 CTC Analysis

2.2.3.1 CellSearch®

For human samples, 7.5mL of whole blood was processed on the CellSearch® Autoprep system using the CellSearch® CTC kit (Menarini Silicon Biosystems), analyzed on the CellSearch® Analyzer, and assessed for the presence of CTCs as previously described¹¹. For mouse samples, 50 μ L of whole blood was incubated with components of the CellSearch® CTC kit including anti-EpCAM ferrofluid (25 μ L), Capture Enhancement Reagent (25 μ L), Nucleic Acid Dye (50 μ L), Staining Reagent (50 μ L), Permeabilization Reagent (100 μ L), as well as anti-mouse CD45-APC (1.5 μ L) (eBiosciences, San Diego, CA) as described previously¹¹. Samples were manually immuno-magnetically separated and transferred to a CellSearch® MagNest™ cartridge for analysis using the CellSearch® Analyzer. In all cases, cells displaying the phenotype of EpCAM⁺/CK⁺/DAPI⁺/CD45⁻ cells with a round/oval morphology were classified as CTCs.

2.2.3.2 Parsortix®

Whole human blood (7.5mL) was processed on the EMT-independent Parsortix® using 6.5µm cartridges (Angle PLC, Surrey, UK). Cartridges were stained using a combination of 20µL anti-human EpCAM-PE (Becton Dickinson), 10µL anti-human N-Cadherin-PE (eBiosciences), 20µL anti-human CD45 AlexaFluor-488 (Becton Dickinson), and 5µL of DAPI (Life Technologies). Cells displaying the phenotype of EpCAM⁺/DAPI⁺/CD45⁻ or N-Cadherin⁺/DAPI⁺/CD45⁻ with a round intact morphology were considered CTCs. Identified CTCs were manually counted on the cartridge using an AX70 microscope (Olympus, Tokyo, JA).

2.2.3.3 VyCap

For the EMT-independent VyCap CTC assay, 3.5µL of Transfix (Caltag MedSystems, Buckingham, EN) was added to each spiked 50µL mouse blood sample and incubated at room temperature for 24-48 hrs. Samples were then incubated for 20 min each with a primary monoclonal anti-human HLA anti-FITC antibody (5µL, Sigma, Darmstadt, DE), followed by a secondary oligoclonal anti-rabbit unconjugated anti-FITC antibody (5µL, Thermofisher), tertiary goat anti-rabbit IgG secondary AlexaFluor-488 antibody (5µL, Invitrogen), and monoclonal anti-mouse CD45-PE antibody (10µL, Invitrogen) with 2x washing with PBS + 0.5% BSA (BioShop LifeScience Products, Burlington, ON) between each antibody step. Samples were then processed through the VyCap microsieve on the PU-250 pump unit (VyCap, Enschede, NL). Vectashield (5µL) antifade mounting media with DAPI (Vector Laboratories, Burlingame, CA) was added to the top and bottom of each microsieve prior to being covered with custom cover glass slips (VyCap). Cells displaying the phenotype of HLA⁺/DAPI⁺/CD45⁻ cells with intact round morphology were considered to be CTCs. Identified CTCs were manually counted on the microseives using an AX70 microscope and an LUCPLFLN UPlanFLN 20x Microscope Objective (Olympus).

2.2.4 *In Vivo* Metastasis Studies

Prostate cancer cells were prepared in sterile Hank's buffered saline (Life Technologies) and injected (1×10^6 cells/40µL per mouse) orthotopically into 6-8 week old male athymic nude mice (Harlan Sprague-Dawley) via the right dorsolateral lobe of the prostate as described previously¹¹. Prostate cancer tumor growth and progression to metastasis was allowed to develop for 9 weeks.

At endpoint, blood (150 μ L) was collected and analyzed for CTCs as described above. Tissues (primary tumors and distant organs) were harvested and formalin-fixed, paraffin-embedded, sectioned (4 μ m) and stained with hematoxylin and eosin (H&E).

2.2.5 CTC Characterization

2.2.5.1 CTC Harvesting

After CTC enumeration on VyCap microseives, coverslips were removed and 50 μ L of lysis/binding buffer from the Dynabeads® mRNA Purification Kit (Thermofisher) was added directly onto microseives. CTCs were lysed via manual pipetting up and down before transfer to 1.5mL RNase/DNase-free microtubes (Diamed, Mississauga, ON). This was repeated twice to ensure total lysis and capture of RNA from all CTCs on each microsieve. For the Parsortix®, cells were collected via the platform's "harvest protocol" into 1.5mL RNase/DNase-free microtubes (Diamed). CTCs were centrifuged at 700 x g for 10 min, supernatants were discarded without disturbing the pellet, and CTCs were lysed via manual pipetting using 50 μ l lysis/binding buffer as described above. Harvested CTCs in lysis/binding buffer were stored at -80°C prior to analysis as described below.

2.2.5.2 Quantitative Real-Time PCR Analysis

The RNA collected from harvested CTCs was eluted using the Dynabeads® mRNA Purification Kit protocol (Thermofisher) and reverse transcribed using SuperScript™ IV VILO™ Master Mix (Invitrogen) on a T100 Thermal Cycler (BioRad). Samples were then subjected to quantitative reverse transcription polymerase chain reactions (RT-qPCR) using Advanced qPCR MasterMix (Wisent Bioproducts, St.Bruno, QC) on a Stratagene Mx3000P qPCR system (Life Technologies) using primers described in **Table 2.1**. mRNA values from recovered cells were compared to matched controls of the same number of cells directly from cell culture. GAPDH was used as a reference gene.

2.2.6 Statistical Analysis

Statistical analysis was performed using GraphPad Prism 7 for MacOS Mojave (La Jolla, CA). Data is presented as mean \pm standard error of the mean (SEM). Paired t-tests were used to analyze

Table 2-1. Forward and reverse primers used for RT-qPCR analysis

Target Gene	Forward Primer (5'→3')	Reverse Primer (5'→3')
E-Cadherin	TGCTGATGCCCCCAATACCCCA	GTGATTTCTGGCCCACGCCAA
EpCAM	CGACTTTTGCCGCAGCTCAGGA	GGGCCCCTTCAGGTTTTGCTCT
N-Cadherin	TGACTCCAACGGGGACTGCACA	AGCTCAAGGACCCAGCAGTGGA
Vimentin	AACCAACGACAAAGCCCGCGTC	TTCCGGTTGGCAGCCTCAGAGA
GAPDH	TCCATGGCACCGTCAAGGCTGA	GCCAGCATCGCCCCACTTGATT

differences between matched samples. For all experiments, $p \leq 0.05$ was considered statistically significant.

2.3 Results

2.3.1 The Parsortix® and CellSearch® platforms provide similar recovery of epithelial CTCs in human blood samples, but Parsortix® is superior for recovering mesenchymal CTCs

In order to detect innate differences in capture between the Parsortix® and CellSearch® CTC technologies for human samples, we first pre-stained epithelial MDA-MB-468 human breast cancer cells and spiked either 5, 10, 100, or 1000 cells into 7.5mL of whole human blood. We then enriched for CTCs using the clinical CellSearch® human protocol (with the added GFP channel to identify pre-stained cells), and Parsortix® (without the staining protocol) in matched samples. We observed that baseline recovery for CTCs in human blood was not significantly different between the two systems (**Figure 2.1a,b** and **Table 2.2**). We next wanted to determine differences in CTC recovery in human blood when enumerating epithelial versus mesenchymal CTCs using the clinical epithelial-dependent CellSearch® staining protocol (DAPI⁺/CK-PE⁺/CD45⁻), and our developed epithelial-independent Parsortix® staining protocol (DAPI⁺/EpCAM⁺ or N-Cadherin⁺/CD45⁻). We spiked 5, 10, 100, or 1000 unstained human MDA-MB-468 breast cancer cells (epithelial phenotype) or human PC-3 prostate cancer cells (mesenchymal phenotype) into whole human blood and analyzed CTCs using the two technologies in matched samples. We observed that overall recovery of epithelial CTCs in human blood was not significantly different between the two systems (**Figure. 2.1c,d** and **Table 2.2**), but when assessing cell recovery based on serial numbers of expected cells, CellSearch® was able to enumerate significantly more epithelial CTCs in the cell group of 1000 expected cells compared to Parsortix® ($p \leq 0.05$) (**Figure 2.1d** and **Table 2.2**). However, recovery of mesenchymal CTCs in human blood was significantly higher using Parsortix® ($54.9 \pm 4.7\%$) compared to CellSearch® ($39.5 \pm 3.5\%$) ($p \leq 0.05$) (**Figure 2.1e,f** and **Table 2.2**). Parsortix® was also able to enumerate significantly more CTCs in the 100 and 1000 cell groups compared to CellSearch® ($p \leq 0.05$) (**Figure 2.1f** and **Table 2.2**). Representative images of positive CTCs isolated using CellSearch® and Parsortix® are shown in **Supplemental Figure 1.1**. Taken together, these results indicate that while Parsortix® and CellSearch® provide equivalent recovery of epithelial CTCs in human blood samples, Parsortix® is superior for recovery of mesenchymal CTCs.

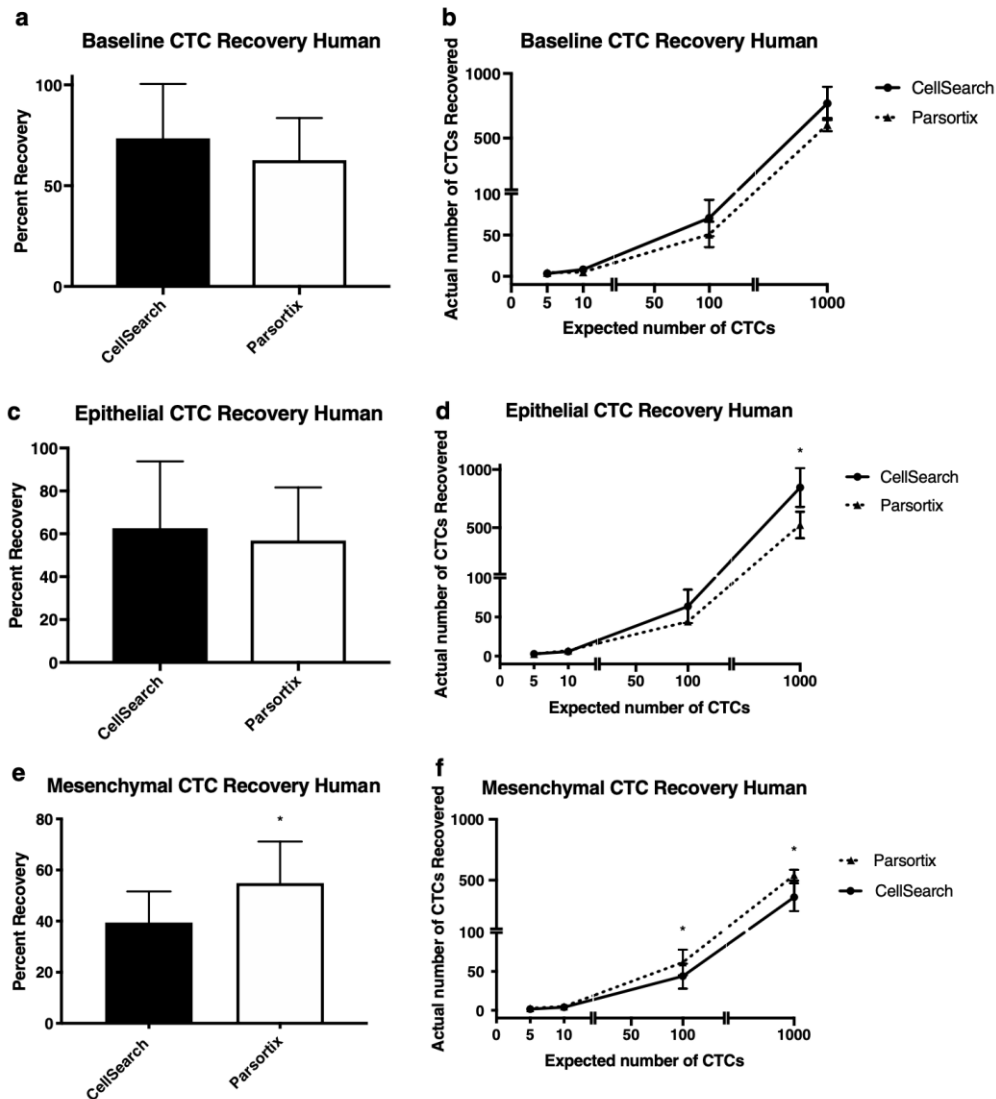


Figure 2.1. The Parsortix® and CellSearch® CTC platforms provide equivalent recovery of epithelial CTCs in human blood samples, but Parsortix® is superior for recovery of mesenchymal CTCs. Epithelial MDA-MB-468 human breast cancer cells or mesenchymal PC-3 human prostate cancer cells were spiked into whole human blood (5, 10, 100, or 1000 cells per 7.5 ml/blood) and recovered using the human protocols for CellSearch® (epithelial-dependent) or Parsortix® (EMT-independent). (a-b) Pre-stained (CellTrace™) epithelial MDA-MB-468 human breast cancer cells spiked into human blood; (c-d) Epithelial MDA-MB-468 human breast cancer cells and (e-f) Mesenchymal PC-3 human prostate cancer cells spiked into human blood and stained using the human CellSearch® or Parsortix® protocols. Data are presented as mean ± SEM (n ≥ 3), * = significantly different than CellSearch® (p ≤ 0.05)

Table 2-2. CTC recovery in spiked human blood samples using Parsortix® versus CellSearch®

Cell Type	Number of Cells Spiked	Cells Recovered (Parsortix®)	Cells Recovered (CellSearch®)	P-Value
Baseline (Pre-stained MDA-MB-468)	5	4.4 ± 0.1 (88%)	3.3 ± 1.0 (66%)	0.4226
	10	5.1 ± 1.5 (51%)	8.0 ± 2.1 (80%)	0.1994
	100	50.5 ± 7.8 (50%)	70.4 ± 11.0 (70%)	0.0989
	1000	604.2 ± 25.4 (60%)	768.6 ± 64.9 (77%)	0.1213
Epithelial (MDA-MB-468)	5	2.8 ± 0.45 (56%)	3.3 ± 1.5 (66%)	0.6349
	10	7.3 ± 2.4 (73%)	5.8 ± 0.5 (58%)	0.6968
	100	44.5 ± 1.6 (45%)	63.9 ± 10.8 (64%)	0.2236
	1000	547.7 ± 43.9 (55%)	846.4 ± 83.6 (85%)	0.0417*
Mesenchymal (PC-3)	5	2.9 ± 0.7 (58%)	1.8 ± 0.4 (36%)	0.2254
	10	4.6 ± 0.9 (46%)	4.2 ± 0.6 (42%)	0.2254
	100	61.7 ± 8.5 (62%)	43.9 ± 8.0 (44%)	0.0489*
	1000	540.6 ± 23.0 (54%)	362.0 ± 57.2 (36%)	0.0473*

2.3.2 The VyCap CTC platform provides enhanced recovery of epithelial and mesenchymal CTCs in mouse blood samples compared to CellSearch®

In order to compare CTC capture between the VyCap and CellSearch® technologies for mouse blood samples, we first pre-stained epithelial MDA-MB-468 human breast cancer cells and spiked either 5, 10, 100, or 1000 cells into 50 μ L of whole mouse blood. We then enriched for CTCs using our previously developed CellSearch® mouse protocol (with the added GFP channel to identify pre-stained cells), and the VyCap (without the staining protocol) in matched samples. We observed that baseline recovery for CTCs in mouse blood was significantly higher with VyCap ($71.9 \pm 3.4\%$) compared to CellSearch® ($33.9 \pm 6.3\%$) ($p \leq 0.05$; **Figure 2.2a** and **Table 2.3**). When assessing cell recovery based on serial numbers of expected CTCs, VyCap was able to enumerate significantly more CTCs in cell groups of 5, 100, and 1000 expected cells compared CellSearch® in matched samples ($p \leq 0.05$) (**Figure 2.2b** and **Table 2.3**). We next wanted to determine differences in CTC recovery in mouse blood from the perspective of isolation based on an epithelial versus a mesenchymal cell phenotype. To investigate this, we compared the CellSearch® staining protocol (DAPI⁺/CK⁻PE⁺/CD45⁻) versus an epithelial-independent VyCap staining protocol (DAPI⁺/HLA⁺/CD45⁻) that we developed for this study. We spiked 5, 10, 100, or 1000 unstained human MDA-MB-468 cells breast cancer cells (epithelial phenotype) or human PC-3 prostate cancer cells (mesenchymal phenotype) into whole mouse blood and analyzed CTCs using the two technologies in matched samples. We observed that recovery of epithelial MDA-MB-468 human CTCs in mouse blood was significantly higher using VyCap ($79.9 \pm 6.2\%$) compared to CellSearch® ($27.7 \pm 10.2\%$) ($p \leq 0.05$) (**Figure 2.2c** and **Table 2.3**). When assessing cell recovery based on serial numbers of expected cells, VyCap was able to enumerate significantly more epithelial CTCs in cell groups of 10, 100, and 1000 expected cells compared to CellSearch® ($p \leq 0.05$) (**Figure 2.2d** and **Table 2.3**). The difference between CTC platforms was even more marked when assessing the recovery of mesenchymal human CTCs in mouse blood, which was significantly higher using VyCap ($65.3 \pm 6.5\%$) compared to CellSearch® ($14.3 \pm 5.4\%$) ($p \leq 0.05$) (**Figure 2.2e,f** and **Table 2.3**). VyCap was able to enumerate significantly more mesenchymal CTCs in cell groups of 10, 100, and 1000 expected cells compared to CellSearch® ($p \leq 0.05$) (**Figure 2.2f** and **Table 2.3**). Representative images of positive CTCs isolated using CellSearch® and VyCap in each technical condition are shown in **Supplemental Figure 2.2**. Taken together,

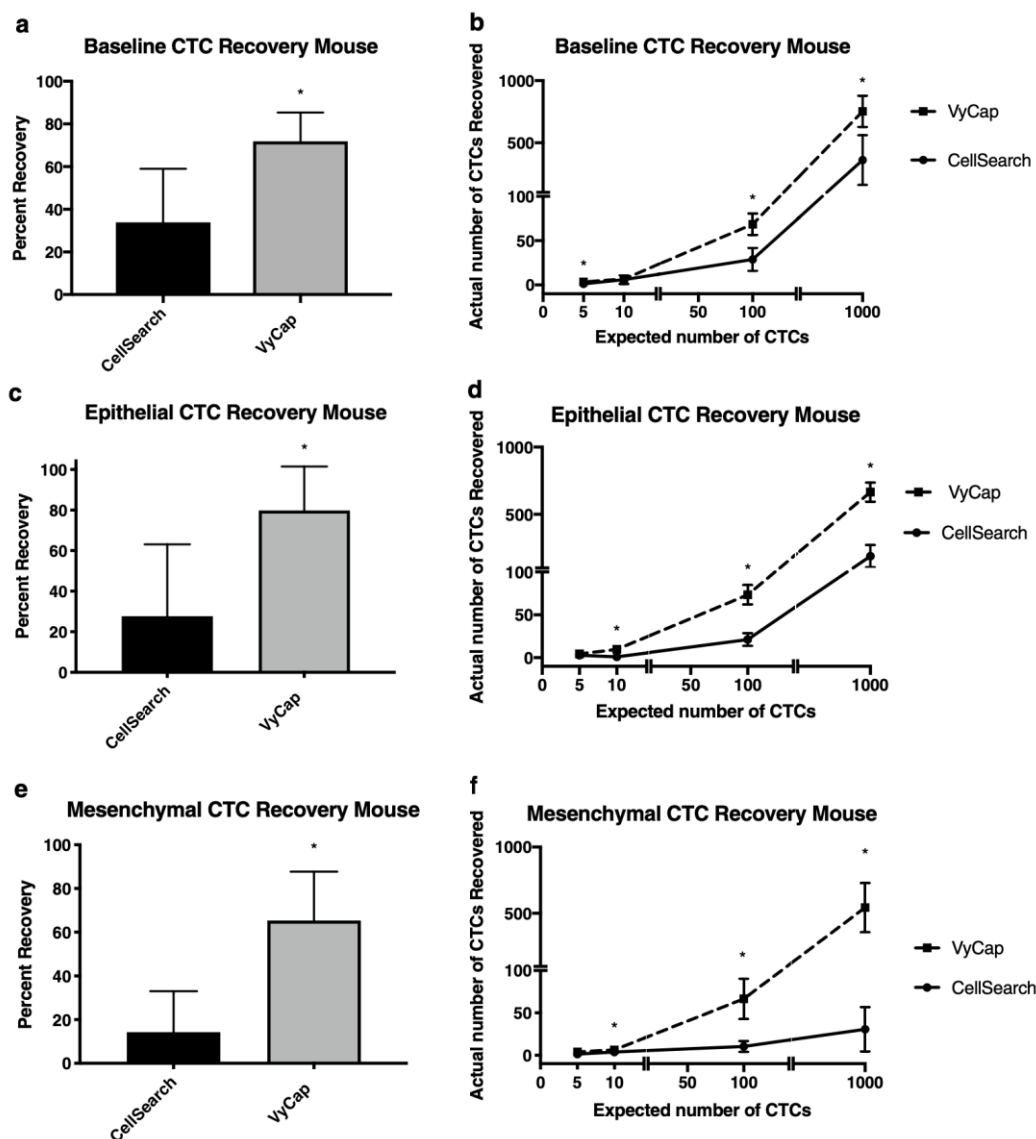


Figure 2.2. The VyCap CTC platform provides enhanced recovery of spiked-in epithelial and mesenchymal CTCs in mouse blood samples compared to the CellSearch®. Epithelial MDA-MB-468 human breast cancer cells or mesenchymal PC-3 human prostate cancer cells were spiked into whole mouse blood (5, 10, 100, or 1000 cells per 50 μ l/blood) and recovered using the mouse protocols for CellSearch® (epithelial-dependent) or VyCap (EMT-independent). (*a-b*) Pre-stained (CellTrace™) epithelial MDA-MB-468 human breast cancer cells spiked into mouse blood; (*c-d*) Epithelial MDA-MB-468 human breast cancer cells and (*e-f*) Mesenchymal PC-3 human prostate cancer cells spiked into mouse blood and stained using the human CellSearch® or VyCap protocols. Data are presented as mean \pm SEM ($n \geq 3$), * = significantly different than CellSearch® ($p \leq 0.05$).

Table 2-3. CTC recovery in spiked mouse blood samples using VyCap versus CellSearch®

Cell Type	Number of Cells Spiked	Cells Recovered (VyCap)	Cells Recovered (CellSearch®)	P-Value
Baseline (Pre-stained MDA-MB-468)	5	3.9 ± 0.3 (78%)	1.4 ± 0.8 (28%)	0.0182*
	10	6.6 ± 1.1 (66%)	4.3 ± 2.3 (43%)	0.6971
	100	68.6 ± 7.1 (69%)	28.7 ± 7.6 (28%)	0.0042*
	1000	753.0 ± 73.6 (75%)	360.5 ± 116.1 (36%)	0.0151*
Epithelial (MDA-MB-468)	5	4.1 ± 1.0 (80%)	3.0 ± 2.0 (60%)	0.3828
	10	9.8 ± 1.3 (98%)	1.1 ± 0.6 (10%)	0.0102*
	100	73.2 ± 6.4 (73%)	21.4 ± 4.5 (21%)	0.0026*
	1000	664.7 ± 41.8 (66%)	187.6 ± 47.7 (19%)	0.0003*
Mesenchymal (PC-3)	5	3.9 ± 0.8 (78%)	1.0 ± 0.8 (20%)	0.0572
	10	6.0 ± 1.3 (60%)	2.3 ± 1.6 (23%)	0.0131*
	100	66.7 ± 13.8 (67%)	10.5 ± 3.8 (11%)	0.0474*
	1000	566.7 ± 130.1 (57%)	31.0 ± 15.0 (3%)	0.0422*

these results indicate that both baseline CTC recovery and overall recovery of CTCs with either an epithelial or mesenchymal phenotype is enhanced through independent VyCap system versus the standard CellSearch® protocol.

2.3.3 The VyCap CTC platform provides enhanced recovery of mesenchymal CTCs from *in vivo* mouse models of prostate cancer metastasis

In order to assess the value of our developed mouse VyCap EMT-independent protocol compared to the mouse CellSearch® protocol *in vivo*, we orthotopically injected 12 mice with mesenchymal PC-3 human prostate cancer cells. After 9 weeks of primary tumor growth and disease progression, mice were sacrificed, blood samples were collected, and CTCs were enumerated using our two protocols. We observed that the VyCap was able to recover a CTCs in all 12 mice, whereas the CellSearch® was only able to capture CTCs in 10/12 mice with metastatic prostate cancer (**Figure 2.3a,b**). The VyCap also provided significantly enhanced recovery of CTCs in mice with metastatic prostate cancer ($13,094 \pm 5719$ CTCs/mouse) compared to CellSearch® (171 ± 117 CTCs/mouse) ($p \leq 0.05$) (**Figure 2.3a,c**). Of these mice, we observed that 8/12 mice developed metastatic disease in one or more organs as determined by histopathological analysis (**Figure 2.3d**). In addition to detecting CTCs in the 8 mice with detectable metastases, VyCap was also able to detect a significant number of CTCs in all 4 mice in which metastases were histologically undetectable, although the numbers of CTCs observed were lower. In contrast, the CellSearch® was only able to detect CTCs in 2 of these mice. These results support our observations from the spiking studies and validate our newly developed EMT-independent VyCap protocol for use in pre-clinical mouse studies of CTCs and metastasis.

2.3.4 CTCs can be harvested from the VyCap and Parsortix® for downstream molecular characterization

Finally, we wanted to assess the feasibility of harvesting CTCs from the two EMT-independent platforms and using them for downstream molecular characterization. Following CTC enumeration by either Parsortix® or VyCap, CTCs were harvested, and RNA was isolated for RT-qPCR to assess expression of EMT markers in MDA-MB-468 (epithelial) and PC-3 (mesenchymal) CTC samples. Overall, we observed that EMT gene expression could be detected in isolated epithelial or mesenchymal CTCs harvested both platforms, although the expression patterns were

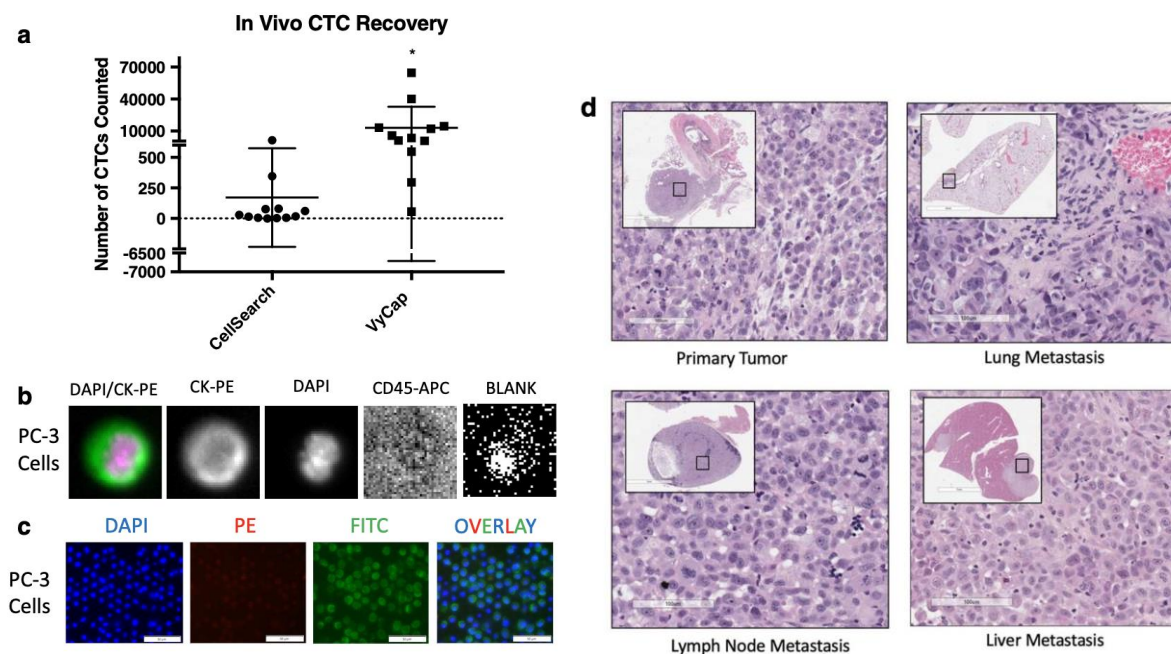


Figure 2.3. The VyCap CTC platform provides enhanced recovery of mesenchymal CTCs from *in vivo* mouse models of prostate cancer metastasis. PC-3 cells were orthotopically injected into the prostate gland of male nude mice. Prostate cancer tumor growth and progression to metastasis was allowed to develop for 9 weeks. At endpoint, blood was collected and analyzed for CTCs using mouse protocols for CellSearch® (epithelial-dependent) or VyCap (EMT-independent). **(a)** Recovery of *in vivo* CTCs by CellSearch® versus VyCap. Data are presented as mean ± SEM CTCs/50 µl of blood/mouse (n =12), * = significantly different than CellSearch® ($p \leq 0.05$). **(b)** Representative images of positive CTCs isolated using CellSearch®. DAPI⁺/CK-PE⁺/CD45⁻ cells are considered to be positive CTCs in samples processed with the CellSearch® CTC kit (DAPI = nuclear stain, PE= cytokeratins, APC = CD45, Blank = no stain). **(c)** Representative images of positive CTCs isolated using VyCap. DAPI⁺/PE⁻/FITC⁺ cells are considered to be positive CTCs in samples processed using VyCap (DAPI (*blue*) = nuclear stain, PE (*red*) = CD45, FITC (*green*) = HLA). **(d)** Representative H&E staining of primary tumor and metastatic sites. Low power 5X, high power 100X.

more consistent with what was expected using the VyCap (**Figure 2.4a,b**) ($p \leq 0.05$). In particular, MDA-MB-468 CTCs harvested from Parsortix® did not show the expected epithelial gene expression pattern ($p > 0.05$). These results demonstrate the ability to isolate RNA and characterize gene expression from CTC samples via the VyCap or Parsortix® for further downstream characterization after CTC enumeration.

2.4 Discussion

Analysis of CTCs hold tremendous promise for tracking metastatic progression and treatment response in both human cancer patients and pre-clinical mouse models of metastasis. However, current clinical assays such as CellSearch® rely on epithelial cell characteristics for CTC detection and enumeration, and thus may be limiting our ability to capitalize on the full potential of CTCs. In the current study we developed and validated two EMT-independent CTC enumeration and harvest protocols, one for use with human patient samples using the Parsortix® (EpCAM⁺ or N-Cadherin⁺ phenotype), and one for use with pre-clinical mouse samples using VyCap (HLA⁺ phenotype) and compared them to the clinical “gold standard” FDA-approved CellSearch®.

For analysis of human samples, we observed no significant differences in CTC capture for epithelial CTCs between CellSearch® and Parsortix®. Thus, either system may be appropriate for enumeration of epithelial CTCs from human blood samples depending on the study design. For example, studies evaluating early-stage cancers, the initiating steps of metastasis, or epithelial marker expression on CTCs could be carried out using either CellSearch® and Parsortix®. However, in studies of more advanced and/or aggressive cancers where a greater proportion of mesenchymal CTCs or mixed epithelial/mesenchymal CTCs are expected, Parsortix® might be a more appropriate CTC platform based on our observations that significantly enhanced detection of mesenchymal CTCs is possible with Parsortix® versus CellSearch®. For CTC capture in pre-clinical mouse models, our results indicate that our developed VyCap protocol (EMT-independent) is superior to our previously developed mouse CellSearch® protocol (EpCAM-dependent) regardless of cell phenotype. This is likely due to both the epithelial-dependent nature of the CellSearch® platform as well as the manual CTC enrichment step in the CellSearch® mouse protocol (including multiple wash steps) which may cause loss of CTCs during the isolation process¹¹.

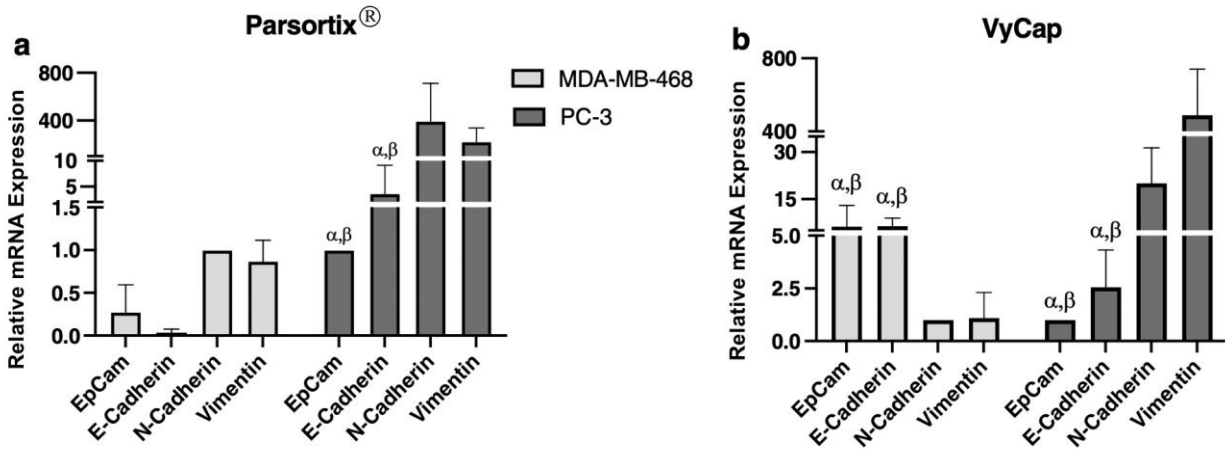


Figure 2.4. CTCs can be harvested from the VyCap and Parsortix systems for downstream molecular characterization. Epithelial MDA-MB-468 human breast cancer CTCs or mesenchymal PC-3 human prostate cancer CTCs were enumerated on the (a) Parsortix® or (b) VyCap platforms and CTCs were harvested after enumeration. RNA was isolated from captured CTC samples and assessed for expression of the EMT markers EpCAM, E-Cadherin, N-Cadherin, and Vimentin using RT-qPCR. MDA-MB-468 RNA is relative to N-cadherin expression while PC-3 RNA is relative to EpCAM expression. Data are presented as mean \pm SEM (n=3), α = significantly different than N-Cadherin ($p \leq 0.05$), β = significantly different than Vimentin ($p \leq 0.05$).

Additionally, the ability to harvest CTCs from the different platforms for downstream analysis is an important consideration when choosing which technology is most appropriate, since it is difficult to recover enumerated CTCs using the CellSearch®. Therefore, for investigators interested in tracking evolving molecular characteristics throughout disease progression or assessing expression of specific therapeutic targets, our results suggest that VyCap or Parsortix® may be a more appropriate platform to use compared to CellSearch®. Our results also indicate that the VyCap platform may be slightly more optimal for cell harvesting compared to the Parsortix®, potentially due to the differences in isolation procedure. With the VyCap, the RNA lysis buffer is added directly to the microsieve, with full exposure to all CTCs present and potentially improved recovery and RNA extraction. In contrast, with the Parsortix® system, tumor cells move through an increasingly smaller area until they become lodged within the stepwise system of the chip. It is possible that some larger CTCs may become stuck within the chip and are not dislodged by the backflow pressure in the harvest protocol and thus do not get harvested. This may result in an insufficient cell number for RNA extraction and accurate RT-qPCR analysis, especially with low numbers of CTCs. This may be of particular concern when using immortalized cell lines for CTC studies, which have been demonstrated to have a greater diameter in circulation (~15-20µm) than primary patient CTCs (~10-13µm) [27]. Similarly, breast cancer CTCs are typically larger than prostate cancer CTCs [27] which may help explain why we did not obtain the expected epithelial EMT gene expression results from MDA-MB-468 breast cancer cells harvested from the Parsortix®. Thus, recovery of CTCs from the Parsortix® for downstream analysis may be further optimized by careful selection of the most appropriately sized cartridge (6.5, 8 or 10µm) for the disease site and/or experimental question being investigated.

Each of the three CTC platforms described in this Technical Note have a number of advantages and disadvantages that researchers should consider when designing their CTC studies and choosing an appropriate analysis platform (**Table 2.4**). For example, the FDA-approved status and the significant body of clinical prognostic data available for CellSearch® supports its use in clinical studies, particularly those where mostly epithelial CTCs are expected. However, it may potentially miss aggressive mesenchymal CTCs and it provides very limited capacity for recovery and downstream analysis of CTCs. The Parsortix® addresses many of these limitations, and although it is not yet FDA-approved, its potential clinical validity is supported by a CE mark in Europe and a number of promising clinical studies²⁰. For example, in a recently completed clinical

trial, Parsortix® was successfully used to isolate and harvest CTCs from metastatic breast cancer patients for further downstream analysis in support of an upcoming FDA submission (ClinicalTrials.gov; NCT03427450). Ongoing clinical studies are also using Parsortix® for the isolation of rare CTCs in ovarian cancer (ClinicalTrials.gov; NCT02781272), to evaluate multiple biomarkers in ovarian cancer (ClinicalTrials.gov; NCT02785731), in an EMT-independent prostate cancer study (ClinicalTrials.gov; NCT04021394), and for evaluating heterogeneity and predicting clinical relapse in non-small cell lung carcinoma patients (ClinicalTrials.gov; NCT03771404). Pending FDA approval, the unique attributes of Parsortix® such as easy marker customization and the ability to harvest CTCs for downstream analysis^{27,28} will position Parsortix® as an ideal CTC platform for use in clinical trials and clinical management. However, one of the main limitations of the Parsortix® is the time it takes to process a single sample; approximately seven hours to separate, stain, harvest, and clean the instrument in preparation for the next sample. The low-throughput nature of Parsortix® is challenging but manageable for clinical samples, which typically arrive in the lab one at a time. However, for pre-clinical studies, researchers often have multiple mice in each group with set endpoints or blood collection points. Using the VyCap^{23,29,30}, mouse blood samples can be pre-stained in batches in two hours using custom antibody panels, enriched in less than a minute per sample, and CTC RNA harvested in approximately five minutes off the disposable microsieves. This allows the user to stain, separate, enumerate, and harvest up to twelve samples in one day. Due to the increased sample throughput of the VyCap compared to the Parsortix®, it is a better platform to assess CTCs in pre-clinical mouse experiments where multiple samples need to be collected and analyzed together. With the ability to further enhance analysis capacity through the additional use of VyCap's semi-automated microscopy system³¹ and/or single CTC isolation puncher³², this system provides a high degree of flexibility for CTC studies. However, similar to the Parsortix®, VyCap does not yet have FDA approval for clinical use and has not yet demonstrated clinical validity in terms of association with patient prognosis or response to treatment; and this is the major limitation of this system³³.

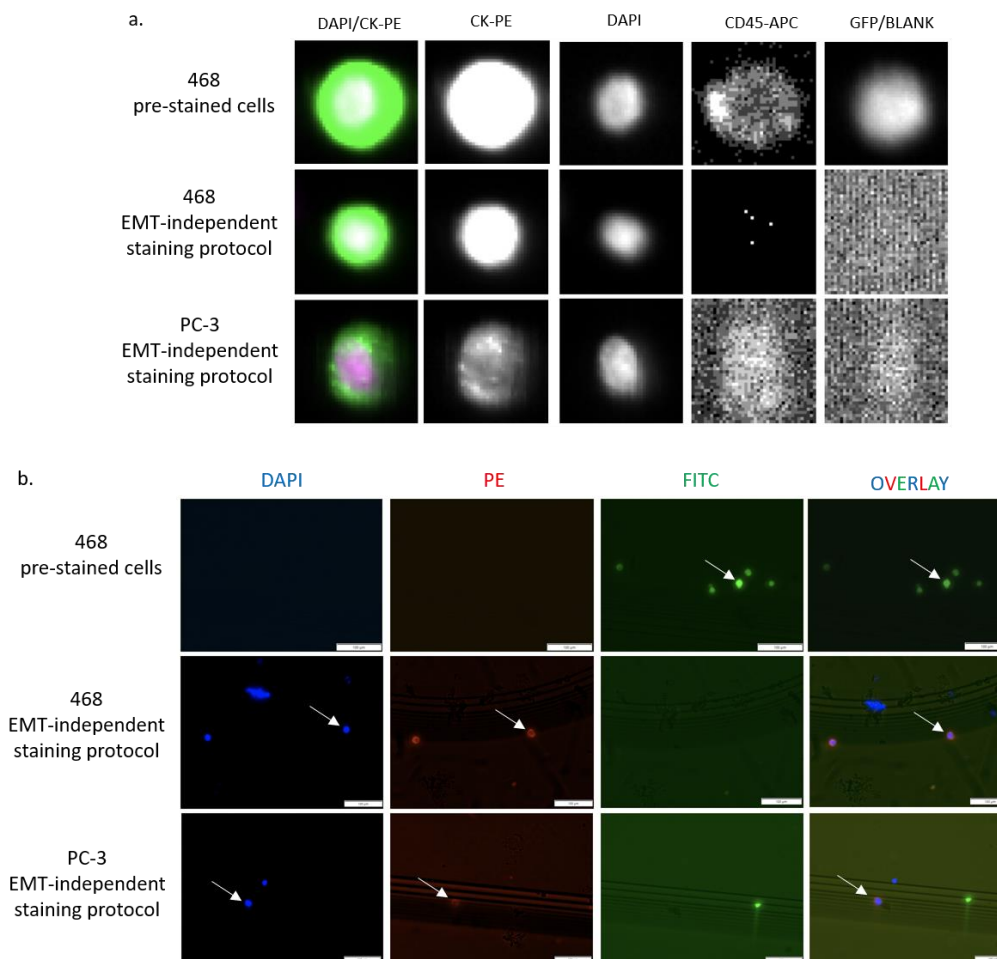
In summary, we believe that this Technical Note will be valuable for aiding researchers in decision-making regarding which CTC platform is best for their specific studies. Taken together, this will help enhance knowledge in the areas of CTC generation, metastasis, and EMT to ultimately assist in treating patients with aggressive metastatic disease.

Table 2-4. Advantages and disadvantages of CellSearch®, Parsortix® and VyCap CTC analysis platforms

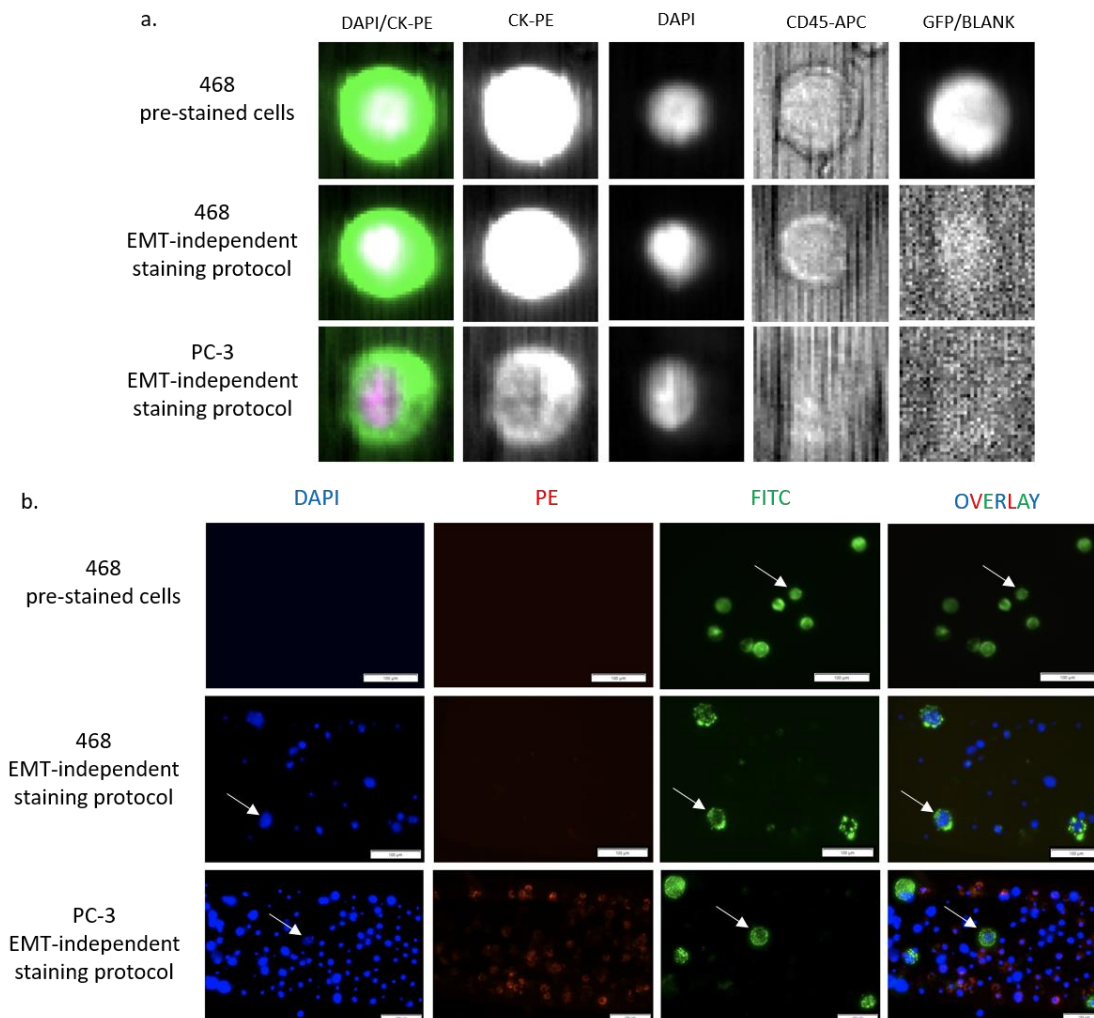
	CellSearch®	Parsortix®	VyCap
Clinically Validated ¹ ?	✓✓✓	✓✓	✗
Captures all types of CTC/phenotype-independent	✗	✓✓✓	✓✓✓
Provides user flexibility for development of custom antibody panels for CTC analysis	✗	✓✓✓	✓✓✓
Ability to harvest viable cells for downstream analysis	✗	✓✓	✓✓✓
Quick processing time/high sample throughput	✓✓✓	✗	✓✓✓
Affordability/cost	✓	✓✓	✓✓✓
Recommended for use in analyzing CTCs in clinical samples from cancer patients?	✓✓✓	✓✓	✓
Recommended for use in analyzing CTCs in pre-clinical mouse models of metastasis?	✗	✗	✓✓✓

¹Based on regulatory approval and/or published clinical data demonstrating an association with patient prognosis and/or response to therapy

2.5 Supplemental Data – Chapter 2



Supplemental Figure 2-1. Representative images of positive CTCs isolated from human blood using CellSearch® and Parsortix®. For baseline recovery experiments, MDA-MB-468 human breast cancer cells (epithelial) were pre-stained with the CellTrace™ carboxyfluorescein succinimidyl ester (CFSE) Cell Proliferation Kit. For all other experiments, human MDA-MB-468 cells or human PC-3 mesenchymal cells were stained using the human staining protocols outlined in the Materials & Methods. (a) Representative positive CTCs isolated using the human CellSearch® protocol. DAPI⁺/CK-PE⁺/CD45⁻/GFP(CFSE)⁺ cells are considered to be positive CTCs in pre-stained samples. DAPI⁺/CK-PE⁺/CD45⁻ cells are considered to be positive CTCs in samples processed with the CellSearch® CTC kit. (b) Representative positive CTCs isolated using the human Parsortix® protocol (*white arrows*). FITC (CFSE)⁺ are considered to be positive CTCs in pre-stained samples. For samples stained with the EMT-independent staining protocol, DAPI⁺/PE⁺/FITC⁻ cells are considered positive (DAPI (*blue*) = nuclear stain, PE (*red*) = EpCAM or N-Cadherin, FITC (*green*) = CD45).



Supplemental Figure 2-2. Representative images of positive CTCs isolated from mouse blood using CellSearch® and VyCap. For baseline recovery experiments, MDA-MB-468 human breast cancer cells (epithelial) were prestained with the CellTrace™ carboxyfluorescein succinimidyl ester (CFSE) Cell Proliferation Kit. For all other experiments, human MDA-MB-468 cells or human PC-3 mesenchymal cells were stained using the mouse staining protocols outlined in the Materials & Methods. (a) Representative positive CTCs isolated using the mouse CellSearch® protocol. DAPI⁺/CK-PE⁺/CD45⁻/GFP(CFSE)⁺ cells are considered to be positive CTCs in pre-stained samples. DAPI⁺/CK-PE⁺/CD45⁻ cells are considered to be positive CTCs in samples processed with the CellSearch® CTC staining protocol. (b) Representative positive CTCs isolated using the mouse VyCap protocol (*white arrows*). FITC (CFSE)⁺ are considered to be positive CTCs in pre-stained samples. For samples stained with the EMT-independent staining protocol, DAPI⁺/PE⁻/FITC⁺ cells are considered positive (DAPI (*blue*) = nuclear stain, PE (*red*) = CD45, FITC (*green*) = HLA).

2.6 References

1. Siegel RL, Miller KD, Jemal A. Cancer statistics, 2020. *CA Cancer J Clin.* 2020. doi:10.3322/caac.21590
2. Seyfried TN, Huysentruyt LC. On the Origin of Cancer Metastasis. *Crit Rev Oncog.* 2012. doi:10.1615/critrevoncog.v18.i1-2.40
3. Mittal V. Epithelial Mesenchymal Transition in Tumor Metastasis. *Annu Rev Pathol Mech Dis.* 2018. doi:10.1146/annurev-pathol-020117-043854
4. Kalluri R, Weinberg RA. The basics of epithelial-mesenchymal transition. *J Clin Invest.* 2009;119(6):1420-1428. doi:10.1172/JCI39104
5. Albanese C, Rodriguez OC, VanMeter J, et al. Preclinical magnetic resonance imaging and systems biology in cancer research: current applications and challenges. *Am J Pathol.* 2013;182(2):312-318. doi:10.1016/j.ajpath.2012.09.024
6. Chambers AF, Groom AC, MacDonald IC. Dissemination and growth of cancer cells in metastatic sites. *Nat Rev Cancer.* 2002;2(8):563-572. doi:10.1038/nrc865
7. Cristofanilli M, Budd GT, Ellis MJ, et al. Circulating tumor cells, disease progression, and survival in metastatic breast cancer. *N Engl J Med.* 2004;351(8):781-791. doi:10.1056/NEJMoa040766
8. De Bono JS, Scher HI, Montgomery RB, et al. Circulating tumor cells predict survival benefit from treatment in metastatic castration-resistant prostate cancer. *Clin Cancer Res.* 2008. doi:10.1158/1078-0432.CCR-08-0872
9. Graves H, Czerniecki BJ. Circulating Tumor Cells in Breast Cancer Patients: An Evolving Role in Patient Prognosis and Disease Progression. *Patholog Res Int.* 2011. doi:10.4061/2011/621090
10. Goldkorn A, Ely B, Quinn DI, et al. Circulating tumor cell counts are prognostic of overall survival in SWOG S0421: A phase III trial of docetaxel with or without atrasentan for metastatic castration-resistant prostate cancer. *J Clin Oncol.* 2014;32(11):1136-1142. doi:10.1200/JCO.2013.51.7417
11. Lowes LE, Goodale D, Xia Y, et al. Epithelial-to-mesenchymal transition leads to disease-stage differences in circulating tumor cell detection and metastasis in pre-clinical models of prostate cancer. *Oncotarget.* 2016. doi:10.18632/oncotarget.12682
12. Cohen SJ, Punt CJ a, Iannotti N, et al. Prognostic significance of circulating tumor cells in patients with metastatic colorectal cancer. *Ann Oncol.* 2009;20(7):1223-1229. doi:10.1093/annonc/mdn786
13. Allard WJ, Matera J, Miller MC, et al. Tumor cells circulate in the peripheral blood of all major carcinomas but not in healthy subjects or patients with nonmalignant diseases. *Clin*

- Cancer Res.* 2004;10(20):6897-6904. doi:10.1158/1078-0432.CCR-04-0378
14. Jolly MK. Implications of the Hybrid Epithelial/Mesenchymal Phenotype in Metastasis. *Front Oncol.* 2015;5. doi:10.3389/fonc.2015.00155
 15. Gorges TM, Tinhofer I, Drosch M, et al. Circulating tumour cells escape from EpCAM-based detection due to epithelial-to-mesenchymal transition. *BMC Cancer.* 2012;12. doi:10.1186/1471-2407-12-178
 16. Armstrong AJ, Marengo MS, Oltean S, et al. Circulating tumor cells from patients with advanced prostate and breast cancer display both epithelial and mesenchymal markers. *Mol Cancer Res.* 2011. doi:10.1158/1541-7786.MCR-10-0490
 17. Bulfoni M, Gerratana L, Del Ben F, et al. In patients with metastatic breast cancer the identification of circulating tumor cells in epithelial-to-mesenchymal transition is associated with a poor prognosis. *Breast Cancer Res.* 2016. doi:10.1186/s13058-016-0687-3
 18. Lindsay CR, Le Moulec S, Billiot F, et al. Vimentin and Ki67 expression in circulating tumour cells derived from castrate-resistant prostate cancer. *BMC Cancer.* 2016. doi:10.1186/s12885-016-2192-6
 19. Yu M, Bardia A, Wittner BS, et al. Circulating breast tumor cells exhibit dynamic changes in epithelial and mesenchymal composition. *Science (80-).* 2013. doi:10.1126/science.1228522
 20. Kitz J, Lowes L, Goodale D, Allan A. Circulating Tumor Cell Analysis in Preclinical Mouse Models of Metastasis. *Diagnostics.* 2018. doi:10.3390/diagnostics8020030
 21. Lowes LE, Hedley BD, Keeney M, Allan AL. Adaptation of semiautomated circulating tumor cell (CTC) assays for clinical and preclinical research applications. *J Vis Exp.* 2014. doi:10.3791/51248
 22. Angle. How the Parsortix System Works. www.angleplc.com. Accessed April 24, 2018.
 23. Zweitzig DR, Tibbe AG, Nguyen AT, et al. Feasibility of a simple microsieve-based immunoassay platform. *J Immunol Methods.* 2016. doi:10.1016/j.jim.2016.07.002
 24. Lampignano R, Schneck H, Neumann M, et al. Detection of EpCAM-negative circulating tumor cells by using VyCAP filters technology. *Senol - Zeitschrift für Mammadiagnostik und -therapie.* 2015. doi:10.1055/s-0035-1550523
 25. Price JE, Polyzos A, Zhang RD, Daniels LM. Tumorigenicity and Metastasis of Human Breast Carcinoma Cell Lines in Nude Mice. *Cancer Res.* 1990.
 26. Kaighn ME, Narayan KS, Ohnuki Y, Lechner JF, Jones LW. Establishment and characterization of a human prostatic carcinoma cell line (PC-3). *Invest Urol.* 1979.

27. Hvichia GE, Parveen Z, Wagner C, et al. A novel microfluidic platform for size and deformability based separation and the subsequent molecular characterization of viable circulating tumor cells. *Int J Cancer*. 2016;138(12):2894-2904. doi:10.1002/ijc.30007
28. Xu L, Mao X, Imrali A, et al. Optimization and evaluation of a novel size based circulating tumor cell isolation system. *PLoS One*. 2015;10(9). doi:10.1371/journal.pone.0138032
29. Coumans FAW, van Dalum G, Beck M, Terstappen LWMM. Filtration Parameters Influencing Circulating Tumor Cell Enrichment from Whole Blood. *PLoS One*. 2013. doi:10.1371/journal.pone.0061774
30. De Wit S, Van Dalum G, Lenferink ATM, et al. The detection of EpCAM+ and EpCAM- circulating tumor cells. *Sci Rep*. 2015. doi:10.1038/srep12270
31. Pailler E, Oulhen M, Billiot F, et al. Method for semi-automated microscopy of filtration-enriched circulating tumor cells. *BMC Cancer*. 2016. doi:10.1186/s12885-016-2461-4
32. Stevens M, Oomens L, Broekmaat J, et al. VyCAP's puncher technology for single cell identification, isolation, and analysis. *Cytom Part A*. 2018. doi:10.1002/cyto.a.23631
33. Neumann MHD, Bender S, Krahn T, Schlange T. ctDNA and CTCs in Liquid Biopsy – Current Status and Where We Need to Progress. *Comput Struct Biotechnol J*. 2018. doi:10.1016/j.csbj.2018.05.002

Chapter 3

3 Comparison of EMT dependent and independent circulating tumor cell enumeration and downstream molecular characterization in metastatic prostate cancer patients

Abstract

Prostate cancer is the second leading cause of cancer related deaths among American men. While early-stage prostate cancers can be effectively managed by surgery, radiation and/or androgen-deprivation therapies, over time these tumors often adapt to the androgen-deprived environment and become “castrate-resistant”. Patients with castrate-resistant prostate cancer invariably experience disease progression and most prostate cancer related deaths are due to the resulting metastases. In the current study we aimed to develop further insight into the biology of prostate cancer metastatic progression by assessing circulating tumor cells (CTCs) from 3 patient cohorts: 1) Low-volume metastatic hormone-sensitive prostate cancer (LV-mHSPC); 2) High-volume metastatic hormone-sensitive prostate cancer (HV-mHSPC); and 3) Metastatic castrate-resistant prostate cancer (mCRPC). We assessed patient CTCs using the clinically available epithelial-based CellSearch® assay versus our developed and validated EMT-independent Parsortix® CTC protocol. When assessing the numbers of CTCs captured between groups, we did not observe any significant differences between the two technologies, although CellSearch® was able to identify a greater number of CTCs in the HV-mHSPC cohort compared to LV-mHSPC. However, we observed that the Parsortix® was able to identify more patients in all cohorts with ≥ 5 CTCs, which has potential prognostic value. Furthermore, patient CTCs were harvested from Parsortix® in order to carry out downstream molecular analysis using the novel HyCEAD mRNA multiplex assay. We identified 19 differentially expressed genes between the three patient cohorts that may contribute to disease progression in prostate cancer. Taken together, the results of study provide a promising panel of potential biomarkers that could be used alone or as a molecular signature in order to develop a comprehensive, real-time CTC liquid biopsy strategy for the personalized clinical management of metastatic prostate cancer patients in the future.

3.1 Introduction

Prostate cancer is the most commonly diagnosed cancer and second most common cause of cancer death in American men¹. Early-stage prostate cancers are dependent on androgen stimulation for growth, and thus androgen-deprivation therapy by chemical and/or surgical castration is a treatment mainstay for hormone-dependent disease. However, as tumors adapt to the androgen-deprived environment and become “castrate-resistant”, many patients will invariably experience disease progression. Deaths from prostate cancer are primarily a result of castrate-resistant metastatic disease, as current therapies are largely non-curative in this setting^{2,3}. Further insight into the biology of disease progression and metastasis is therefore essential in order to develop better strategies for treatment. In addition, the use of Gleason score and/or prostate-specific antigen (PSA) levels is helpful but imperfect for predicting disease outcome, and this uncertainty often results in under-treatment or over-treatment of prostate cancer patients⁴. There is therefore a clear need for improved biomarkers that can be used to accurately assess disease progression and treatment response. One such biomarker may be circulating tumor cells (CTCs).

The presence of circulating tumor cells (CTCs) in the blood of prostate cancer patients has been shown to be an important indicator of metastatic disease and poor prognosis^{5,6}. Additionally, changes in CTC number throughout treatment have been demonstrated to reflect therapy response⁷. Although these cells are very rare (~1 CTC per 10^5 - 10^7 leukocytes)^{8,9}, recent technological advances have now facilitated sensitive enumeration and characterization of CTCs. Techniques to enrich and analyze CTCs include size- and/or density-based separation and antibody-based techniques with/without the aid of microfluidics, while detection techniques rely almost exclusively on protein- (immunofluorescence/flow cytometry) or nucleic acid-based (RT-PCR/RT-qPCR) assays^{10,11}. However, CellSearch® (Menarini-Silicon Biosystems)¹² is the only FDA- and Health Canada-cleared CTC platform available at the present time, and is thus considered the current “gold standard” for clinical CTC analysis^{10,11}.

CellSearch® uses an epithelial-based marker approach for immunomagnetic enrichment, isolation, and quantitative immunofluorescence of CTCs. Using this assay, it has been demonstrated that CTCs are readily detectable in ~65% of castrate-resistant prostate cancer (CRPC) patients¹³ and that the presence of ≥ 5 CTCs in 7.5ml of blood is indicative of progressive metastatic disease and reduced overall survival^{5,6}. Notably, CTCs are undetectable in ~35% of metastatic CRPC

patients¹³. This suggests that either CTCs are truly not present in >1/3 of patients with advanced metastatic disease, and/or that CTCs are present but not detectable as they do not meet the standard CellSearch® definition of CTCs (EpCAM+/Cytokeratin 8/18/19 [CK]+/DAPI+/CD45-). Given the accumulating evidence that prostate cancer cells can lose epithelial characteristics as they evolve towards a more metastatic phenotype¹⁴, we hypothesize that the latter scenario is most likely.

The epithelial-to-mesenchymal transition (EMT) is a critical process during embryonic development and cancer metastasis^{15,16}. Activation of EMT leads to profound phenotypic changes resulting in loss of cell polarity, loss of cell-cell adhesion, resistance to apoptosis, and acquisition of migratory/invasive properties^{14,17,18}. It has also been proposed that tumor cells (via the mesenchymal-to-epithelial transition [MET]) may revert back to an epithelial phenotype in order to facilitate metastatic growth in secondary sites, suggesting a role for phenotypic plasticity during metastatic progression^{14,15,19}. At the molecular level, EMT is mediated by decreased expression of epithelial proteins (E-cadherin, CK, EpCAM), as well as corresponding increases in mesenchymal factors (N-cadherin, Vimentin, Twist, Zeb), with MET mediated by the opposite changes^{15,16}.

Clinically, Gleason grading can arguably be viewed as morphological evidence of EMT¹⁴, since increasing Gleason score is associated with progressive loss of epithelial architecture, loss of defined basement membrane/cell polarity, and increased invasion²⁰. In support of this, studies have demonstrated that decreased expression of E-Cadherin^{21,22} or increased expression of mesenchymal markers (Vimentin, N-Cadherin, Snail)²³⁻²⁷ in primary prostate tumors is associated with advanced Gleason score, metastasis, and/or poor prognosis. Although the role of androgen receptor (AR) signaling in EMT is poorly understood, studies have also demonstrated that EMT may be facilitated by androgen deprivation²⁸, castration-resistance²⁹, and/or disruption of androgen signaling^{30,31}.

Importantly, several clinical studies have demonstrated that CTCs with a purely mesenchymal phenotype are undetectable by CellSearch®, but that the presence of mesenchymal marker expression on CTCs with a hybrid epithelial-mesenchymal phenotype is indicative of poor prognosis^{19,32-36}. In addition, previous pre-clinical data from our laboratory^{37,38} has demonstrated that in animal models, prostate cancers with a mesenchymal phenotype shed greater numbers of

CTCs more quickly and with greater metastatic capacity than those with an epithelial phenotype. Notably, the clinically used CellSearch®-based assay captured the majority of CTCs shed during early-stage disease *in vivo*, and only after the establishment of metastases were a significant number of undetectable CTCs present. This suggests that current clinical assays may be limiting our ability to capitalize on the full potential of CTCs, and that a greater understanding of CTC biology is necessary in order to guide future technology development and translation to the clinic.

CTCs hold enormous promise as surrogate biomarkers for cancer progression and treatment response. However, several scientific and technical issues remain to be resolved before CTC analysis and characterization can be considered for widespread application in the clinic. In particular, previous clinical biomarker studies and our pre-clinical animal studies suggest that the epithelial-based, clinical gold standard CellSearch® CTC assay may be missing the most invasive and highly metastatic cells driving prostate cancer disease progression, and that characterization of CTCs with a mesenchymal or hybrid phenotype may be more informative than analysis of those with a purely epithelial phenotype^{6,11}. To address this challenge, the EMT-independent CTC platform Parsortix® has been developed by ANGLE plc³⁹⁻⁴². The company has already received CE Mark authorization for *in vitro* diagnostic (IVD) use of the system in the European Union and is moving towards FDA approval in the United States. To complement this technology, ANGLE has also developed a sophisticated downstream analysis system for gene expression profiling of cells called HyCEAD (Hybrid Capture Enrichment Amplification and Detection), which allows for the simultaneous multiplex analysis of 100+ mRNA species⁴³. The overall goal of this study is to test the hypothesis that patients at later stages of prostate cancer progression will have a greater number of CTCs with enhanced EMT characteristics. We investigated this in metastatic prostate cancer patients at different disease progression stages along the spectrum of hormone-sensitive to castrate-resistant, using comparative CTC enumeration by CellSearch® and Parsortix® and CTC molecular characterization with HyCEAD.

3.2 Materials and Methods

3.2.1 Patient Population and Study Eligibility

All studies were carried out under a protocol approved by the Western University's Health Sciences Research Ethics Board (protocol #109759). A total of 29 evaluable patients were accrued

from the London Regional Cancer Program (LRCP) at the London Health Sciences Centre (LHSC; London, ON Canada) following informed consent. Patients were accrued based on 3 progressive disease stage cohorts including (1) Low-volume metastatic hormone-sensitive prostate cancer (LV-mHSPC)⁴⁴ (n=10 patients) (<4 bone lesions); (2) High-volume metastatic hormone-sensitive prostate cancer (HV-mHSPC)⁴⁴ (n=9 patients) (≥ 4 bone lesions and at least 1 outside of the vertebral column or pelvis); and (3) Metastatic castrate-resistant prostate cancer (mCRPC)^{5,6} (n=10 patients) (evidence of disease progression while on androgen deprivation therapy). All patients were 18 years of age or older with histologically diagnosed prostate cancer and documented evidence of metastatic disease. Specific inclusion criteria for the LV-mHSPC cohort included previous treatment with androgen deprivation therapy for <90 days and/or recommended but not yet started new line of androgen deprivation therapy; and bone only metastatic disease (less than 4 lesions contained within vertebral column or pelvis)⁴⁴. Inclusion criteria for the HV-mHSPC cohort included previous treatment with androgen deprivation therapy for <90 days and/or recommended but not yet started new line of androgen deprivation therapy; and visceral metastases (extranodal) and/or bone metastases (≥ 4 bone lesions with ≥ 1 lesion outside vertebral column or pelvis)⁴⁴. Inclusion criteria for the mCRPC cohort included documented evidence of progression while receiving androgen ablation therapy (medical or surgical castration) according to PCWG2 criteria; and bone and/or visceral metastatic disease⁴⁵.

3.2.2 Clinical Data Collection

Following confirmation of eligibility and written informed consent, a unique study ID was assigned and clinical characteristics and data for each patient were collected by the LRCP Clinical Research Unit (CRU) using study Case Report Forms (CRFs). All data was entered into REDCap, an electronic case report form database. De-identified source documents were uploaded directly into REDCap to support the data. Upon study registration, baseline data including patient demographics, disease information, previous cancer treatments, results from routine blood tests and concomitant medications were collected. Patients are being followed annually for 5 years after study registration, with survival and disease status captured by CRF.

3.2.3 Blood Collection and CTC Enumeration

Blood samples (2x10 ml) were collected from each patient by routine phlebotomy at LRCP into CellSave preservative blood collection tubes (Menarini Silicon Biosystems, Huntingdon Valley, PA, USA) for pre-analytical stabilization of CTCs for up to 96 hours. One sample (7.5 mL of whole blood) was analyzed by CellSearch® (Menarini Silicon Biosystems) and CTCs were enumerated based on an EpCAM+/CK+/CD45-/DAPI+ cell phenotype as previously described⁴⁶. The other sample (7.5 mL of whole blood) was analyzed using Parsortix® (Angle, Toronto, ON, CA) as described previously^{39-42,47}, using 6.5 µm cassettes. CTCs were enumerated based on the standard Parsortix® in-cassette staining protocol with a custom antibody panel⁴⁷. In reagent tubes one and two, 1-2 mL of flow buffer, consisting of phosphate buffer solution (PBS) and 3% fetal bovine serum (FBS), was added in place of 4% paraformaldehyde fixative and permeabilization reagents, respectively. Reagent tube three consisted of 1 mL flow buffer and 10 µL anti-human N-Cadherin- PE (Invitrogen, 12-3259-42, Waltham, MA, US), 20 µL anti-Human EpCam- PE (BD, 347198, Franklin Lakes, NJ, US), 20 µL anti-Human CD-45 FITC (Beckman Coulter, IM0782U, Brea, CA, US), and 5 µL DAPI (Sigma Aldrich, Ref: D9542, St. Louis, MO, US). Reagent tube three and cassette holder were covered in aluminum foil to protect antibodies from light during CTC staining. EpCAM and N-Cadherin antibodies were both labeled with the same fluorochrome in order to identify CTCs regardless of EMT phenotype. EpCAM+ or N-Cadherin+/CD45-/DAPI+ cells were considered positive CTCs.

3.2.4 CTC Harvest, RNA Isolation and HyCEAD Analysis

Following enumeration, CTCs were collected via the platform's harvest protocol into one 1.5 mL RNase/DNase-free microtube (Diamed, Mississauga, ON, CA) per patient sample as previously described⁴⁷. Patient CTCs were centrifuged at 700 x g for 10 min, supernatants were discarded without disturbing the pellet, and CTCs were lysed via manual pipetting using 50 µL lysis/binding buffer from the Dynabeads® mRNA Purification Kit (ThermoFisher, 61021). Harvested CTCs in lysis/binding buffer were stored at -80 °C prior to analysis. Hybrid Capture Extension and Detection (HyCEAD) mRNA analysis was performed by ANGLE as described previously⁴³. Briefly, polyA⁺ mRNA was captured directly from cell lysates and multiplex amplification and labeling targeted two sequences for each gene of interest. Products were sorted and quantified by chemiluminescent detection on flow-through chips. Two gene expression chips including the

prostate cancer (“PC”) chip and the high expression (“HE”) chip (**Supplemental Table 3.1**) were developed by ANGLE and previously validated on a separate mCRPC patient cohort (*ANGLE’s confidential unpublished data*). Automated analysis was completed based on signal intensity compared to control cell/tissue RNA. Genes identified during HyCEAD analysis were considered significantly upregulated if they had an amplification of >20-fold compared to the average amplification of non-template controls (NTC).

3.2.5 TCGA Analysis

Follow-up analysis on upregulated HyCEAD genes was completed using online patient data from The Cancer Genome Atlas (TCGA). Using the gene analysis [Ualcan database](#) (accessed on December 12, 2021), each gene with altered expression between clinical groups was analyzed. Utilizing the TCGA dataset, genes were assessed for changes in expression in prostate adenocarcinoma versus normal tissues and metastatic prostate cancer versus non-metastatic prostate cancer (MET500 dataset) as well as correlation with overall survival.

3.2.6 Statistical Data Analysis

Statistical analysis was completed using GraphPad Prism 9 for MacOS (San Diego, CA, US). Data is presented as the mean \pm standard deviation (SD). For matched samples, two-tailed non-parametric Wilcoxon matched-pairs signed rank tests were performed. For analysis between patient groups non-paired, non-parametric Kruskal-Wallis tests, with Dunn’s multiple comparisons follow up tests were performed. For all experiments, $p \leq 0.05$ was considered statistically significant.

3.3 Results

3.3.1 Patient characteristics

Metastatic hormone-sensitive prostate cancer (mHSPC) is diagnosed when a patient’s cancer has spread from the primary site to other parts of the body but can still be treated with hormone deprivation therapy to block, stop, or slow cancer growth⁴⁸. The most common place for prostate cancer to metastasize is to bone⁴⁹, so we assessed patients with low-volume mHSPC (LV-mHSPC) (<4 bone lesions) and high-volume mHSPC (HV-mHSPC) (≥ 4 bone lesions and at least 1 lesion outside of the vertebral column or pelvis). In HV-mHSPC, high burden of disease includes more

bone lesions (specifically lesions outside of the vertebral column and pelvis) and/or visceral metastasis⁴⁸. This is indicative of advancing metastatic disease compared to LV-mHSPC patients⁴⁸. Lastly, we assessed metastatic castrate resistant prostate cancer (mCRPC) patients. These patients have disease progression while receiving androgen deprivation therapy such as increased tumor size or rising PSA levels⁵⁰. Patients with mCRPC may undergo systemic chemotherapy and/or radiation targeted at primary/metastatic sites, however there are currently no curative therapies in this setting and the range of survival for CRPC is 9-36 months⁵⁰. As such, mCRPC represents the disease stage where prostate cancer patients have the poorest prognoses and/or the most impaired quality of life⁵⁰.

Study population characteristics are summarized in **Table 3.1**. In all three cohorts, the majority of patients (72.4%) had a Gleason score of >6 and the majority of all metastases (86.2%) were to bone. For the LV-mHSPC group, most patients had ≤ 1 site of bone metastasis, whereas in the HV-mHSPC group the majority of patients had ≥ 8 sites of bone metastases. In all cohorts the majority of patients (with a known number of metastatic lesions) had 1 lesion per site. Of patients in the HV-mHSPC and mHSPC cohorts, 63.2% had metastases to the lymph node. In these two more advanced cohorts, 47.4% had visceral metastasis and the majority (with a known number of metastatic lesions) had 1 lesion per site. There was a large diversity of sites of bone and visceral metastasis, with few distinct patterns of reoccurring sites except 2 patients in each of HV-mHSPC and mCRPC groups that had visceral metastases to the lung.

3.3.2 CTC enumeration in metastatic prostate cancer patients is similar between CellSearch[®] and Parsortix[®]

We were first interested in determining if there were any differences in CTC enumeration ability between the epithelial-based CellSearch[®] versus the EMT-independent Parsortix[®] platforms in metastatic prostate cancer patients with increasingly progressive disease. Blood samples from a total of 29 patients in 3 cohorts (LV-mHSPC, HV-mHSPC, and mCRPC) were collected and used to enumerate CTCs with both platforms. In the LV-mHSPC cohort (n=10 patients), we observed a mean of 3.9 ± 7.7 CTCs with the CellSearch[®] and a mean of 3.6 ± 3.2 CTCs with the Parsortix[®] (**Figure 3.1a**). In the HV-mHSPC cohort (n=9 patients), we observed a mean of 305.1 ± 790.6 CTCs with the CellSearch[®] and 23.8 ± 35.4 CTCs with the Parsortix[®] (**Figure 3.1b**). In the mCRPC cohort (n=10 patients), we observed a mean of 33.3 ± 60.3 CTCs with the CellSearch[®]

Table 3-1. Patient Characteristics.

<i>N</i>	LV-mHSPC (10)	HV-mHSPC (9)	mCRPC (10)	Total
Gleason score				
≤6	2	1	4	7 (24.1%)
7	2	3	2	7 (24.1%)
8	2	2	0	4 (13.8%)
9	3	3	4	10 (34.5%)
Unknown	1	0	0	1 (3.4%)
Bone metastasis (BM)	7	9	9	25 (86.2%)
Number of sites of BM				
0	3	0	1	4 (13.8%)
1	3	0	0	3 (10.3%)
2	0	1	1	2 (6.9%)
3	4	1	1	6 (20.7%)
4	0	0	3	3 (10.3%)
5	0	2	0	2 (6.9%)
6	0	0	1	1 (3.4%)
8	0	1	1	2 (6.9%)
9	0	3	2	5 (17.2%)
10	0	1	0	1 (3.4%)
Number of lesions of BM				
1	7	23	38	68 (54.8%)
2	0	6	6	12 (9.7%)
3	0	2	1	3 (2.4%)
4	0	1	1	2 (1.6%)
6	0	1	0	1 (0.8%)
7	1	0	2	3 (2.4%)
Unknown	7	27	1	35 (28.2%)
Metastasis to lymph node	N/A	7	5	12 (63.2%)
Visceral metastasis (VM)	N/A	4	5	9 (47.4%)
Number of sites of VM	N/A			
0		5	5	10 (52.6%)
1		1	4	5 (26.3%)
2		2	1	4 (21.1%)
4		1	0	1 (5.3%)
Number of lesions of VM	N/A			
1		3	4	7 (46.7%)
2		0	2	2 (13.3%)
3		0	0	0 (0.0%)
4		1	0	1 (6.7%)
Unknown		5	0	5 (33.3%)
Lung as a site of VM	N/A	2	2	4 (21.1%)

and 7.3 ± 10.7 CTCs with the Parsortix® (**Figure 3.1c**). We did not observe any statistical differences in CTC enumeration between CTC platforms in any of the three patient cohorts (**Figure 3.1a-c**). However, in the HV-mHSPC and mCRPC cohorts (**Figure 3.1b,c**) we observed a trend towards higher CTC recovery using the epithelial-based CellSearch® compared to the EMT-independent Parsortix®. The presence of ≥ 5 CTCs in 7.5ml of blood has previously demonstrated to be prognostic for progressive metastatic disease and reduced overall survival in prostate cancer using CellSearch®^{5,6}. The red line on **Figures 3.1** and **3.2** identifies where 5 CTCs is on the y-axis. Individual patient CTC recovery using the CellSearch® and Parsortix® is summarized in **Table 3.2**.

3.3.3 CellSearch® identifies the presence of increased CTCs in HV-mHSPC versus LV-mHSPC prostate cancer patients

We next wanted to assess whether there were differences in the number of CTCs present between disease cohorts assessed by the same CTC analysis platform. We observed that there were a significantly greater number of CTCs identified in the HV-mHSPC cohort versus the LV-mHSPC group using the CellSearch® ($p \leq 0.05$) (**Figure 3.2a**). No significant differences between CTC number were observed between disease cohorts analyzed with the Parsortix® (**Figure 3.2b**).

3.3.4 HyCEAD chip analysis identified increased expression of 119 genes including 11 biologically relevant genes which may contribute to prostate cancer progression

After CTC enumeration and quantification, CellSearch® samples are not able to be used for any further analysis, however Parsortix® possesses the unique advantage whereby CTCs can be harvested for downstream mRNA analysis. This presents the opportunity to assess for unique mRNA species across all three patient cohorts in order to identify potential molecular markers of metastasis and/or EMT. Pre-analytical variables related to preservatives in CellSave and EDTA tubes were confirmed the ability the analyze samples from CellSave tubes using HyCEAD analysis prior to study sample evaluation (data not shown). HyCEAD analysis identified a total of 119 genes with increased expression in at least 1 patient across the 3 patient sample cohorts, where a >20 -fold increase in expression compared to NTC was considered significant. This included 49 genes identified using the PC chip (**Figure 3.3** and **Supplemental Tables 3.1, 3.2**) and 70 additional genes identified with the HE chip (**Figure 3.4** and **Supplemental Tables 3.1, 3.3**) ($n \geq$

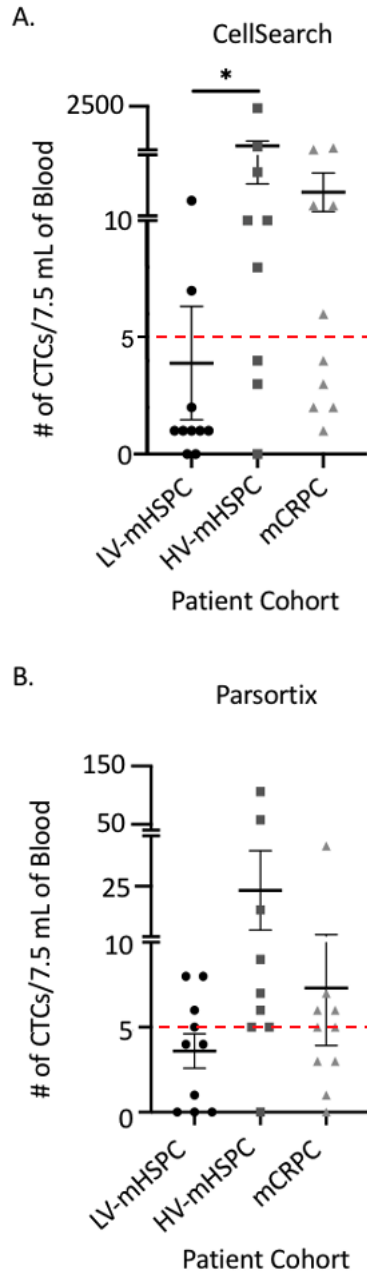


Figure 3.2. CellSearch® identifies the presence of increased CTCs in HV-mHSPC versus LV-mHSPC prostate cancer patients. Whole blood samples (7.5 ml) were collected from prostate cancer patients after informed consent and analyzed for CTCs using CellSearch® and Parsortix® as described in the Materials and Methods. Comparison between LV-mHSPC, HV-mHSPC, and mCRPC cohorts (n=9-10/cohort) using the (a) CellSearch® or (b) Parsortix® platforms for CTC enumeration. * = significantly different between patient cohorts ($p \leq 0.05$). Red line indicates pre-established CellSearch prognostic cut-off of ≥ 5 CTCs^{5,6}.

Table 3-2. Individual patient CTC recovery for each cohort using the CellSearch® and Parsortix®

Cohort	Patient	CellSearch® CTC Recovery	Parsortix® CTC Recovery
LV-mHSPC	1	1-----0	0
	2	7-----8	8
	3	2-----4	4
	4	1-----4	4
	5	0-----6	6
	6	1-----8	8
	7	1-----0	0
	8	1-----5	5
	9	25-----1	1
	10	0-----0	0
HV-mHSPC	1	2402-----106	106
	2	10-----18	18
	3	8-----5	5
	4	10-----58	58
	5	3-----9	9
	6	0-----0	0
	7	53-----6	6
	8	256-----7	7
	9	4-----5	5
mCRPC	1	2-----0	0
	2	87-----1	1
	3	188-----37	37
	4	1-----6	6
	5	3-----3	3
	6	20-----5	5
	7	6-----6	6
	8	20-----7	7
	9	2-----5	5
	10	4-----3	3

8/cohort). Interestingly, the HV-mHSPC cohort had the greatest number of altered transcripts (103 genes) followed the mCRPC cohort (89 genes) and the LV-mHSPC cohort (69 genes) (**Figures 3.3, Figure 3.4, and Supplemental Figure 3.1**).

Further investigation of the biological relevance of these transcripts via a PubMed literature search identified 3 genes whose lower expression has the potential to contribute to more advanced disease (**Table 3.3**). These genes had significantly higher expression in the LV-mHSPC cohort and less expression in the HV-mHSPC and/or mCRPC cohorts. Additional analysis also identified 16 genes whose higher expression may contribute to more advanced disease (**Table 3.4**). These genes had significantly lower expression in the LV-mHSPC cohort and higher expression in the HV-mHSPC and/or mCRPC cohorts. Notably, 11 of the genes with differential expression in one or more patients between the cohorts have established links to EMT and/or invasive behavior, including NKX3-1, TOP2A, ERG, GHR, PRSS8, ITGBL1, NID2, ZNF217, VEGFA, MAP2K7, and ST14⁵¹⁻⁶¹.

Finally, we were interested in examining the expression of genes identified by CTC HyCEAD analysis in our prostate patient cohorts relative to a larger patient dataset. We thus analyzed the 19 identified potentially biologically relevant HyCEAD genes using TCGA and [Ualcan](#) online clinical databases (accessed December 12, 2021). We observed significantly lower expression of 2 of the 3 identified HyCEAD downregulated genes (FAM107A and FERMT2) in primary prostate cancer patient tumors (n = 497) compared to normal prostatic samples (n=52) ($p \leq 0.05$) (**Figure 3.5a**). Additionally, all 3 of these genes (FAM107A, FERMT2, and NKX3-1) had significantly lower expression in metastatic prostate cancer patients (n = 44) relative to non-metastatic prostate cancer patients (n = 497) ($p \leq 0.05$) (**Figure 3.5b**). We also observed significantly higher expression of 9 of the 16 identified HyCEAD upregulated genes (TOP2A, ERG, CCNE2, GHR, VSTM2L, PRSS8, ITGBL1, ST14, and ZNF217) in primary prostate cancer patient tumors (n = 497) compared to normal prostatic samples (n = 44) (**Figure 3.6a**), with 4 genes (TOP2A, ERG, CCNE2, and GHR) also having significantly higher expression in metastatic prostate cancer patients (n = 44) relative to non-metastatic prostate cancer patients (n = 497) ($p \leq 0.05$) (**Figure 3.6b**). Lastly, patients with high expression of TBP (n=125) had decreased overall survival compared to patients with low expression (n=372) ($p = 0.0038$) (**Figure 3.6c**).

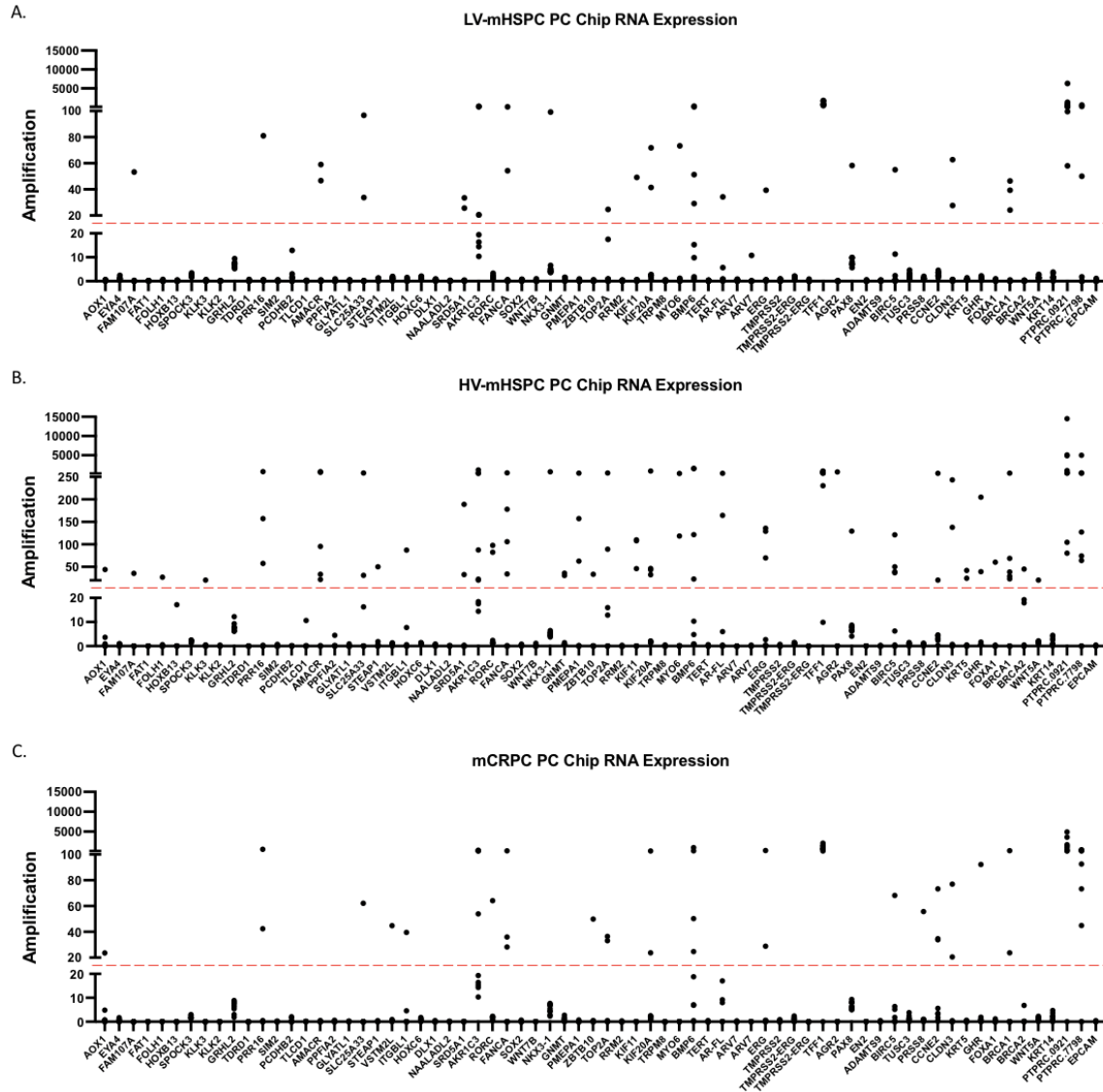


Figure 3.3. HyCEAD prostate cancer (PC) chip analysis identified 49 genes with increased expression in the three prostate cancer patient cohorts. Patient CTCs were isolated using Parsortix® using the harvest protocol and dissolved in Dynabead® RNA lysis buffer as a pooled CTC population for each individual patient. CTC samples were assessed for RNA expression using HyCEAD Zplex chip technology (Angle PLC). Samples with an amplification of >20 compared to the average NTC amplification were considered overexpressed. (a-c) HyCEAD prostate cancer (PC) chip analysis identified increased expression of genes (*above the red line*) in all three cohorts compared to NTC control, including (a) 21 genes in the LV-mHSPC cohort; (b) 36 genes in the HV-mHSPC cohort; and (c) 20 genes in the CRPC cohort ($n \geq 8$ patient samples/cohort).

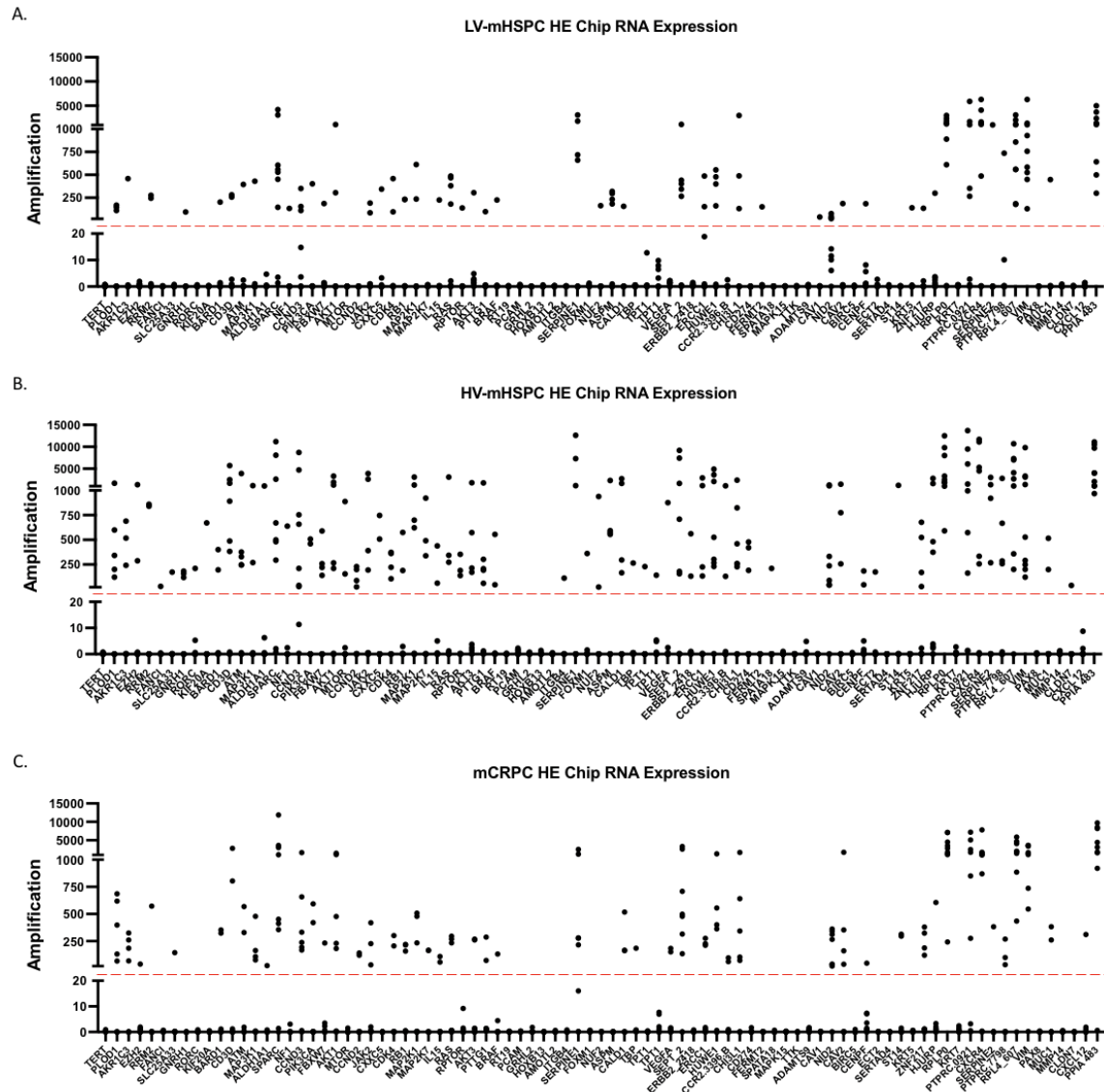


Figure 3.4. HyCEAD high expression chip analysis identified 70 genes with increased expression in the three prostate cancer patient cohorts. Patient CTCs were isolated using Parsortix® using the harvest protocol and dissolved in Dynabead® RNA lysis buffer as a pooled CTC population for each individual patient. CTC samples were assessed for RNA expression using HyCEAD Zplex chip technology (Angle PLC). Samples with an amplification of >20 compared to the average NTC amplification were considered over expressed. HyCEAD high expression (HE) chip analysis identified increased expression of genes (*above the red line*) in all three cohorts compared to NTC control, including (*a*) 48 genes in the LV-mHSPC cohort; (*b*) 67 genes in the HV-mHSPC cohort and (*c*) 69 genes in the mCRPC cohort ($n \geq 8$ patient samples/cohort).

Table 3-3. Expression and functional relevance of HyCEAD-identified genes that lose expression in CTCs with advancing prostate cancer disease progression

Gene name	Average expression/group			Loss of function contributes to cancer progression
	LV-HSPC	HV-HSPC	mCRPC	
Prostate cancer chip				
NKX3-1	15.2±31.5	82.5±282.5	5.4±2.0	Tumor suppressor downregulated in mPC ⁵¹
FAM107A	6.1±17.7	3.9±11.8	0±0	Inhibits the progression of PC ⁶²
High expression chip				
FERMT2	17.0±50.6	0±0	0±0	Tumor suppressor in OC and CRC ⁶³

PC-Prostate cancer, mPC- Metastatic prostate cancer, OC- Ovarian cancer, CRC- Colorectal cancer

Table 3-4. Expression and functional relevance of HyCEAD-identified genes that gain expression in CTCs with advancing prostate cancer disease progression

Gene name	Average expression/group			Gain of function contributes to cancer progression
	LV-HSPC	HV-HSPC	mCRPC	
Prostate cancer chip				
TOP2A	5.1±9.3	57.5±131.3	7.8±15.3	Associated with PC progression ⁶⁴
ERG	4.7±13.0	37.6±58.4	28.9±75.7	Overexpression promotes metastasis in PC ⁵⁴
CCNE2	3.4±2.0	38.0±98.1	17.4±25.1	Associated with poor prognosis in BC ⁶⁵
GHR	1.4±1.0	27.7±67.6	10.8±30.5	Promotes growth/metastasis in PaC ⁵⁵
VSTM2L	1.3±1.0	3.0±0.7	5.3±14.8	Associated with chemoresistance in RC ⁶⁶
PRSS8	1.3±0.5	2.2±0.5	6.7±18.4	Suppresses tumor growth/metastasis in HC ⁵⁶
ITGBL1	0.8±0.8	2.0±10.7	4.9±13.1	Promotes EMT, invasion and migration in PC ⁵⁷
High expression chip				
PIK3CA	44.6±133.8	107.4±213.5	112.7±227.6	Increases cell division in PC ^{67,68}
NID2	24.4±24.4	345.4±489.0	153.2±161.6	Linked to poor prognosis and invasion ⁵⁸
BARD1	22.8±67.2	66.4±141.1	75.6±149.6	Isoforms are linked to poor outcomes ⁶⁹
CAV2	20.8±62.0	276.4±512.1	252.8±564.1	Associated with PC progression ⁷⁰
ZNF217	15.3±44.9	155.6±260.9	112.9±152.0	Promotes PC tumor growth ⁵⁹
VEGFA	1.1±0.8	97.7±292.0	37.7±74.2	Associated with tumor recurrence in PC ⁷¹
TBP	0.2±0.3	29.7±88.4	20.8±61.3	Drives VEGFR expression in colon cancer ⁶⁰
MAP2K7	0.2±0.3	194.8±329.1	36.8±73.0	Cancer stemness/EMT associated gene ⁶¹
ST14	0.1±0.1	135.1±405.2	68.0±134.4	Linked to BC metastasis/poor survival ⁵³

PC-Prostate cancer, PaC- Pancreatic cancer, BC-Breast cancer, RC- Rectal Cancer, HC, Hepatocellular carcinoma

- ≥2 patients/group with increased expression (amplification of >20 compared to NTC)
- 1 patient/group with increased expression (amplification of >20 compared to NTC)
- 0 patients/group with increased expression (amplification of >20 compared to NTC)

3.4 Discussion

Prostate cancer remains a leading cause of cancer diagnosis and cancer-related death in American men¹. The majority of deaths from prostate cancer are due to metastatic, castrate-resistant disease, as current therapies are largely non-curative in this setting^{2,3}. Further insight into the biology of disease progression and metastasis is therefore essential in order to develop better strategies for treatment. In addition, the use of Gleason score and/or prostate-specific antigen (PSA) levels is helpful but imperfect for predicting disease outcome, and this uncertainty often results in under-treatment or over-treatment of prostate cancer patients⁴. There is therefore a clear need for improved biomarkers such as circulating tumor cells (CTCs) that can be used to accurately assess disease progression and treatment response.

The current study assessed CTCs in metastatic prostate cancer patients at different disease progression stages along the spectrum of hormone-sensitive to castrate-resistant. Overall, we assessed CTCs from 29 prostate cancer patients using the epithelial-based CellSearch® and the EMT-independent Parsortix® CTC analysis platforms. The least aggressive cohort examined was low-volume metastatic hormone sensitive prostate cancer (LV-mHSPC)⁴⁴, the “middle” cohort was high-volume metastatic hormone sensitive prostate cancer (HV- mHSPC)⁴⁴, and the most advanced cohort was metastatic castrate-resistant prostate cancer (mCRPC)^{5,6}. We hypothesized that as the disease cohorts became more advanced, we would observe a greater number of CTCs overall, as well as increased CTC capture by the EMT-independent Parsortix® compared to the epithelial-based CellSearch® based on a predicted evolution of CTCs to a more mesenchymal phenotype.

Interestingly, we did not see any significant differences in CTC enumeration between technologies within any of the patient cohorts. This highlights that Parsortix® is able to capture and enumerate CTCs just as effectively as CellSearch®; the clinical “gold standard” based on its FDA- and Health Canada approved status^{10,11}. We also assessed differences in CTC enumeration between the 3 progressive patient cohorts and observed significantly greater CTC numbers in the HV-mHSPC cohort relative to the LV-mHSPC cohort using the CellSearch®. Although this result was in contrast to our original hypothesis that the EMT-independent Parsortix® would have enhanced CTC capture in the more

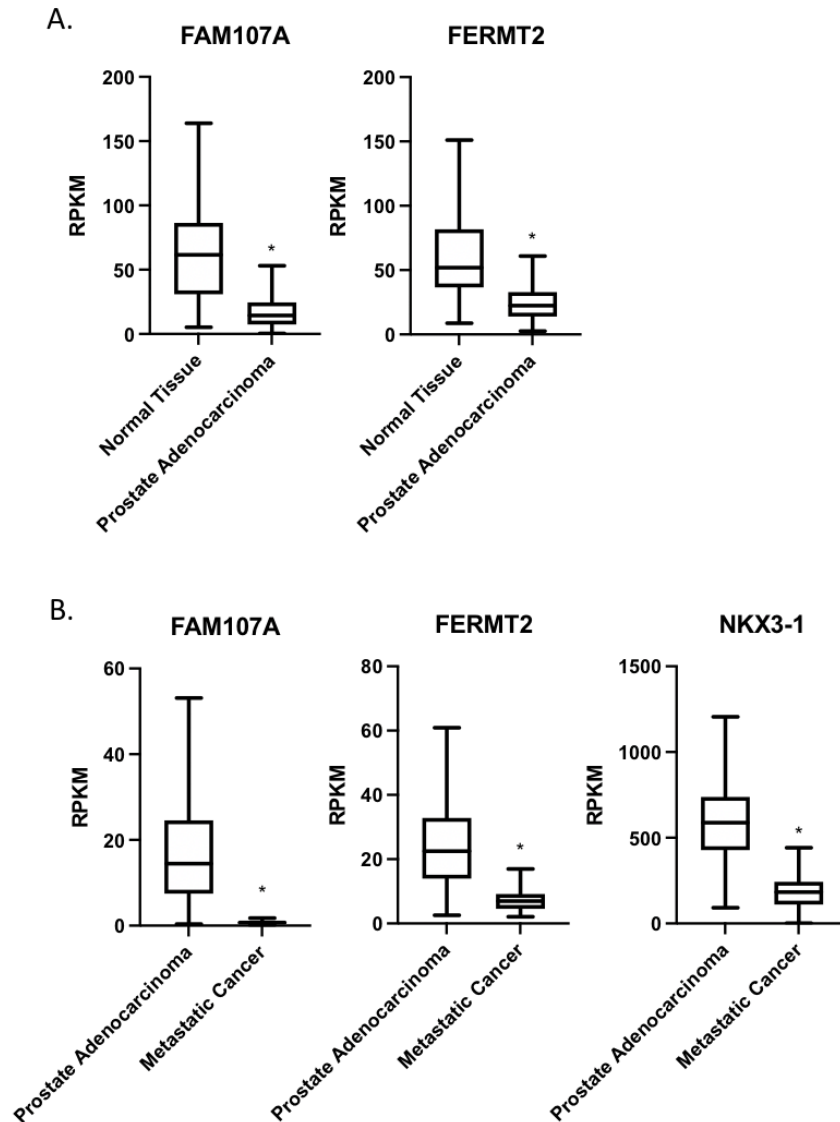


Figure 3.5. TCGA analysis reveals that FAM107A, FERMT2, and NKX3-1 have lower expression in prostate cancer patients with primary and/or metastatic disease. Ualcan analysis identified lower expression of (a) FAM107A and FERMT2 in primary prostate cancer tumors (n = 497) compared to normal prostatic samples (n = 52); and lower expression of (b) FAM107A, FERMT2, and NKX3-1 in metastatic prostate cancer (n = 44) vs. non-metastatic prostate cancer (n = 497). * = significant difference between patient groups ($p \leq 0.05$).

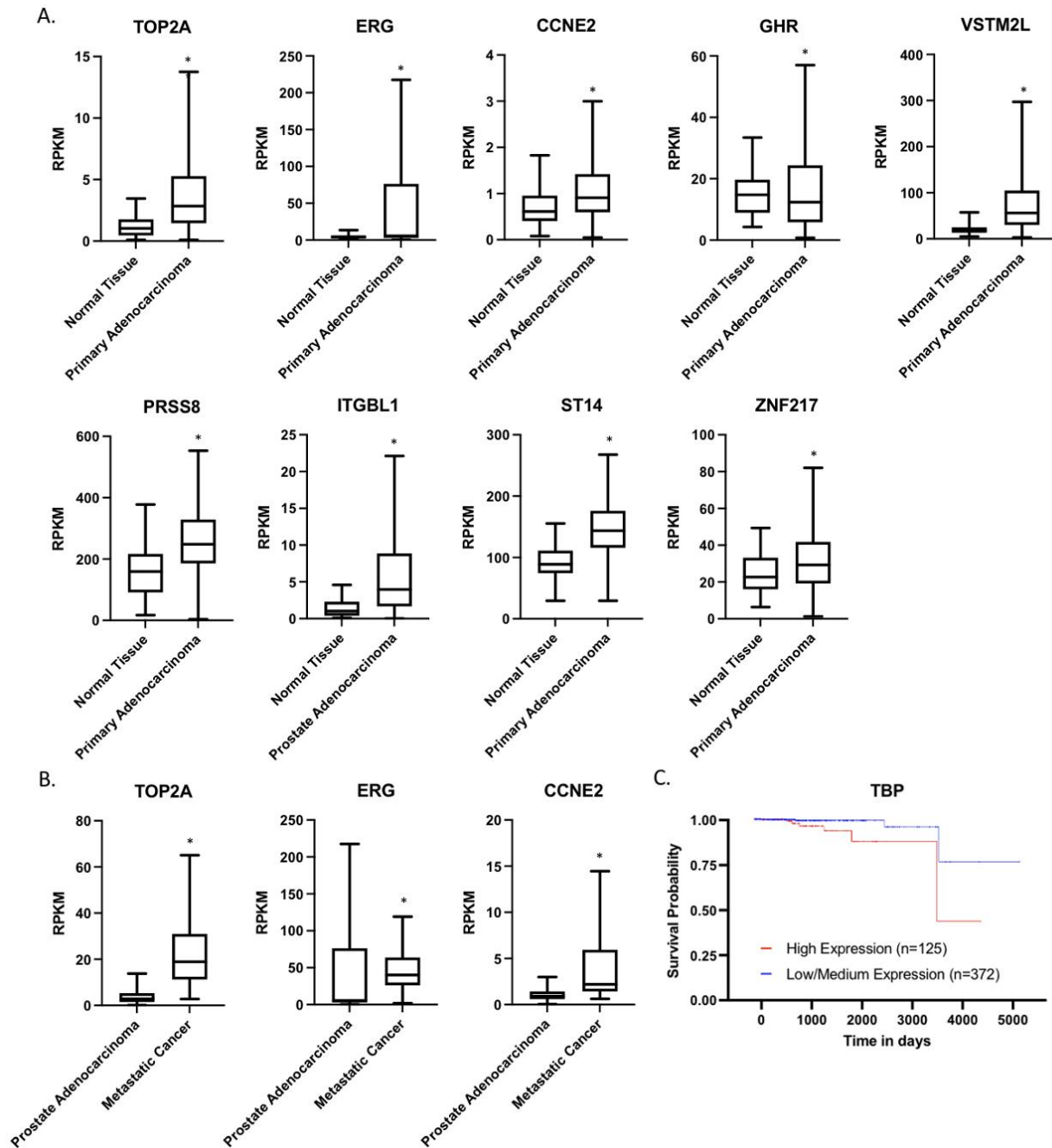


Figure 3.6. TCGA analysis reveals that **TOP2A**, **ERG**, **CCNE2**, **GHR**, **VSTM2L**, **PRSS8**, **ITGBL1**, **ST14**, **ZNF217**, and **TBP** have higher expression in prostate cancer patients with primary and/or metastatic disease. Ualcan analysis identified higher expression of (a) TOP2A, ERG, CCNE2, GHR, VSTM2L, PRSS8, ITGBL1, ST14 and ZNF217 in primary prostate cancer tumors (n = 502) compared to normal prostatic samples (n = 50), and higher expression of (b) TOP2A, ERG, and CCNE2 in metastatic prostate cancer (PC) (n = 44) vs. non-metastatic prostate cancer (n = 497). * = significant difference between patient groups ($p \leq 0.05$). (c) Decreased overall survival in prostate cancer patients with high expression of TBP (n=125) compared to patients with low expression of TBP (n=372) ($p = 0.0038$).

advanced disease cohorts compared to the epithelial-based CellSearch®, it does highlight the ability of both platforms to capture CTCs throughout disease progression, thus providing support for the continued clinical use of CellSearch® for prostate cancer patients at all stages of metastatic progression.

The observation that the HV-mHSPC cohort (versus the more advanced mCRPC cohort) had the greatest number of CTCs was also somewhat unexpected and provided a rationale for further CTC analysis at the molecular level, something that is only feasible with the Parsortix® but not the CellSearch®⁷³. Assessing patient CTCs is becoming increasingly more important within the context of personalized medicine and advancing the utility of CTC research⁷⁴. In support of this, ANGLE has developed a novel RNA analysis approach that can be used in conjunction with the Parsortix® CTC harvest protocol. This HyCEAD mRNA assay uses multiplex (Ziplex) technology to assess up to 100 genes/chip with as little as 1 CTC per sample⁴³. In the current study, we used HyCEAD to assess the expression of 155 genes in individual pooled CTC populations from 27 of our 29 patients using two analysis chips (prostate cancer [PC] and high expression [HE]). Using these two chips, we were able to identify a total of 119 genes with increased expression among the 3 patient cohorts. Importantly, 3 of the genes that demonstrated lower expression as our disease cohorts became more advanced (NKX3-1, FAM107A, and FERMT2) have previously been shown to have a loss of function during cancer progression^{51,62,63}. Additionally, 16 of the genes that demonstrated higher expression as our disease cohorts became more advanced (TOP2A, ERG, CCNE2, GHR, VSTM2L, PRSS8, ITGBL1, PIK3CA, NID2, BARD1, CAV2, ZNF217, VEGFA, TBP, MAP2K7, and ST14) have been associated with a gain of function as cancer progresses^{53-61,64-71}.

We then further validated these 19 potentially biologically significant genes in a larger cohort of prostate cancer patient tissues samples using the TCGA online database. We observed that 2 of 3 of the identified lower expression HyCEAD genes (FAM107A and FERMT2) have decreased expression in prostate tumor tissue compared to normal prostatic tissue, with FAM107A, FERMT2, and NKX3-1 also having decreased expression in metastatic prostate cancer compared to primary tumors. Similarly, of the genes that HyCEAD identified as having higher expression in the more advanced cohorts, 9 of 16 genes (TOP2A, ERG, CCNE2, GHR, VSTM2L, PRSS8, ITGB1, ST14, and ZNF217) were validated through TCGA as having increased expression in

prostate tumor tissue compared to normal tissue. TOP2A, ERG, CCNE2, and GHR also had higher expression in metastatic prostate cancer compared to primary tumors, and increased TBP expression was correlated with decreased overall survival.

Notably, 11 of the identified HyCEAD genes with differential expression between cohorts have been identified within the literature as being involved in processes that promote cancer aggressiveness including EMT and partial-EMT, metastasis, invasion, proliferation, cell motility, and cancer stemness. Specifically, NKX3-1 has been shown as a prostatic tumor suppressor gene and a marker of metastatic prostate cancer carcinoma⁵¹. TOP2A has been shown to promote cell migration, invasion, and EMT in cervical cancer⁵². ERG is associated with prostate cancer progression through gene fusion in the promoter region of the androgen-induced TMPRSS2 gene⁵⁴. GHR has been shown to induce molecular mechanisms that cause EMT⁵⁵. The downregulation of PRSS8 is associated with suppression of tumor growth and metastasis in hepatocellular carcinoma⁵⁶. ITGBL1 has been shown to promote EMT, invasion, and migration in prostate cancer. NID2 promotes invasion and migration in gastric cancer⁵⁸. ZNF217 is associated with invasion, metastasis, and EMT⁸³. VEGFA increases motility, and invasion through Slug induction in breast cancer cells⁸⁴. Upregulation of MAP2K7 is associated with cancer stemness⁶¹. Lastly, ST14 is involved in the metastasis of breast cancer and poor survival. The HyCEAD analysis of these CTCs demonstrates substantial differences within and between metastatic patient cohorts which was not apparent through CTC enumeration alone. This underscores the importance of downstream molecular CTC characterization for elucidating the biology of EMT, its impact on disease progression, and the resulting implications for personalized medicine.

In summary, the results of this study support the continued clinical use of CellSearch® for enumerating CTCs in all progression stages of metastatic prostate cancer. Our findings also support the combined implementation of Parsortix® and HyCEAD for CTC enumeration, harvest, and downstream analysis after further validation studies. In particular, the HyCEAD molecular characterization of CTCs in this study provides a promising panel of potential biomarkers that could be used alone or as a molecular signature in order to develop a comprehensive, real-time CTC liquid biopsy strategy for the personalized clinical management of metastatic prostate cancer patients in the future.

3.5 Supplemental Data – Chapter 3

Supplemental Table 3-1. HyCEAD gene expression panels used to analyze prostate cancer CTC samples.

Prostate Cancer (PC) Chip					
ADAMTS9	CCNE2	FOXA1	KLK3	PRSS8	TERT
AGR2	CLDN3	GHR	KRT14	PTPRC	TFF1
AKR1C3	DLX1	GLYATL1	KRT5	RORC	TLCD1
AMACR	EN2	GNMT	MYO6	RRM2	TMPRSS2
AOX1	EPCAM	GRHL2	NAALADL2	SIM2	TMPRSS2-ERG
AR-FL	ERG	HOXB13	NKX3-1	SLC25A33	TOP2A
ARV7	EYA4	HOXC6	PAX8	SOX2	TRPM8
BIRC5	FAM107A	ITGBL1	PCDHB2	SPOCK3	TUSC3
BMP6	FANCA	KIF11	PMEPA1	SRD5A1	VSTM2L
BRCA1	FAT1	KIF20A	PPFIA2	STEAP1	WNT5A
BRCA2	FOLH1	KLK2	PRR16	TDRD1	
High Expression (HE) Chip					
ADAMTS9	CCND3	FANCI	MAP2K1	PTPRC	SPARC
AKR1C3	CCR2	FBXW7	MAP2K7	PTTG1	SPATA18
AKT1	CD274	FERMT2	MAP3K1	RAS	ST14
AKT3	CD3D	FOXM1	MAPK15	RB1	TBP
ALDH1A1	CDK4	GNRH1	MMP14	RORC	TERT
AMOTL2	CENPF	GRHL2	MTOR	RPL4	TPT1
ASPM	CHI3L1	HJURP	MUC1	RPLP0	TTK
ATM	CLDN7	HOXB13	NF1	RPTOR	VEGFA
BARD1	CXCL12	HUWE1	NID2	RRM2	VIM
BIRC5	CXCR4	IL15	NUF2	RT19	ZNF217
BRAF	CXXC5	ITGB4	PAX8	SEPT2	
CALD1	ECT2	JAK2	PCAM	SERPINE1	
CAV1	ERBB2	KIF20A	PIK3CA	SERPINE2	
CAV2	ERCC1	KRT5	PLOD1	SERTAD4	
CCND2	EZH2	KRT7	PPIA	SLC25A33	

Supplemental Table 3-2. Summary of HyCEAD Prostate Cancer (PC) chip gene expression analysis^a

LV-mHSPC							
Gene Name	Average Expression						
TFF1	1126.9±486.7	KIF20A	14.3±25.2	MOY6	8.6±24.3	AR-FL	4.9±11.2
AKR1C3	81.5±94.4	PAX8	14.0±16.6	BIRC5	7.9±18.1	ERG	4.7±13.0
BMP6	58.9±101.0	BRCA1	12.4±19.1	SRD5A1	6.8±13.1		
FANCA	21.9±48.0	AMACR	11.9±23.4	FAM107A	6.1±17.7		
NKX3	15.2±31.5	CLDN3	10.4±21.6	KIF11	5.7±16.3		
SLC25A33	14.6±32.7	PRR16	9.2±26.9	TOP2A	5.1±9.3		
HV-mHSPC							
TFF1	474.2±274.8	PMEP1	63.9±121.3	KIF11	29.3±47.6	KRT5	.5±15.2
BMP6	364.2±678.0	TOP2A	57.5±131.3	BIRC5	28.2±40.2	FOXA1	6.8±20.1
AKR1C3	230.3±386.9	BRCA1	54.9±107.4	GHR	27.7±67.6	STEAP1	5.9±16.6
AMACR	160.6±282.8	AR-FL	51.8±106.1	SRD5A1	24.7±62.6	AOX1	5.5±14.5
KIF20A	116.4±300.6	SLC25A33	46.7±122.7	RORC	21.2±39.2	FAM107A	3.9±11.8
PRR16	109.0±251.9	MYO6	42.8±92.5	PAX8	20.6±40.8	ZBTB10	3.8±11.2
FANCA	83.2±144.4	CLDN3	42.6±88.0	ITGBL1	10.7±28.9	WNT5A	3.7±6.3
NKX3-1	82.5±232.5	CCNE2	38.0±98.1	BRCA2	9.2±15.6	FOLH1	3.1±9.0
AGR2	72.3±216.8	ERG	37.6±58.4	GNMT	8.0±14.3	KLK3	2.4±6.8
mCRPC							
TFF1	861.1±677.5	BRCA1	26.0±69.4	GHR	10.8±30.5	PRSS8	6.7±18.4
BMP6	138.4±317.5	FANCA	24.2±50.5	BIRC5	9.1±22.3	ZBTB10	5.7±16.6
AKR1C3	78.3±101.9	CCNE2	17.4±25.1	RORC	8.5±20.9	VSTM2L	5.3±14.8
PRR16	64.3±177.4	KIF20A	16.0±35.4	TOP2A	7.8±15.3	ITGBL1	4.9±13.1
ERG	28.9±75.7	CLDN3	10.9±25.7	SLC25A33	6.9±20.7	AOX1	3.4±7.7

^a Samples with an amplification of >20 compared to the average NTC amplification were considered overexpressed.

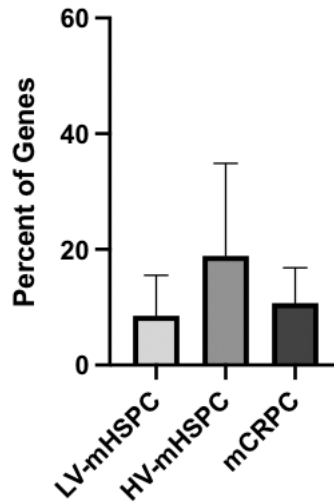
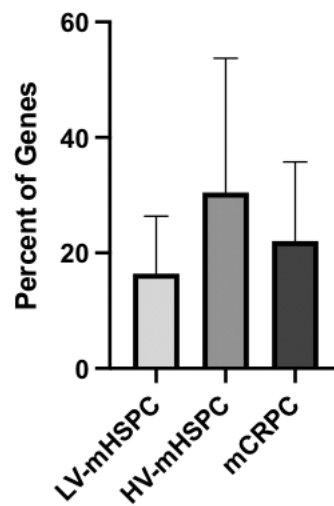
- ≥2 patients/group with increased expression (amplification of >20 compared to NTC)
- 1 patient/group with increased expression (amplification of >20 compared to NTC)

Supplemental Table 3-3. Summary of HyCEAD High Expression (HE) chip gene expression analysis^a

LV-mHSPC							
Gene Name	Average Expression						
PPIA	1816.8±1596.7	SERPINE2	116.0±348.0	PLOD1	47.2±72.4	FBXW7	21.3±62.3
CXCR4	1670.2±2164.5	ASPM	114.8±141.0	PIK3CA	44.6±133.8	CAV2	20.8±62.0
VIM	1349.6±1893.3	MAP2K1	94.3±209.6	ATM	44.2±131.6	NUF2	18.1±54.4
RPLP0	1263.9±1025.0	ERCC1	73.3±162.9	CXXC5	38.6±114.5	CALD1	17.5±52.4
RPL4	1081.1±947.6	CCND3	70.5±119.8	AKT3	35.7±101.2	FERMT2	17.0±50.6
SPARC	1064.1±1504.9	CDK4	61.7±152.1	HJURP	34.6±99.4	KRT5	15.9±47.2
SERPINE1	700.6±1088.6	CD3D	60.4±118.8	JAK2	31.3±66.8	RPTOR	15.4±46.2
CHI3L1	402.2±987.2	RRM2	58.1±115.2	BRAF	25.3±75.3	ZNF217	15.3±44.9
SEPT2	289.3±373.0	RB1	51.7±102.4	IL15	25.2±75.4	NF1	14.9±44.7
HUWE1	177.4±234.5	AKR1C3	51.1±153.1	NID2	24.4±24.4	PTTG1	11.2±32.8
RAS	168.9±217.2	MUC1	49.9±149.6	BARD1	22.8±67.2	GNRH1	10.5±31.6
AKT1	159.4±377.3	MAP3K1	48.0±143.6	CENPF	22.4±60.8	CAV1	4.5±13.4
HV-mHSPC							
PPIA	4940.4x±4292.3	CALD1	535.4±972.7	CCR2	138.1±367.3	BARD1	66.4±141.1
RPLP0	4603.2±4344.1	CHI3L1	491.8±762.8	ST14	135.1±405.2	CCND2	59.9±91.9
RPL4	3703.9±3836.6	ERCC1	487.3±975.1	FBXW7	134.4±200.2	IL15	56.3±145.0
CXCR4	3687.7±4824.0	ASPM	446.8±748.4	CD274	121.1±196.7	GNRH1	51.1±78.3
SPARC	2646.9±4114.0	RAS	413.0±1016.1	CDK4	118.2±160.2	FOXO1	40.5±120.6
SERPINE1	2336.5±4530.0	NID2	345.4±489.0	ALDH1A1	116.6±347.4	TBP	29.7±88.4
SEPT2	2143.5±3558.6	PLOD1	328.4±549.9	MTOR	116.1±293.9	CENPF	26.5±61.3
VIM	2110.0±3140.7	AKT3	308.4±593.5	PIK3CA	107.4±213.5	TPT1	25.3±76.0
CCND3	1677.1±3029.7	PTTG1	280.7±566.8	NUF2	106.8±311.8	RORC	24.0±69.8
HUWE1	1323.5±1804.1	CAV2	276.4±512.1	VEGFA	97.7±292.0	SPATA18	23.4±70.2
CD3D	1291.9±1859.7	MAP2K7	194.8±329.1	RB1	85.3±193.8	ECT2	19.6±58.4
JAK2	787.1±1439.0	RRM2	189.0±375.1	MUC1	79.5±176.5	SLC25A33	19.3±57.9
AKT1	775.9±1168.6	EZH2	184.0±453.9	ERBB2	77.4±186.9	TPT1	17.0±46.8
MAP2K1	633.0±1031.1	AKR1C3	160.9±266.4	RPTOR	76.0±126.9	ITGB4	12.5±37.4
SERPINE2	614.3±1019.8	MAP3K1	156.7±379.1	KIF20A	74.5±223.6	CLDN7	4.3±12.9
HJURP	582.4±974.9	ZNF217	155.6±260.9	NF1	71.3±213.0	FANCI	3.3±9.7
ATM	565.6±1257.5	CXXC5	139.3±282.9	BRAF	66.8±183.9		
mCRPC							
PPIA	4241.2±3660.5	CAV2	252.8±564.1	BARD1	75.6±149.6	CCND2	29.2±58.2
RPLP0	3262.9±2530.6	PLOD1	211.3±281.3	MUC1	71.5±145.1	FBXW7	26.6±77.5
RPL4	2366.2±2045.4	NID2	153.2±161.6	HJURP	68.2±201.5	TBP	20.8±61.3
SPARC	2306.7±3824.4	MAP2K1	135.6±216.7	ST14	68.0±134.4	IL15	18.5±39.0
VIM	1777.1±1400.1	ZNF217	112.9±152.0	RB1	66.0±100.0	CCR2	17.7±35.7
CXCR4	1559.0±2431.3	PIK3CA	112.7±227.6	RRM2	63.7±190.9	SLC25A33	16.1±48.1
SEPT2	892.6±1202.7	ATM	99.9±206.4	AKT3	59.3±116.8	BRAF	15.2±43.7
SERPINE1	502.5±844.0	CALD1	94.1±173.9	CDK4	56.4±114.5	CENPF	7.6±15.1
CD3D	400.6±938.2	AKR1C3	93.4±129.7	SERPINE2	42.6±127.6	EZH2	4.7±12.7
AKT1	385.9±545.1	MAP3K1	92.0±157.0	PTTG1	40.7±95.5	ALDH1A1	2.9±8.2
CCND3	360.5±527.8	RAS	89.1±134.0	VEGFA	37.7±74.2		
CHI3L1	316.1±557.3	ERCC1	79.8±120.1	MAP2K7	36.8±73.0		
HUWE1	293.4±443.0	JAK2	75.8±148.8	CXCL12	35.0±03.7		

^a Samples with an amplification of >20 compared to the average NTC amplification were considered overexpressed.

- ≥2 patients/group with increased expression (amplification of >20 compared to NTC)
 1 patient/group with increased expression (amplification of >20 compared to NTC)

A. Upregulated Genes on the PC chip**B. Upregulated Genes on the HE chip**

Supplemental Figure 3-1. Percent of upregulated genes in each cohort. Each sample was assessed for the percent of upregulated genes (>20 amplification) compared to NTCs. (n ≥ 8/cohort).

3.6 References

1. Siegel RL, Miller KD, Jemal A. Cancer statistics, 2020. *CA Cancer J Clin.* 2020. doi:10.3322/caac.21590
2. Chambers AF, Groom AC, MacDonald IC. Dissemination and growth of cancer cells in metastatic sites. *Nat Rev Cancer.* 2002;2(8):563-572. doi:10.1038/nrc865
3. Pantel K, Brakenhoff RH. Dissecting the metastatic cascade. *Nat Rev Cancer.* 2004. doi:10.1038/nrc1370
4. Lilja H, Ulmert D, Vickers AJ. Prostate-specific antigen and prostate cancer: Prediction, detection and monitoring. *Nat Rev Cancer.* 2008. doi:10.1038/nrc2351
5. Danila DC, Heller G, Gignac GA, et al. Circulating tumor cell number and prognosis in progressive castration-resistant prostate cancer. *Clin Cancer Res.* 2007. doi:10.1158/1078-0432.CCR-07-1506
6. De Bono JS, Scher HI, Montgomery RB, et al. Circulating tumor cells predict survival benefit from treatment in metastatic castration-resistant prostate cancer. *Clin Cancer Res.* 2008. doi:10.1158/1078-0432.CCR-08-0872
7. Goldkorn A, Ely B, Quinn DI, et al. Circulating tumor cell counts are prognostic of overall survival in SWOG S0421: A phase III trial of docetaxel with or without atrasentan for metastatic castration-resistant prostate cancer. *J Clin Oncol.* 2014;32(11):1136-1142. doi:10.1200/JCO.2013.51.7417
8. Allan AL, Keeney M. Circulating tumor cell analysis: Technical and statistical considerations for application to the clinic. *J Oncol.* 2010;2010. doi:10.1155/2010/426218
9. Tibbe AGJ, Miller MC, Terstappen LWMM. Statistical considerations for enumeration of circulating tumor cells. *Cytom Part A.* 2007;71(3):154-162. doi:10.1002/cyto.a.20369
10. Ferreira MM, Ramani VC, Jeffrey SS. Circulating tumor cell technologies. *Mol Oncol.* 2016;10(3):374-394. doi:10.1016/j.molonc.2016.01.007
11. Lowes LE, Allan AL. Recent advances in the molecular characterization of circulating tumor cells. *Cancers (Basel).* 2014;6(1):595-624. doi:10.3390/cancers6010595
12. Biosystems M-S. CellSearch CTC Test. <https://www.cellsearchctc.com>. Published 2021.
13. Allard WJ, Matera J, Miller MC, et al. Tumor cells circulate in the peripheral blood of all major carcinomas but not in healthy subjects or patients with nonmalignant diseases. *Clin Cancer Res.* 2004;10(20):6897-6904. doi:10.1158/1078-0432.CCR-04-0378
14. Nauseef JT, Henry MD. Epithelial-to-mesenchymal transition in prostate cancer: Paradigm or puzzle? *Nat Rev Urol.* 2011;8(8):428-439. doi:10.1038/nrurol.2011.85

15. Kalluri R, Weinberg RA. The basics of epithelial-mesenchymal transition. *J Clin Invest.* 2009;119(6):1420-1428. doi:10.1172/JCI39104
16. Thiery JP, Acloque H, Huang RYJ, Nieto MA. Epithelial-Mesenchymal Transitions in Development and Disease. *Cell.* 2009. doi:10.1016/j.cell.2009.11.007
17. Gupta PB, Chaffer CL, Weinberg RA. Cancer stem cells: Mirage or reality? *Nat Med.* 2009;15(9):1010-1012. doi:10.1038/nm0909-1010
18. Hess D, Alison A. Migratory strategies of normal and malignant stem cells. *Stem Cell Migr.* 2011;750:25-44.
19. Jolly MK. Implications of the Hybrid Epithelial/Mesenchymal Phenotype in Metastasis. *Front Oncol.* 2015;5. doi:10.3389/fonc.2015.00155
20. Gleason D. Classification of prostatic carcinomas. *Cancer Chemother Rep.* 1966;50(3):125-128.
21. De Marzo AM, Knudsen B, Chan-Tack K, Epstein JI. E-cadherin expression as a marker of tumor aggressiveness in routinely processed radical prostatectomy specimens. *Urology.* 1999;53(4):707-713. doi:10.1016/S0090-4295(98)00577-9
22. Schaafsma HE, Bringuier PP, Oosterhof GON, Debruyne FMJ, Schalken JA. Decreased E-Cadherin Expression Is Associated with Poor Prognosis in Patients with Prostate Cancer. *Cancer Res.* 1994;54(14):3929-3933.
23. Jaggi M, Nazemi T, Abrahams NA, et al. N-cadherin switching occurs in high Gleason grade prostate cancer. *Prostate.* 2006;66(2):193-199. doi:10.1002/pros.20334
24. Kwok WK, Ling MT, Lee TW, et al. Up-regulation of TWIST in prostate cancer and its implication as a therapeutic target. *Cancer Res.* 2005;65(12):5153-5162. doi:10.1158/0008-5472.CAN-04-3785
25. Lang SH, Hyde C, Reid IN, et al. Enhanced expression of vimentin in motile prostate cell lines and in poorly differentiated and metastatic prostate carcinoma. *Prostate.* 2002;52(4):253-263. doi:10.1002/pros.10088
26. Poblete CE, Fulla J, Gallardo M, et al. Increased SNAIL expression and low syndecan levels are associated with high Gleason grade in prostate cancer. *Int J Oncol.* 2014;44(3):647-654. doi:10.3892/ijo.2014.2254
27. Whiteland H, Spencer-Harty S, Thomas DH, et al. Putative prognostic epithelial-to-mesenchymal transition biomarkers for aggressive prostate cancer. *Exp Mol Pathol.* 2013;95(2):220-226. doi:10.1016/j.yexmp.2013.07.010
28. Sun Y, Wang BE, Leong KG, et al. Androgen deprivation causes epithelial-mesenchymal transition in the prostate: Implications for androgen- deprivation therapy. *Cancer Res.* 2012;72(2):527-536. doi:10.1158/0008-5472.CAN-11-3004

29. Jennbacken K, Tešan T, Wang W, Gustavsson H, Damber JE, Welén K. N-cadherin increases after androgen deprivation and is associated with metastasis in prostate cancer. *Endocr Relat Cancer*. 2010;17(2):469-479. doi:10.1677/ERC-10-0015
30. Miao L, Yang L, Li R, et al. Disrupting androgen receptor signaling induces Snail-mediated epithelial-mesenchymal plasticity in prostate cancer. *Cancer Res*. 2017;77(11):3101-3112. doi:10.1158/0008-5472.CAN-16-2169
31. Zhu M, Kyprianou N. Role of androgens and the androgen receptor in epithelial-mesenchymal transition and invasion of prostate cancer cells. *FASEB J*. 2010;24(3):769-777. doi:10.1096/fj.09-136994
32. Armstrong AJ, Marengo MS, Oltean S, et al. Circulating tumor cells from patients with advanced prostate and breast cancer display both epithelial and mesenchymal markers. *Mol Cancer Res*. 2011. doi:10.1158/1541-7786.MCR-10-0490
33. Bulfoni M, Gerratana L, Del Ben F, et al. In patients with metastatic breast cancer the identification of circulating tumor cells in epithelial-to-mesenchymal transition is associated with a poor prognosis. *Breast Cancer Res*. 2016. doi:10.1186/s13058-016-0687-3
34. Gorges TM, Tinhofer I, Drosch M, et al. Circulating tumour cells escape from EpCAM-based detection due to epithelial-to-mesenchymal transition. *BMC Cancer*. 2012;12. doi:10.1186/1471-2407-12-178
35. Lindsay CR, Le Moulec S, Billiot F, et al. Vimentin and Ki67 expression in circulating tumour cells derived from castrate-resistant prostate cancer. *BMC Cancer*. 2016. doi:10.1186/s12885-016-2192-6
36. Yu M, Bardia A, Wittner BS, et al. Circulating breast tumor cells exhibit dynamic changes in epithelial and mesenchymal composition. *Science* (80-). 2013. doi:10.1126/science.1228522
37. Lowes LE, Hedley BD, Keeney M, Allan AL. Adaptation of semiautomated circulating tumor cell (CTC) assays for clinical and preclinical research applications. *J Vis Exp*. 2014. doi:10.3791/51248
38. Lowes LE, Goodale D, Xia Y, et al. Epithelial-to-mesenchymal transition leads to disease-stage differences in circulating tumor cell detection and metastasis in pre-clinical models of prostate cancer. *Oncotarget*. 2016. doi:10.18632/oncotarget.12682
39. Chudziak J, Burt DJ, Mohan S, et al. Clinical evaluation of a novel microfluidic device for epitope-independent enrichment of circulating tumour cells in patients with small cell lung cancer. *Analyst*. 2016;141(2):669-678. doi:10.1039/C5AN02156A
40. Gorges TM, Kuske A, Röck K, et al. Accession of tumor heterogeneity by multiplex transcriptome profiling of single circulating tumor cells. *Clin Chem*. 2016;62(11):1504-1515. doi:10.1373/clinchem.2016.260299

41. Hvichia GE, Parveen Z, Wagner C, et al. A novel microfluidic platform for size and deformability based separation and the subsequent molecular characterization of viable circulating tumor cells. *Int J Cancer*. 2016;138(12):2894-2904. doi:10.1002/ijc.30007
42. Xu L, Mao X, Imrali A, et al. Optimization and Evaluation of a Novel Size Based Circulating Tumor Cell Isolation. *PLoS One*. 2015;10(9). doi:10.1371/journal.pone.0138032
43. Englert DF, Kolesnikova M, Zaman N, Hustler A, Wishart G, O'Shannessy DJ. Abstract 1375: Multiplex gene expression using the HyCEAD assay in CTCs isolated with the Parsortix™ system. *Cancer Res*. 2019;79(13_Supplement):1375. doi:10.1158/1538-7445.AM2019-1375
44. Kyriakopoulos CE, Chen YH, Carducci MA, et al. Chemohormonal therapy in metastatic hormone-sensitive prostate cancer: long-term survival analysis of the randomized phase III E3805 chaarted trial. *J Clin Oncol*. 2018. doi:10.1200/JCO.2017.75.3657
45. Scher HI, Morris MJ, Basch E, Heller G. End points and outcomes in castration-resistant prostate cancer: from clinical trials to clinical practice. *J Clin Oncol Off J Am Soc Clin Oncol*. 2011;29(27):3695-3704. doi:10.1200/JCO.2011.35.8648
46. Lowes LE, Lock M, Rodrigues G, et al. The significance of circulating tumor cells in prostate cancer patients undergoing adjuvant or salvage radiation therapy. *Prostate Cancer Prostatic Dis*. 2015. doi:10.1038/pcan.2015.36
47. Kitz J, Goodale D, Postenka C, Lowes LE, Allan AL. EMT-independent detection of circulating tumor cells in human blood samples and pre-clinical mouse models of metastasis. *Clin Exp Metastasis*. 2021;38(1):97-108. doi:10.1007/s10585-020-10070-y
48. Sweeney CJ, Chen Y-H, Carducci M, et al. Chemohormonal Therapy in Metastatic Hormone-Sensitive Prostate Cancer. *N Engl J Med*. 2015;373(8):737-746. doi:10.1056/nejmoa1503747
49. Msaouel P, Pissimissis N, Halapas A, Koutsilieris M. Mechanisms of bone metastasis in prostate cancer: clinical implications. *Best Pract Res Clin Endocrinol Metab*. 2008;22(2):341-355. doi:10.1016/j.beem.2008.01.011
50. Apoun O, Mikulová V, Janíková M, et al. Prognosis of castration-resistant prostate cancer patients-use of the adnatest system for detection of circulating tumor cells. *Anticancer Res*. 2016;36(4):2019-2026.
51. Gurel B, Ali TZ, Montgomery EA, et al. NKX3.1 as a marker of prostatic origin in metastatic tumors. *Am J Surg Pathol*. 2010;34(8):1097-1105. doi:10.1097/PAS.0b013e3181e6cbf3
52. Wang B, Shen Y, Zou Y, et al. TOP2A Promotes Cell Migration, Invasion and Epithelial-Mesenchymal Transition in Cervical Cancer via Activating the PI3K/AKT Signaling. *Cancer Manag Res*. 2020;12:3807-3814. doi:10.2147/CMAR.S240577

53. Kim KY, Yoon M, Cho Y, et al. Targeting metastatic breast cancer with peptide epitopes derived from autocatalytic loop of Prss14/ST14 membrane serine protease and with monoclonal antibodies. *J Exp Clin Cancer Res*. 2019;38(1):363. doi:10.1186/s13046-019-1373-y
54. Adamo P, Lodomery MR. The oncogene ERG: A key factor in prostate cancer. *Oncogene*. 2016;35(4):403-414. doi:10.1038/onc.2015.109
55. Subramani R, Lopez-Valdez R, Salcido A, et al. Growth hormone receptor inhibition decreases the growth and metastasis of pancreatic ductal adenocarcinoma. *Exp Mol Med*. 2014;46(10):1-11. doi:10.1038/emm.2014.61
56. Zhang L, Jia G, Shi B, Ge G, Duan H, Yang Y. PRSS8 is Downregulated and Suppresses Tumour Growth and Metastases in Hepatocellular Carcinoma. *Cell Physiol Biochem*. 2016;40(3-4):757-769. doi:10.1159/000453136
57. Li W, Li S, Yang J, Cui C, Yu M, Zhang Y. ITGBL1 promotes EMT, invasion and migration by activating NF- κ B signaling pathway in prostate cancer. *Onco Targets Ther*. 2019;12:3753-3763. doi:10.2147/OTT.S200082
58. Yu Z, Wang Y, Jiang Y, et al. NID2 can serve as a potential prognosis prediction biomarker and promotes the invasion and migration of gastric cancer. *Pathol - Res Pract*. 2019;215(10):152553. doi:https://doi.org/10.1016/j.prp.2019.152553
59. Jiang X, Zhang C, Qi S, et al. Elevated expression of ZNF217 promotes prostate cancer growth by restraining ferroportin-conducted iron egress. *Oncotarget*. 2016;7(51):84893-84906. doi:10.18632/oncotarget.12753
60. Johnson SAS, Lin JJ, Walkey CJ, Leathers MP, Coarfa C, Johnson DL. Elevated TATA-binding protein expression drives vascular endothelial growth factor expression in colon cancer. *Oncotarget*. 2017;8(30):48832-48845. doi:10.18632/oncotarget.16384
61. Ray D, Epstein DM. Tumorigenic de-differentiation: the alternative splicing way. *Mol & Cell Oncol*. 2020;7(6):1809959. doi:10.1080/23723556.2020.1809959
62. Nakajima H, Koizumi K. Family with sequence similarity 107: A family of stress responsive small proteins with diverse functions in cancer and the nervous system (Review). *Biomed reports*. 2014;2(3):321-325. doi:10.3892/br.2014.243
63. Su X, Liu N, Wu W, et al. Comprehensive analysis of prognostic value and immune infiltration of kindlin family members in non-small cell lung cancer. *BMC Med Genomics*. 2021;14(1):119. doi:10.1186/s12920-021-00967-2
64. Schaefer-Klein JL, Murphy SJ, Johnson SH, Vasmatazis G, Kovtun I V. Topoisomerase 2 Alpha Cooperates with Androgen Receptor to Contribute to Prostate Cancer Progression. *PLoS One*. 2015;10(11):1-17. doi:10.1371/journal.pone.0142327
65. Lee C, Fernandez KJ, Alexandrou S, et al. Cyclin E2 promotes whole genome doubling in

- breast cancer. *Cancers (Basel)*. 2020;12(8):1-19. doi:10.3390/cancers12082268
66. Liu H, Zhang Z, Zhen P, Zhou M. High Expression of VSTM2L Induced Resistance to Chemoradiotherapy in Rectal Cancer through Downstream IL-4 Signaling. *J Immunol Res*. 2021;2021. doi:10.1155/2021/6657012
 67. Arafeh R, Samuels Y. PIK3CA in cancer: The past 30 years. *Semin Cancer Biol*. 2019;59:36-49. doi:https://doi.org/10.1016/j.semcancer.2019.02.002
 68. García Z, Kumar A, Marqués M, Cortés I, Carrera AC. Phosphoinositide 3-kinase controls early and late events in mammalian cell division. *EMBO J*. 2006;25(4):655-661. doi:10.1038/sj.emboj.7600967
 69. Ratajska M, Matusiak M, Kuzniacka A, et al. Cancer predisposing BARD1 mutations affect exon skipping and are associated with overexpression of specific BARD1 isoforms. *Oncol Rep*. 2015;34(5):2609-2617. doi:10.3892/or.2015.4235
 70. Sugie S, Mukai S, Yamasaki K, Kamibeppu T, Tsukino H, Kamoto T. Significant Association of Caveolin-1 and Caveolin-2 with Prostate Cancer Progression. *Cancer Genomics Proteomics*. 2015;12(6):391-396.
 71. Nordby Y, Andersen S, Richardsen E, et al. Stromal expression of VEGF-A and VEGFR-2 in prostate tissue is associated with biochemical and clinical recurrence after radical prostatectomy. *Prostate*. 2015;75(15):1682-1693. doi:10.1002/pros.23048
 72. de Bono JS, Scher HI, Montgomery RB, et al. Circulating tumor cells predict survival benefit from treatment in metastatic castration-resistant prostate cancer. *Clin Cancer Res*. 2008;14(19):6302-6309. doi:10.1158/1078-0432.CCR-08-0872
 73. Alunni-Fabbroni M, Sandri MT. Circulating tumour cells in clinical practice: Methods of detection and possible characterization. *Methods*. 2010;50(4):289-297. doi:10.1016/j.ymeth.2010.01.027
 74. Toss A, Mu Z, Fernandez S, Cristofanilli M. CTC enumeration and characterization: moving toward personalized medicine. *Ann Transl Med*. 2014;2(11):108. doi:10.3978/j.issn.2305-5839.2014.09.06
 75. Vestergaard EM, Nexø E, Tørring N, Borre M, Ørntoft TF, Sørensen KD. Promoter hypomethylation and upregulation of trefoil factors in prostate cancer. *Int J cancer*. 2010;127(8):1857-1865. doi:10.1002/ijc.25209
 76. Darby S, Cross SS, Brown NJ, Hamdy FC, Robson CN. BMP-6 over-expression in prostate cancer is associated with increased Id-1 protein and a more invasive phenotype. *J Pathol*. 2008;214(3):394-404. doi:10.1002/path.2292
 77. Wang B, Gu Y, Hui K, et al. AKR1C3, a crucial androgenic enzyme in prostate cancer, promotes epithelial-mesenchymal transition and metastasis through activating ERK signaling. *Urol Oncol*. 2018;36(10):472.e11-472.e20. doi:10.1016/j.urolonc.2018.07.005

78. Stopsack KH, Gerke T, Zareba P, et al. Tumor protein expression of the DNA repair gene BRCA1 and lethal prostate cancer. *Carcinogenesis*. 2020;41(7):904-908. doi:10.1093/carcin/bgaa061
79. Shang X, Lin X, Alvarez E, Manorek G, Howell SB. Tight Junction Proteins Claudin-3 and Claudin-4 Control Tumor Growth and Metastases. *Neoplasia*. 2012;14(10):974-IN22. doi:https://doi.org/10.1593/neo.12942
80. Xu L, Yu W, Xiao H, Lin K. BIRC5 is a prognostic biomarker associated with tumor immune cell infiltration. *Sci Rep*. 2021;11(1):390. doi:10.1038/s41598-020-79736-7
81. Chopin LK, Veveris-Lowe TL, Philipps AF, Herington AC. Co-expression of GH and GHR isoforms in prostate cancer cell lines. *Growth Horm IGF Res Off J Growth Horm Res Soc Int IGF Res Soc*. 2002;12(2):126-136. doi:10.1054/ghir.2002.0271
82. Xiang L, Kong B. PAX8 is a novel marker for differentiating between various types of tumor, particularly ovarian epithelial carcinomas. *Oncol Lett*. 2013;5(3):735-738. doi:10.3892/ol.2013.1121
83. Cohen PA, Donini CF, Nguyen NT, Lincet H, Vendrell JA. The dark side of ZNF217, a key regulator of tumorigenesis with powerful biomarker value. *Oncotarget*. 2015;6(39):41566-41581. doi:10.18632/oncotarget.5893
84. Kim M, Jang K, Miller P, et al. VEGFA links self-renewal and metastasis by inducing Sox2 to repress miR-452, driving Slug. *Oncogene*. 2017;36. doi:10.1038/onc.2017.4
85. Aggarwal V, Montoya CA, Donnenberg VS, Sant S. Interplay between tumor microenvironment and partial EMT as the driver of tumor progression. *iScience*. 2021;24(2):102113. doi:https://doi.org/10.1016/j.isci.2021.102113

Chapter 4

4 Reduced Zeb1 Expression in Prostate Cancer Cells Leads to an Aggressive Partial-EMT Phenotype Associated with Altered Global Methylation Patterns

A version of this chapter has been published:

Kitz, J.; Lefebvre, C.; Carlos, J.; Lowes, L.E.; Allan, A.L. Reduced *Zeb1* Expression in Prostate Cancer Cells Leads to an Aggressive Partial-EMT Phenotype Associated with Altered Global Methylation Patterns. *Int. J. Mol. Sci.* **2021**, *22*, 12840. <https://doi.org/10.3390/ijms222312840>

Abstract

Prostate cancer is the most common cancer in American men and the second leading cause of cancer-related death. Most of these deaths are associated with metastasis, a process involving the epithelial-to-mesenchymal transition (EMT). Furthermore, growing evidence suggests that partial-EMT (p-EMT) may lead to more aggressive disease than complete EMT. In this study, the EMT-inducing transcription factor Zeb1 was knocked down in mesenchymal PC-3 prostate cancer cells (Zeb1^{KD}) and resulting changes in cellular phenotype were assessed using protein and RNA analysis, invasion and migration assays, cell morphology assays, and DNA methylation chip analysis. Inducible knock down of Zeb1 resulted in a p-EMT phenotype including co-expression of epithelial and mesenchymal markers, a mixed epithelial/mesenchymal morphology, increased invasion and migration, and enhanced expression of p-EMT markers relative to PC-3 mesenchymal controls ($p \leq 0.05$). Treatment of Zeb1^{KD} cells with the global de-methylating drug 5-azacytidine (5-aza) mitigated the observed aggressive p-EMT phenotype. DNA methylation chip analysis revealed 10 potential targets for identifying and/or targeting aggressive p-EMT prostate cancer in the future. These findings provide a framework to enhance prognostic and/or therapeutic options for aggressive prostate cancer in the future by identifying new p-EMT biomarkers to identify patients with aggressive disease who may benefit from 5-aza treatment.

4.1 Introduction

Prostate cancer is the second leading cause of cancer related deaths in American men¹. Most of these deaths are caused by metastasis, which allows cancer to spread beyond the prostate to other parts of the body². Metastasis is associated with an epithelial-to mesenchymal transition (EMT), where epithelial cells lose their epithelial characteristics and gain a mesenchymal phenotype, which aids in the process of metastasis²⁻⁸.

Transcription factors bind to specific promoter sequences within the DNA to influence the expression of target genes⁹. Master EMT-inducing transcription factors upregulate mesenchymal genes and/or inhibit epithelial genes, which can cause the cell to undergo EMT¹⁰. An example of this is zinc finger E-box-binding homeobox 1 (Zeb1), which binds to the E-box promoter sequence, regulates neuronal differentiation, and has important roles in promoting EMT to allow for cell movement during gestation^{11,12}. In cancer progression, Zeb1 promotes metastasis and a loss of cell polarity by repressing the epithelial proteins E-Cadherin and epithelial cell adhesion molecule (EPCAM) and promotes tumorigenicity by repressing stemness-inhibiting microRNAs^{10,13}.

It is well-established that EMT is a dynamic state, utilizing both EMT and a reverse mesenchymal-to-epithelial (MET) transition to switch between epithelial and mesenchymal states during the process of metastasis²⁻⁸. In addition to EMT and MET, recent studies have demonstrated that there is an intermediate state called partial EMT (p-EMT), a phenotype that may result in the most aggressive cancer cells¹⁴. Partial EMT is associated with increased cell-cell interactions and cell proliferation in migrating circulating tumor cells (CTC). Growing evidence suggests that migrating cell clusters and CTC clusters in the blood are more aggressive and have higher metastatic potential than migrating single cells or single CTCs, and that these clusters often exhibit a p-EMT phenotype rather than complete EMT¹⁵. It has also been suggested that epigenetic modifications such as DNA methylation of the promoter region of essential genes may be responsible for this increased cell aggressiveness, and that treatment with a global de-methylating agent may aid in treatment of aggressive prostate cancers¹⁶.

In the current study, we tested the hypothesis that knock down of the EMT-inducing transcription factor Zeb1 in mesenchymal PC-3 cells would produce an MET leading to a more epithelial, less

aggressive phenotype compared to control cells. Unexpectedly, we observed that inducible knockdown of *Zeb1* in PC-3 cells (*Zeb1*^{KD} cells) resulted in a p-EMT phenotype including co-expression of epithelial and mesenchymal markers, a mixed epithelial/mesenchymal morphology, increased invasion and migration, and enhanced expression of p-EMT markers relative to PC-3 mesenchymal controls (ctrl cells). Treatment of *Zeb1*^{KD} cells with the global de-methylating drug 5-azacytidine (5-aza)¹⁷ mitigated the observed aggressive p-EMT phenotype. DNA methylation chip analysis revealed 10 potential targets for identifying and/or targeting aggressive p-EMT prostate cancer in the future. These novel findings provide a framework to enhance prognostic and/or therapeutic options for aggressive prostate cancer in the future by identifying new p-EMT biomarkers to classify patients who may benefit from combination treatment with the clinically relevant inhibitor 5-azacytidine.

4.2 Materials and Methods

4.2.1 Cell Culture

Human mesenchymal PC-3 prostate cancer cells (parental PC-3 cells [#CRL-1435]; ATCC, Manassas, VA, USA) were cultured in F12K media + 10% fetal bovine serum (FBS). Human epithelial LNCaP prostate cancer cells (#CRL-1740, ATCC) were cultured in RPMI-1640 media + 10% FBS. Human epithelial MDA-MB-468 breast cancer cells (#HTB-132, ATCC) were cultured in alpha minimum essential media (α MEM) + 10% FBS. Cell lines were authenticated via third party testing (IDEXX BioAnalytics, Columbia, MO, USA). Primary lung fibroblasts (Lonza, Basel, Switzerland) were cultured in RPMI-1640 media + 5% FBS, 1% 4-(2-hydroxyethyl)-1-piperazineethanesulfonic acid (HEPES), 0.1% bovine serum albumin (BSA) (10%), 0.5% insulin, and 0.05% hydrocortisone. Media and reagents are from Life Technologies (Carlsbad, CA, USA), and FBS is from Sigma (St. Louis, MO, USA).

4.2.2 Cell Transductions

To create PC-3 *Zeb1*^{KD} and ctrl cells, 1×10^6 PC-3 cells/mL were seeded into each well of a 6-well dish 24 h prior to transduction. Twenty-five μ L of SMARTvector Lentiviral *Zeb1* shRNA stock (target region; 3' untranslated region, target sequence 5'-TCTAAACCCAGGCTTCCCT-3') or scrambled control (non-targeting control sequence) (Dharmacon, Lafayette, CO, USA) was added to each well and growth media was exchanged for transduction media containing 0.01%

polybrene. After 24 h, transduction media was exchanged for growth media. One day later, growth media was exchanged for selection media containing 0.025% puromycin. Cells were then cultured as usual, supplementing growth media with 0.025% puromycin to continue selective pressure. Resulting changes in inducible Zeb1 expression (\pm Dox) were analyzed using immunoblotting and RT-qPCR as described below.

4.2.3 Immunoblotting

Cells were harvested by cell scraping, collected in lysis buffer, and quantified using a Lowry Assay. Protein (10 μ g) was subjected to sodium dodecyl sulfate polyacrylamide gel electrophoresis (SDS-PAGE) and transferred onto polyvinylidene difluoride membranes (PVDF; Millipore, Billerica, MA, USA). Membranes were blocked using 5% bovine serum albumin (BSA) in Tris-buffered saline + 0.1% Tween-20 (TBS-T). Anti-human primary antibodies were diluted in 5% BSA in TBS-T prior to use as detailed in **Supplementary Table S4.1**. Goat anti-mouse IgG and goat anti-rabbit IgG secondary antibodies (Calbiochem, Billerica, MA, USA) conjugated to horseradish peroxidase and diluted in 5% BSA/TBS-T were used at concentrations of 1:2000 and 1:5000. Protein expression was visualized using Amersham ECL Prime Detection Reagent (GE Healthcare, Wauwatosa, WI, USA), and normalized to total protein based on amido black (Sigma) staining of membranes or actin immunoblotting.

4.2.4 Quantitative Real-Time PCR

Total RNA was isolated using TRIzol (Life Technologies), and reverse transcribed using SuperScript™ IV VILO Master Mix (Invitrogen, Waltham, MA, USA, 11766050). Samples were then subjected to subsequent RNA analysis using Advanced qPCR Master Mix with Supergreen LO-ROX (Wisent Bioproducts, Saint-Jean-Baptiste, QC, Canada) on a QuantStudio™ 3 Real-Time PCR system (Applied Biosystems, Waltham, WA, USA) with primers detailed in **Supplementary Table S4.2**. GAPDH was used as a reference gene.

4.2.5 Transwell Migration and Invasion Assays

Changes in cell migration and invasion were assessed using transwell migration and invasion assays. Transwell plates were coated with either gelatin (4 μ g/well, migration) or Matrigel (6 μ g/well, invasion). Media in the bottom well included normal media supplemented with

puromycin and 2% FBS (migration) or 5% FBS (invasion) with or without 1 $\mu\text{g}/\text{mL}$ Dox treatment as required. 0% FBS was used as a control for both invasion and migration transwell assays. Human PC-3 prostate cancer cells (parental, ctrl or Zeb1^{KD}; 5×10^4 cells/mL) were seeded onto the top portion of each transwell chamber and incubated for 18 h at 37 °C, 5% CO₂ prior to staining and assessment of differences in migration and invasion. Five high powered fields of view (HP-FOVs) were captured for each well, and the mean number of migrated or invaded cells/HP-FOV was calculated using ImageJ software (National Health Institute, Bethesda, MD, USA).

4.2.6 Physical Barrier Wound Healing Assay

Changes in migratory capacity were also assessed using physical barrier wound healing assays. Cells ($3 \times 10^5/\text{mL}$) were plated in F12K media supplemented with puromycin and doxycycline, DMSO, and/or 5-aza, onto 24 well plates. Cells were incubated at 37 °C, 5% CO₂. After 24 h the physical barrier was removed from each well. Images were captured at 0, 12, 24, and 36 h time points using 5 HP-FOVs for each well. Cell migration, calculated by percent wound closure, was analyzed using ImageJ software.

4.2.7 Spheroid Invasion Assay

Changes in invasion were also assessed using spheroid invasion assays. Cells (5×10^3) were plated onto 96-well ultra-low attachment spheroid microplates (Corning, Kennebunk, ME, USA) using growth media supplemented with puromycin, doxycycline, DMSO, and/or 5-aza and allowed to grow into spheroids for 96 h. Matrigel was added to the spheroids and images were captured at 0, 24, and 48 h time points using 5 HP-FOVs for each well. ImageJ software was used to calculate the area of invasion from spheroids into surrounding Matrigel.

4.2.8 BrdU Proliferation Assay

Cell proliferation was assessed using a bromodeoxyuridine (BrdU) incorporation assay. Cells were plated on 8-well chamber slides, allowed to adhere, and serum-starved for 72 h. Media was then replaced with F12K supplemented with puromycin and 10% FBS \pm Dox, 5-aza, and/or DMSO for 24 h. Following incubation, Cell Proliferation Labelling Reagent (BrdU) (GE Healthcare, Chicago, IL, USA) was added for 30 min, cells were formalin fixed and stained with a 100 $\mu\text{L}/\text{well}$ anti-BrdU primary antibody (BD-347580) and a 1:400 concentration of a PE-conjugated goat anti-

mouse IgG secondary antibody was used for immunofluorescent visualization. Images were captured using 5 HP-FOVs for each well, and nuclei were counted using ImageJ, with results expressed as a percentage of BrdU positive cells to total nuclei (DAPI⁺).

4.2.9 Cell Morphology Assay

Changes in cell morphology were determined by analyzing the roundness versus spindle-like shape of each cell. High powered FOVs were used to capture cell images, and 250 cells per HP-FOV (n = 3) were analyzed for cell shape. The actual area (AA) of each cell was calculating by outlining and measuring the entire cell in ImageJ, which was also used to trace the diameter between the longest two points of each cell and the expected area (EA) was calculated using the equation πr^2 . The AA was then divided by EA to assign each cell with a number from 0 to 1. If AA was equal to the expected area then the number is 1, and the cell is more round in shape. If the AA is less than the expected area then the number is closer to 0, and the cell is more spindle shaped. To determine the limits of what number represented a round or spindle-shaped cell control, epithelial MDA-MB-468 breast cancer cells and mesenchymal primary lung fibroblasts were used as controls for cell shape (250 cells/FOV, n = 3). The average of the epithelial/mesenchymal control cells was attained, and the standard deviation was either added or subtracted from the average respectively in order to create a cutoff point for an epithelial cell, a mesenchymal cell, and a cell of “mixed” morphology (i.e., neither epithelial nor mesenchymal) (**Supplementary Figure 4.1**).

4.2.10 *In Vivo* Studies

To assess the effect of Zeb1^{KD} on *in vivo* CTC generation and metastasis, Ctrl and Zeb^{KD} PC-3 cells were injected orthotopically into the prostate gland of male nude mice (n = 36 mice/group). A schematic of the *in vivo* experimental design is provided in **Supplemental Figure 4.2**. All animal studies were carried out in accordance with the Canadian Council of Animal Care under a protocol approved by the University of Western Ontario Animal Care Committee (#2020-124). Male nude mice (Hsd:Athymic Nude-Foxn1tm; Envigo, Indianapolis, IN, USA) were anesthetized with ketamine (McGill University, Montreal QB) / xylezene (University of Western Ontario, London ON) plus 100 μ l metacam (University of Western Ontario, London ON) for analgesia. A 3-point prep was completed with betadine on the lower abdomen. The abdomen was opened and

a 27g needle with Ctrl or Zeb1^{KD} PC-3 cells ($1 \times 10^6/40 \mu\text{l}$) was inserted into the front lobe of the prostate. The cavity was closed with 5.0 suture once the cells were injected, and the mouse warmed until awake and alert. Mice were given an additional 100 μl metacam subcutaneously 24 h after being returned to their cages. Primary prostate tumors were allowed to develop and Zeb1 knockdown was induced by switching mice to a Dox-containing diet (Envigo; TD.01306) at various time points post-injection (early-2 weeks; midpoint-6 weeks; late-9 weeks; n=12 mice/time point/population) to determine the impact on CTC generation and subsequent metastasis. After 12 weeks of disease progression, mice were sacrificed. Whole blood (150 μl) was drawn from each mouse via cardiac puncture as previously described¹⁸. Blood was collected in EDTA microtubes (Becton Dickinson, Franklin Lakes, NJ, USA) and 50 μl each was analyzed using the previously described EMT-independent VyCap CTC system protocol¹⁹. Tissue from primary tumors and distant organs (bone, lung, liver, brain, heart, kidneys, lymph nodes) were also collected. Tissues were formalin-fixed, randomly sectioned, stained with hematoxylin and eosin (H&E), and evaluated in a blinded fashion to assess the presence and extent of tumor in each tissue as described previously^{20,21,22}.

4.2.11 DNA Extraction and Dot-Blot DNA Analysis

DNA was extracted using a Blood & Cell Culture DNA Mini Kit (Qiagen, Hilden, Germany) and the manufacturer's protocol. For the dot-blot analysis, 180 ng of DNA was added to 3M NaOH and incubated at 42 °C for 12 min to denature the DNA. Samples were immediately transferred to positively charged nylon membranes (Roche, Mannheim, Germany) in the dot-blot apparatus. Membranes were then baked at 120 °C for 30 min to allow DNA-membrane crosslinking. The membrane was then blocked in 1×TBS + 0.05% Tween-20 and 5% powdered milk for 1 h prior to incubation with the anti-5mC primary antibody (ab179898; 1:500 in blocking solution) and agitated for 1.5 h. Membranes were washed 3× with TBS-T for 10 min, and then incubated with a goat anti-mouse IgG secondary antibody (Calbiochem, Billerica, MA, USA; 1:1000) for 1 h. Levels of 5 methyl cytosine (5mC) was visualized using Amersham ECL Prime Detection Reagent (GE Healthcare) on a ChemiDoc™ MP Imaging System, and normalized to total DNA based on methylene blue staining of membranes.

4.2.12 DNA Methylation Chip Analysis

Changes in global DNA methylation profile were analyzed using the Illumina Methylation EPIC BeadChip (Illumina, San Diego, CA, USA) and 1000 ng of DNA input ($n = 4$ per cell group) using the manufacturer's protocol²³. In total, 3 different quality control (QC) methods were carried out. First, raw methylation betas were generated using the Minfi package in R²⁴ and no QC was performed; to provide flexibility for analysis. Secondly, QC was performed with the Chip Analysis Methylation Pipeline (ChAMP)²⁵. This method filtered probes with a detection p -value above 0.01 (removing 3337 probes), bead count <3 in at least 5% of samples (removing 26,519 probes), only keeping CpG methylation measurements (removing 2931 probes), filtering probes with SNPs (removing 95,596 probes) and probes that align to multiple locations (removing 11 probes), filtering XY chromosome probes (removing 16,109 probes). The last method of QC still used ChAMP, but only removed probes failing detection p -value, bead count and non-cpg sites (as explained above). After probe filtering with ChAMP, no samples were removed due to QC issues, and values for each sample were normalized with BMIQ normalization²⁶. The resulting Infinium Methylation EPIC chip dataset was archived in the GEO repository, series number GSE186782, "Treatment of p-EMT prostate cancer cell with the demethylating drug 5-azacytidine reduces cell aggressiveness and changes methylation profile".

4.2.13 Patient Sample Analysis

Follow-up analysis was completed using Ualcan and cBioportal online clinical patient databases. Using the gene analysis [Ualcan database](#) (accessed on November 26, 2021), each aberrantly methylated gene identified was analyzed. Utilizing the TCGA dataset, genes were assessed for promoter methylation in prostate adenocarcinoma compared to normal tissue as well as for expression in metastatic prostate cancer (MET500 dataset) compared to non-metastatic prostate cancer. Additionally, [cBioportal](#) (accessed on November 26, 2021) assessed for survival using mRNA expression level comparisons of aberrantly methylated genes in prostate adenocarcinoma. First, the sample set was identified using Onco Query Language on cBioportal. Patients were stratified based on expression of each identified gene, an mRNA profile was added to the query, and "example gene: EXP>2 EXP<-2" was written in the gene set box. After running the query, the "samples affected" list was downloaded. Next the list of sample IDs was pasted into the homepage into the "user-defined case list" in the "select patient/case set": dropdown. This query only looks

at samples with high or low expression. To stratify into high versus low survival analysis, “example gene: EXP>2” was entered in the gene set box and the same (prostate adenocarcinoma) mRNA profile was selected. The query was run, and the survival tab was selected for results.

4.2.14 Statistical Analysis

Statistical analysis was performed using Prism 9 (GraphPad, San Diego, CA, USA) and Excel 16.5.2 (Microsoft, Redmond, WA, USA). Unless otherwise stated, data is presented as the mean \pm standard error of the mean (SEM), with $p \leq 0.05$ considered to be statistically significant. For normally distributed comparisons of 2 groups, t-tests were performed and for comparisons of more than 2 groups a one-way ANOVA with follow up t-tests for multiple comparisons was performed. Non-matched, non-parametric data of more than two groups was assessed with a one-way Kruskal-Wallis with follow up Mann-Whitney tests for multiple comparisons, with a false discovery rate cutoff = 0.05 considered to be statistically significant.

4.3 Results

4.3.1 Inducible Knockdown of Zeb1 in PC-3 Human Prostate Cancer Cells Results in Enhanced Expression of Epithelial Proteins

Mesenchymal human PC-3 prostate cancer cells were engineered with an inducible lentiviral shRNA system to knockdown expression of the master EMT regulator Zeb1. The following cell lines were created: PC-3 ctrl cells with a non-targeting control sequence of scrambled shRNA, and Zeb1^{KD} cells with shRNA targeting the 3'UTR of Zeb1. This was achieved using the SMARTvector inducible lentiviral shRNA (Dharmacon), which features Tet-on[®] induction of the target shRNA in the presence of doxycycline (Dox) and validation by concurrent induction of TurboGFP (green fluorescent protein). Following Dox induction (72 h), we observed that Zeb1 protein (**Figure 4.1a,b**) and RNA (**Supplementary Figure 4.3a**) expression were significantly decreased compared to all ctrl cells ($p \leq 0.05$), down to a level equivalent to that of human LNCaP cells, an epithelial prostate cancer cell line. Fluorescence microscopy confirmed successful knockdown of Zeb1 via TurboGFP expression following Dox induction (**Supplementary Figure 4.3b**). Immunoblotting (**Figure 4.1c,d**) and RT-qPCR (**Supplementary Figure 4.3c**) was used to assess EMT phenotypic marker expression following Dox induction of Zeb1^{KD} cells. Zeb1^{KD} cells

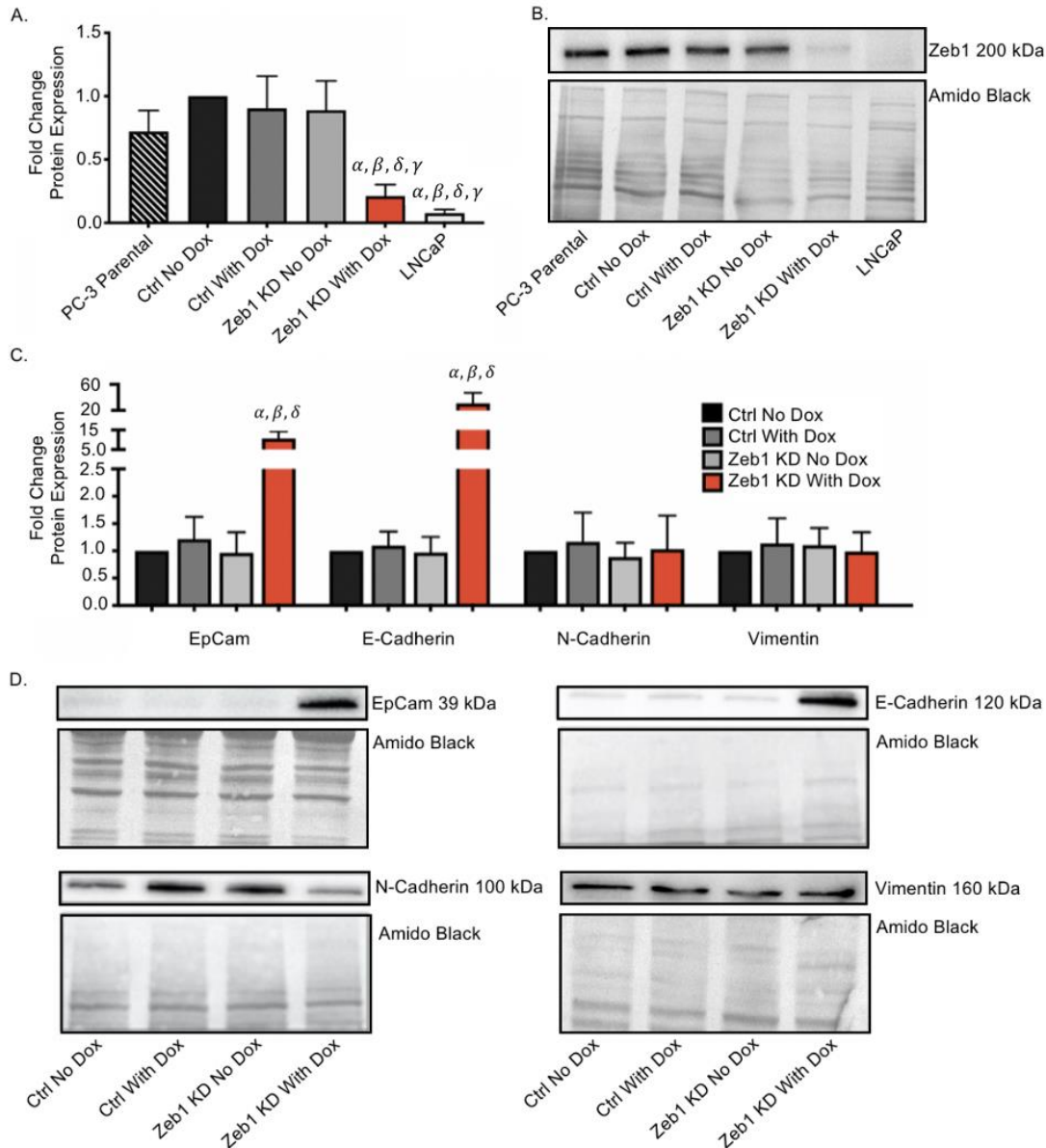


Figure 4-1. Inducible knockdown of Zeb1 in PC-3 human prostate cancer cells results in enhanced expression of epithelial proteins. Mesenchymal human PC-3 prostate cancer cells were engineered to knockdown expression of the master epithelial-to-mesenchymal (EMT) regulator Zeb1 using the SMARTvector inducible lentiviral shRNA system (Dharmacon), which features Tet-on[®] induction of the target shRNA in the presence of doxycycline (Dox). (*a,b*) Immunoblot analysis of Zeb1 protein expression in the presence or absence of Dox (72 h) in Zeb1^{KD} (Zeb1 knockdown), control (ctrl) PC-3 cells, or LNCaP cells. (*c,d*) Immunoblot analysis of E-Cadherin, EpCAM, Vimentin and N-cadherin in Zeb1^{KD} or ctrl cells 72 h after Dox induction. Representative immunoblots are shown and amido black staining of total protein was used as a loading control. Quantitative data is presented as mean \pm standard error of the mean (SEM) fold-change in expression relative to ctrl cells (n = 3). α = significantly different than ctrl no Dox. β = significantly different than ctrl with Dox. δ = significantly different than Zeb1^{KD} no Dox. γ = significantly different than PC-3 ctrl no Dox. ($p \leq 0.05$).

had significantly higher expression of epithelial (EpCAM, E-Cadherin) proteins relative to ctrl cells ($p \leq 0.05$), with no change in expression of mesenchymal proteins (Vimentin, N-Cadherin) (**Figure 4.1c,d**).

4.3.2 Knockdown of Zeb1 in PC-3 Prostate Cancer Cells Increases Migration and Invasion but Does Not Alter Proliferation

Next, we assessed the effect of Zeb1 knockdown on migration and invasion of PC-3 prostate cancer cells using transwell migration (gelatin) and physical barrier wound healing assays. Unexpectedly, we observed that Zeb1^{KD} cells with Dox exhibit significantly increased migration compared to ctrl cells in both transwell (**Figure 4.2a,b**) and wound healing assays (**Figure 4.2c,d**) ($p \leq 0.05$). When Zeb1^{KD} cells were assessed for changes in cell invasion using transwell invasion and spheroid invasion (Matrigel) assays, we similarly observed that Zeb1^{KD} cells with Dox demonstrate significantly enhanced invasion into Matrigel in both the transwell (**Figure 4.3a,b**) and spheroid invasion assays (**Figure 4.3c,d**) ($p \leq 0.05$). BrdU proliferation assays were used to assess differences in cell proliferation between Zeb1^{KD} and ctrl cells, however no significant differences in proliferation were observed (**Supplementary Figure 4.4a,b**).

4.3.3 Knockdown of Zeb1 in PC-3 Prostate Cancer Cells Does Not Alter *In Vivo* CTC Generation or Macrometastases

To assess the influence of Zeb1^{KD} *in vivo*, mice were orthotopically injected with inducible Zeb1^{KD} and ctrl cells. Primary tumors were allowed to grow for 2 (early), 6 (mid), or 10 (late) weeks before *in vivo* induction of Zeb1 knockdown via Dox chow in order to assess the effect on CTC generation and metastasis. While no significant differences in CTC numbers were seen between the early, mid, or late Zeb1^{KD} induction groups compared to ctrl, a trend towards greater numbers of CTCs following late Zeb1^{KD} induction was observed. (**Figure 4.4a**). Relative to ctrl, a trend towards increased metastasis following early and mid Zeb1^{KD} induction groups was also observed (**Figure 4.4b**).

4.3.4 Knockdown of Zeb1 in PC-3 Prostate Cancer Cells Leads to a Partial EMT Phenotype at the Cellular and Molecular Level

We had originally expected that knockdown of Zeb1 in mesenchymal PC-3 prostate cancer cells would lead to a mesenchymal-to-epithelial (MET) transition and reduced metastatic cell behaviors

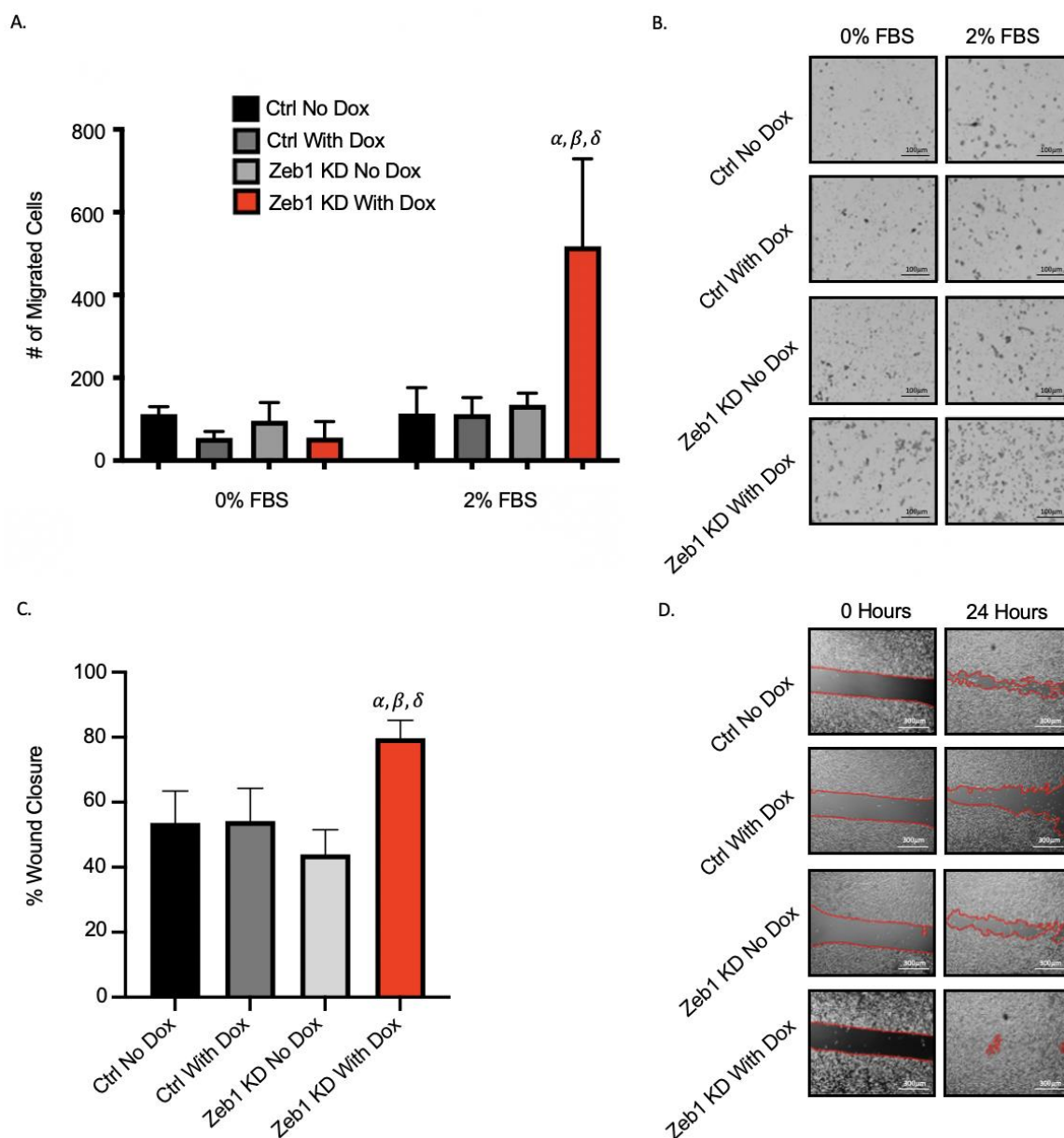


Figure 4-2. Knockdown of Zeb1 in PC-3 prostate cancer cells increases cell migration. (*a,b*) Transwells were coated with 6 $\mu\text{g}/\text{well}$ of gelatin. Cells ($5 \times 10^4/\text{well}$) were added to wells and either control media (0% fetal bovine serum [FBS]) or chemoattractant media (2% FBS) was added and cells were allowed to migrate for 18 h. Cells were fixed with 1% glutaraldehyde and mounted with DAPI-containing mounting media. (*c,d*) For physical barrier wound healing assays, cells were seeded and grown to 90–100% confluency. The physical barrier was removed and cells were allowed to migrate into the wound for 36 h. Representative images are shown for each assay; with migration calculated based on 5 high-powered fields of view (HP-FOV) per well. Black scale bars = 100 μm , white scale bars = 300 μm . Data is presented as the mean \pm standard error of the mean (SEM) ($n = 3$). α = significantly different than control (ctrl) no doxycycline (Dox). β = significantly different than ctrl with Dox. δ = significantly different than Zeb1^{KD} (Zeb1 knockdown) no Dox ($p \leq 0.05$).

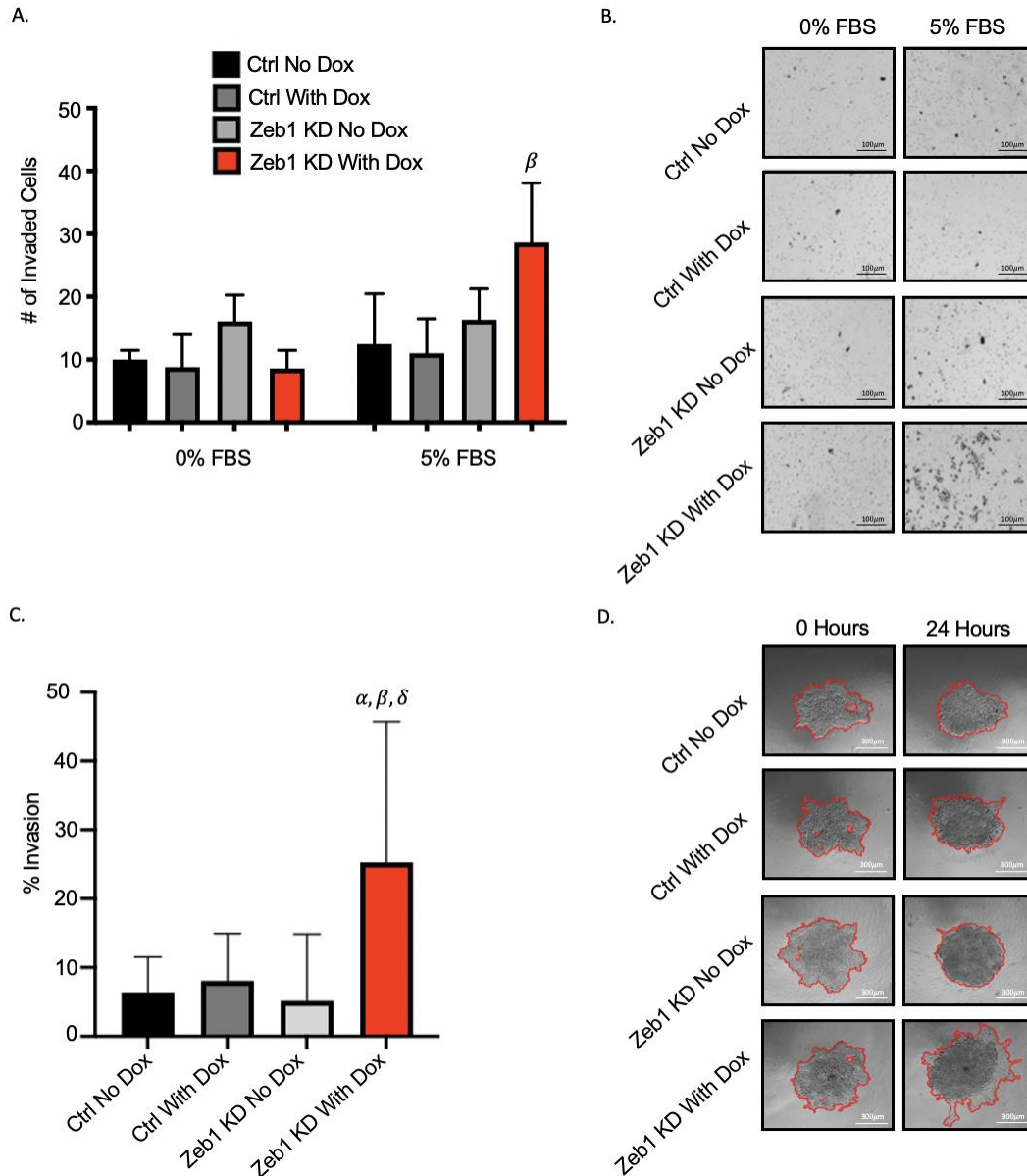


Figure 4-3. Knockdown of Zeb1 in PC-3 prostate cancer cells increases cell invasion. (*a,b*) Transwells were coated with 4 $\mu\text{g}/\text{well}$ of Matrigel. Cells ($5 \times 10^4/\text{well}$) were added to wells and either control media (0% fetal bovine serum [FBS]) or chemoattractant media (5% FBS) was added and cells were allowed to invade for 24 h. Cells were fixed with 1% glutaraldehyde and mounted with DAPI-containing mounting media. (*c,d*) For spheroid invasion assays, cells were seeded onto ultra-low attachment plates and allowed to grow for 96 h to create spheroids. Matrigel was then added and invasion was quantified after 48 h. Representative images are shown for each assay; with invasion calculated based on 5 high-powered fields of view (HP-FOV) per well. Black scale bars = 100 μm , white scale bars = 300 μm . Data is presented as the mean \pm standard error of the mean (SEM) ($n = 3$). α = significantly different than PC-3 control (ctrl) no doxycycline (Dox). β = significantly different than ctrl with Dox. δ = significantly different than Zeb1^{KD} (Zeb1 knockdown) no Dox ($p \leq 0.05$).

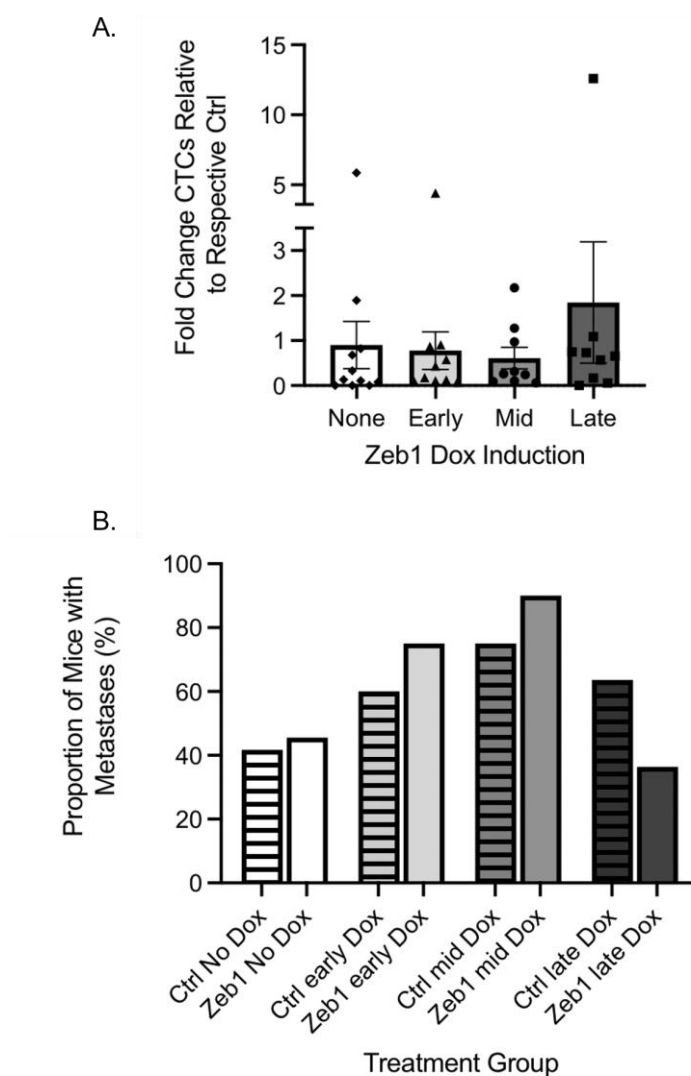


Figure 4-4. Knockdown of Zeb1 in PC-3 prostate cancer cells does not alter *in vivo* CTC generation or macrometastases. Mice were orthotopically injected with inducible Zeb1^{KD} and ctrl cells. Primary tumors were allowed to grow for 2 (early), 6 (mid), or 10 (late) weeks before continuous induction of Zeb1^{KD} via Dox chow. Twelve weeks post-injection mice were sacrificed, and blood and organs were collected for analysis. A schematic of the experimental design is presented in **Supplemental Figure 4.2**. (a) CTCs were enumerated via the EMT-independent VyCap protocol in the ctrl, early, mid, and late Zeb1^{KD} induction groups. (b) Number of mice within each group with detectable macrometastases were assessed and confirmed via H&E staining as shown in **Figure 2.3** (n = 9-12 mice/group).

such as migration and invasion. Our observation that knockdown of Zeb1 instead actually led to more aggressive cell behavior led us to investigate the potential for a partial EMT (p-EMT) phenotype¹⁴. Zeb1^{KD} cells with Dox were assessed for changes in cell morphology as described in the Materials & Methods section and in **Supplementary Figure 4.1**. We observed that Zeb1^{KD} cells with Dox demonstrate a mixed cell morphology, with a significantly higher percentage of epithelial cells and significantly lower percentage of mesenchymal cells compared to ctrl cells ($p \leq 0.05$) (**Figure 4.5a,b**). We next assessed changes in expression of the p-EMT markers P-Cadherin (P-Cad) and integrin $\beta 4$ (ITG $\beta 4$)^{27,28}. We observed that both P-Cad and ITG $\beta 4$ protein expression was significantly enhanced in Zeb1^{KD} cells with Dox compared to ctrl cells ($p \leq 0.05$) (**Figure 4.5c**), while P-Cad RNA expression was also significantly increased in Zeb1^{KD} cells with Dox compared to ctrl cells ($p \leq 0.05$) (**Figure 4.5d**).

4.3.5 Treatment of PC-3 Zeb1^{KD} Prostate Cancer Cells with the Global Demethylating Agent 5-Azacytidine Results in Decreased DNA Methylation, Migration, and Invasion

It has been suggested that epigenetic modifications such as DNA methylation of the promoter region of essential genes may be responsible for increased cell aggressiveness in cancer¹⁶. The global demethylating agent 5-aza is currently used to treat myelodysplastic syndrome²⁹ and is in many phase III clinical trials for cancer ([ClinicalTrials.gov](https://clinicaltrials.gov); accessed on November 25, 2021). To begin investigating whether DNA methylation is involved in the p-EMT phenotype observed in our Zeb1^{KD} cells, we treated cells with 5-aza \pm Dox to assess the effects on cell phenotype. We observed that DNA methylation was decreased in Zeb1^{KD} with Dox and ctrl cells treated with 5-aza compared to DMSO based on decreased expression of 5-mC ($p \leq 0.05$) (**Figure 4.6a,b**). We next assessed the effects of demethylation on cell motility, and observed that treatment with 5-aza significantly mitigated both migration (**Figure 4.6c,d**) and invasion (**Figure 4.6e,f**) compared to treatment with DMSO ($p \leq 0.05$).

4.3.6 Methylation Chip Analysis of Zeb1^{KD} PC-3 Prostate Cancer Cells Identified 10 Genes Associated with a p-EMT Phenotype

To explore specific molecular characteristics in Zeb1^{KD} cells that are being affected by demethylation, DNA was extracted from Dox-induced Zeb1^{KD} cells treated with DMSO (Z0) or

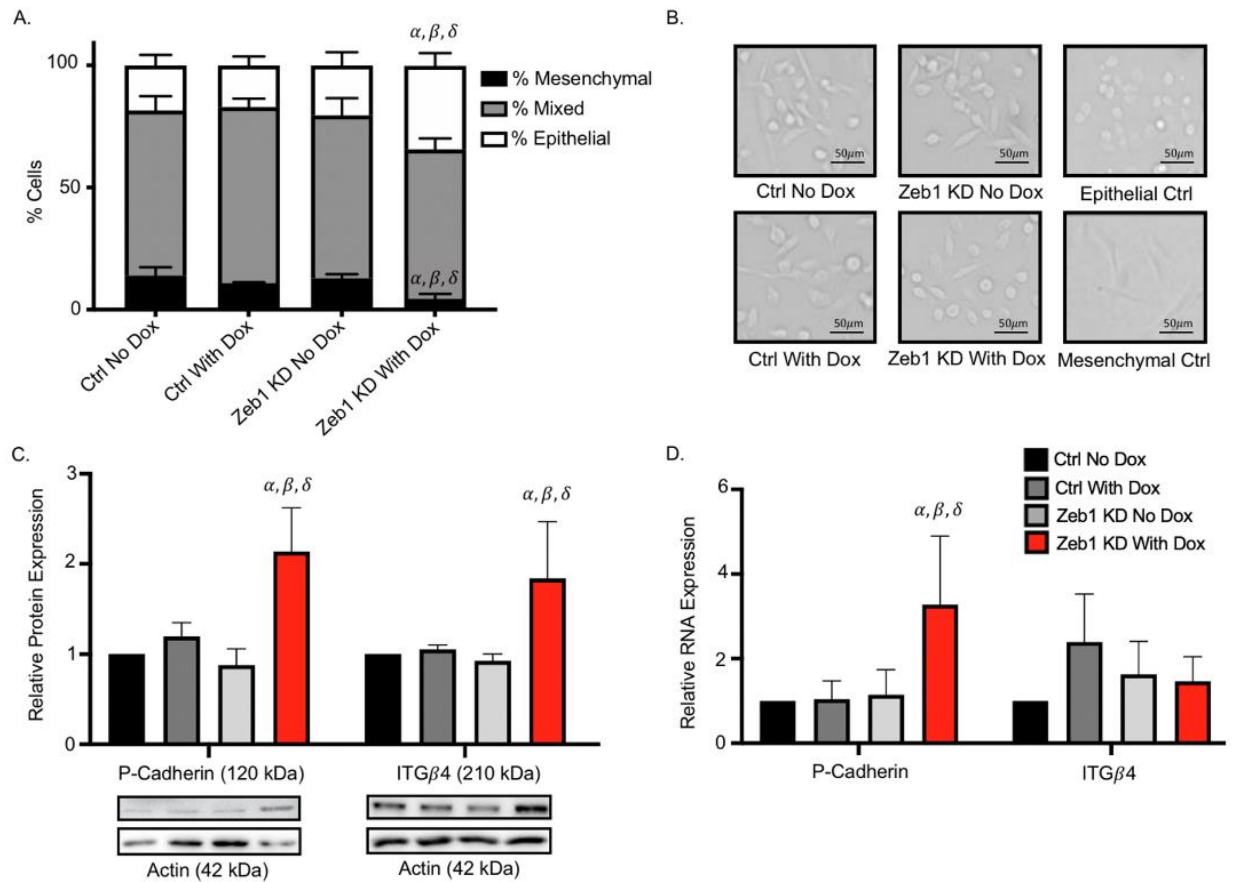


Figure 4-5. Knockdown of Zeb1 in PC-3 prostate cancer cells leads to a partial-EMT phenotype at the cellular and molecular level. (a,b) Cultured PC-3 Zeb1^{KD} (Zeb1 knockdown) and control (ctrl) cells were assessed for cell morphology characteristics as described in the Materials & Methods and in **Supplementary Figure 4.1** (N = 3; n = 250/cells per group). Representative images of each cell group and epithelial (MDA-MB-468) and mesenchymal (primary lung fibroblasts) controls are shown. (c) Immunoblot analysis of P-Cadherin and ITG β 4 in Zeb1^{KD} or ctrl cells. Actin was used as a loading control and representative immunoblots are shown. Blots are aligned with histogram bars above. (d) RT-qPCR analysis of p-EMT marker expression in the presence or absence of Dox in Zeb1^{KD} or ctrl cells. Data is presented as the mean \pm standard error of the mean (SEM) (n = 3) relative to ctrl no Dox. Scale bars = 50 μm . α = significantly different than PC-3 ctrl no Dox. β = significantly different than ctrl with Dox. δ = significantly different than Zeb1^{KD} no Dox ($p \leq 0.05$).

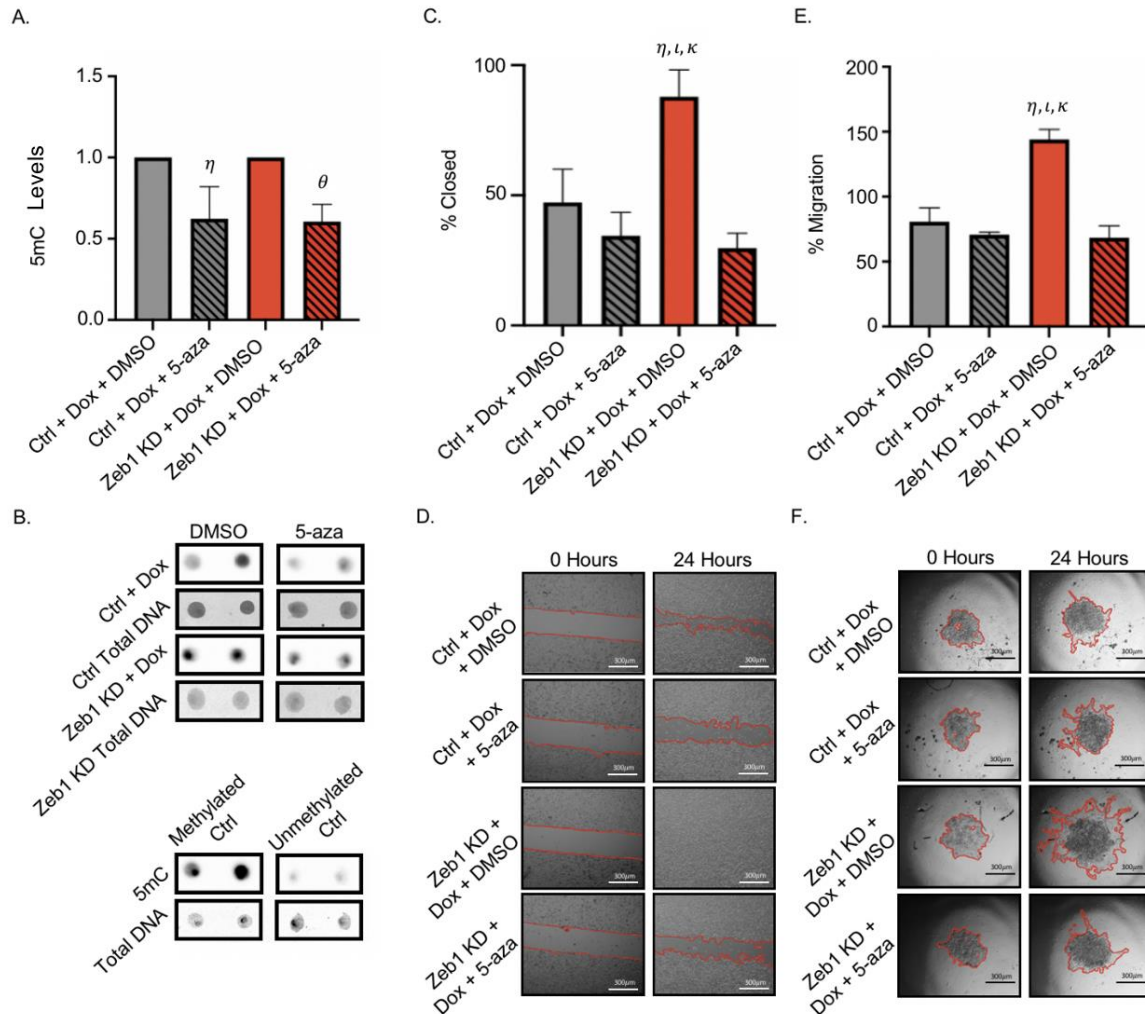


Figure 4-6. Treatment of PC-3 Zeb1KD prostate cancer cells with the global demethylating agent 5-azacitadine (5-aza) results in decreased DNA methylation, migration and invasion. (a,b) PC-3 Zeb1^{KD} (Zeb1 knockdown) with doxycycline (Dox) or control (ctrl) cells were treated with either dimethyl sulfoxide (DMSO) or 5-aza (5 μM) for 24 h and DNA was extracted to assess for global DNA methylation via dot blot assays. Representative dot blots are shown in duplicates side-by-side. Methylated and unmethylated DNA controls were used to validate 5-methylcytosine (5mC) levels. (c,d) Cells were seeded onto physical barrier cell culture dish and grown to 90–100% confluency. Treatments (5 μM 5-aza or DMSO) were added to cells, the physical barrier was removed, and cells were allowed to migrate into the wound. (e,f) Cells were seeded onto ultra-low attachment plates and allowed to grow for 96 h to create spheroids. After 96 h of growth, Matrigel and 5 μM 5-aza or DMSO were added. Representative images are shown for each assay; with migration or invasion calculated based on 5 high-powered fields of view (HP-FOV) per well. Scale bars = 300 μm. Data is presented as the mean ± standard error of the mean (SEM) (n = 3). η = significantly different than ctrl with Dox and treated with DMSO. θ = significantly different than Zeb1^{KD} with Dox and treated with DMSO. ι = significantly different than ctrl with Dox treated with 5 μM 5-aza. κ = significantly different than Zeb1^{KD} with Dox treated with 5 μM 5-aza ($p \leq 0.05$).

5 μ M of 5-aza (Z5), and from Dox-induced ctrl cells treated with DMSO (C0) or 5-aza (C5) and assessed for global changes in DNA methylation using an Infinium MethylationEPIC chip. We observed over 100,000 differentially methylated sites between ctrl + DMSO cells (C0) and Zeb1^{KD} + DMSO cells (Z0) (false discovery rate (FDR) cutoff value = 0.05) (**Figure 4.7a**). We then further assessed only those sites which had an increase in DNA methylation between C0 and Z0 that also demonstrated rescued demethylation in Zeb1^{KD} cells + 5-aza (Z5); resulting in 51 potential sites of importance (FDR cutoff value = 0.05) (**Figure 4.7b**). Of these, 10 sites (LRPPRC, CLDN11, MTOR, EPB41, DAPK1, PPZR2B, ZDHHC2, HSD17B13, MYOM2 and MAN1A1) were have been previously linked to decreased expression and increased aggressiveness/p-EMT, which may be of clinical importance for identifying an aggressive p-EMT phenotype in cancer patients in the future (**Figure 4.7c, Table 4.1**).

4.3.7 MAN1A1, EPB41, HSD17B13 and MYOM2 Are Altered in Prostate Cancer Patients

Finally, we were interested in determining the potential clinical relevance of the identified DNA methylation targets in prostate cancer patients. We analyzed the 10 identified target p-EMT genes using available [Ualcan](#) (accessed on November 26, 2021) and [cBioportal](#) (accessed on November 26, 2021) online clinical databases. We observed significant hypermethylation of 4 of the 10 target genes (MAN1A1, EPB41, HSD17B13, and MYOM2) in primary prostate cancer patient tumors (n = 503) compared to normal prostatic samples (n = 50) ($p \leq 0.05$) (**Figure 4.8a**). Expression of MAN1A1 was also observed to be significantly decreased in metastatic prostate cancer patients (n = 42) relative to non-metastatic prostate cancer patients (n = 44) ($p \leq 0.05$) (**Figure 4.8b**). We observed that decreased expression of MYOM2 correlates with decreased overall survival in prostate cancer patients (**Figure 4.8c**). Taken together, these observations in prostate cancer patients support our pre-clinical findings in aggressive Zeb1^{KD} cells and suggest that these genes merit future investigation as potential biomarkers for combination treatment of prostate cancer patients with 5-aza.

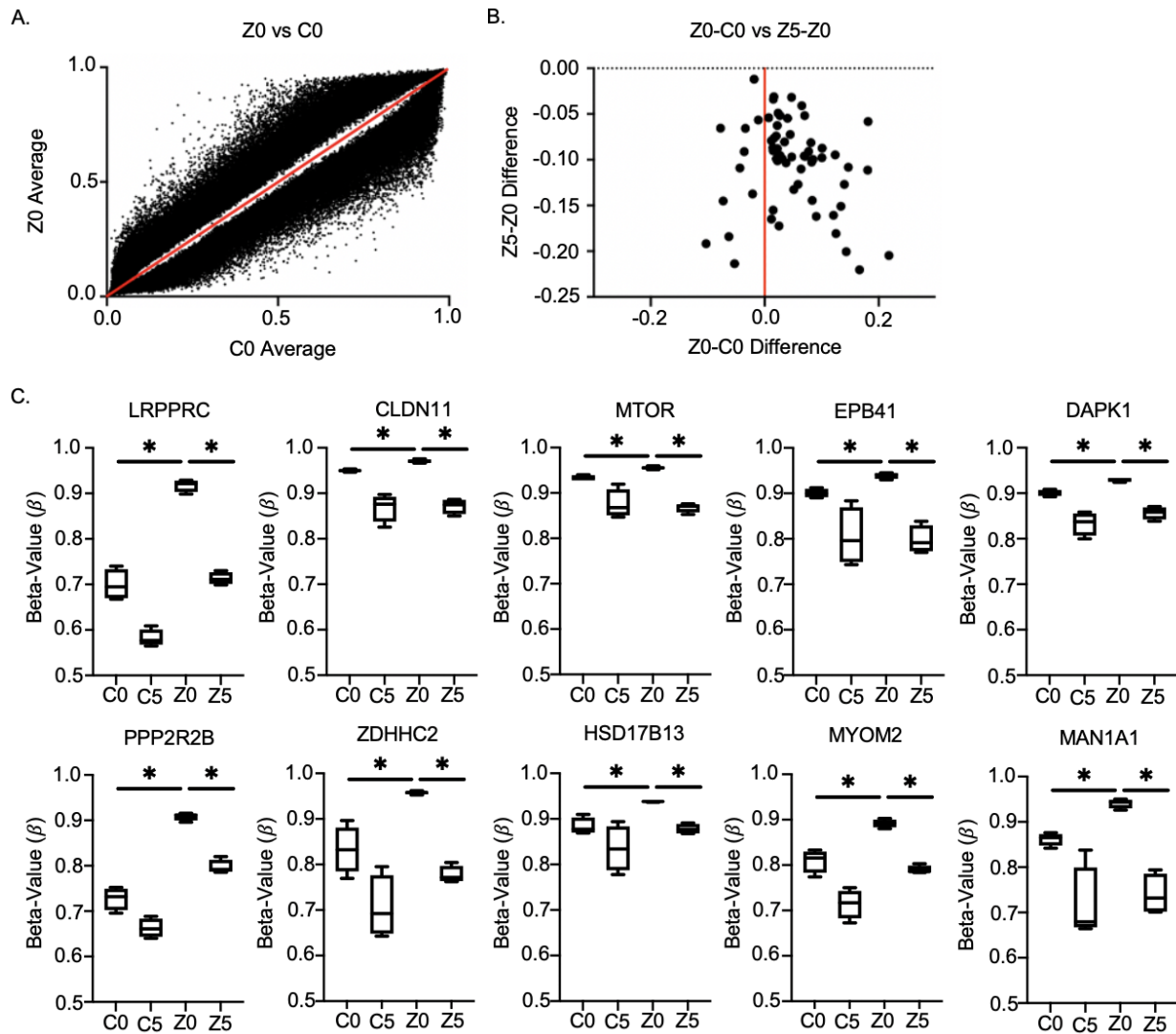


Figure 4-7. DNA methylation chip analysis of *Zeb1*^{KD} PC-3 prostate cancer cells identified 10 genes associated with a p-EMT phenotype. DNA was extracted from PC-3 *Zeb1*^{KD} (*Zeb1* knockdown) cells with doxycycline (Dox) treated with dimethyl sulfoxide (DMSO) (Z0) or 5-azacitadine (5-aza; Z5; 5 μ M), and from Dox-induced control (ctrl) cells treated with DMSO (C0) or 5-aza (C5; 5 μ M) and was assessed for global changes in DNA methylation using an Infinium Methylation EPIC chip. (a) A two-tailed, unpaired, equal variance *t*-test was completed with FDR cut-off value = 0.05 (Benjamini-Hochberg FDR) between C0 and Z0. This was filtered for significant Z0-C0 differences, and 107,971 cg sites were observed. (b) A two-tailed, unpaired, equal variance *t*-test was completed with FDR cut-off value = 0.05 (Benjamini-Hochberg FDR) between Z0 vs. Z5. This was filtered for significant Z0-Z5 differences, and 62 CpG sites were observed. Among the C0-Z0 and Z0-Z5 significant differences, we wanted to identify rescue changes, so we filtered the dataset for cg sites where $Z0-C0 = -(Z5-Z0)$ and identified 51 cg sites (right side of graph (b)). (c) Genes identified in DNA methylation chip analysis (increased DNA methylation from C0 versus Z0 with a corresponding demethylation in Z5). β -values represents the estimate of DNA methylation level at a given locus. Data is presented as the mean \pm standard error of the mean (SEM) (n = 4). * = significant difference between conditions.

Table 4-1. Functional relevance of genes identified in DNA methylation chip analysis.

Gene Symbol	Gene Name	Function Relative to Cancer Aggressiveness
LRPPRC	Leucine rich pentatricopeptide repeat containing	Dysregulation is related to various diseases ranging from tumors to viral infections ³⁰ .
CLDN-11	Claudin-11	Plays an important role in cellular proliferation and migration ³¹ .
mTOR	Mammalian target of rapamycin	Regulates cell growth, proliferation, motility, survival, protein synthesis, autophagy, and transcription ³² .
EPB41	Erythrocyte Membrane Protein Band 4.1	Expression is significantly decreased in HCC tissue specimens, especially in portal vein metastasis or intrahepatic metastasis, compared to normal tissues ³³ .
DAPK1	Death Associated Protein Kinase 1	Downregulation promotes the stemness of cancer stem cells and EMT process by activating Zeb1 in colorectal cancer ³⁴ .
PPP2RR2B	Protein Phosphatase 2 Regulatory Subunit Bbeta	Negative control of cell growth and division ³⁵ .
ZDHHC2	Zinc Finger DHHC-Type Palmitoyltransferase 2	Tumor suppressor in metastasis and recurrence of HCC ³⁶ .
HSD17B13	17- β hydroxysteroid dehydrogenase 13	Downregulated in hepatocellular carcinoma ³⁷ .
MYOM2	Myomesin 2	Downregulation was observed in a clinical assessment of breast cancer patients ³⁸ .
MAN1A1	Mannosidase Alpha Class 1A Member 1	Reduced expression leads to impaired survival in breast cancer ³⁹ .

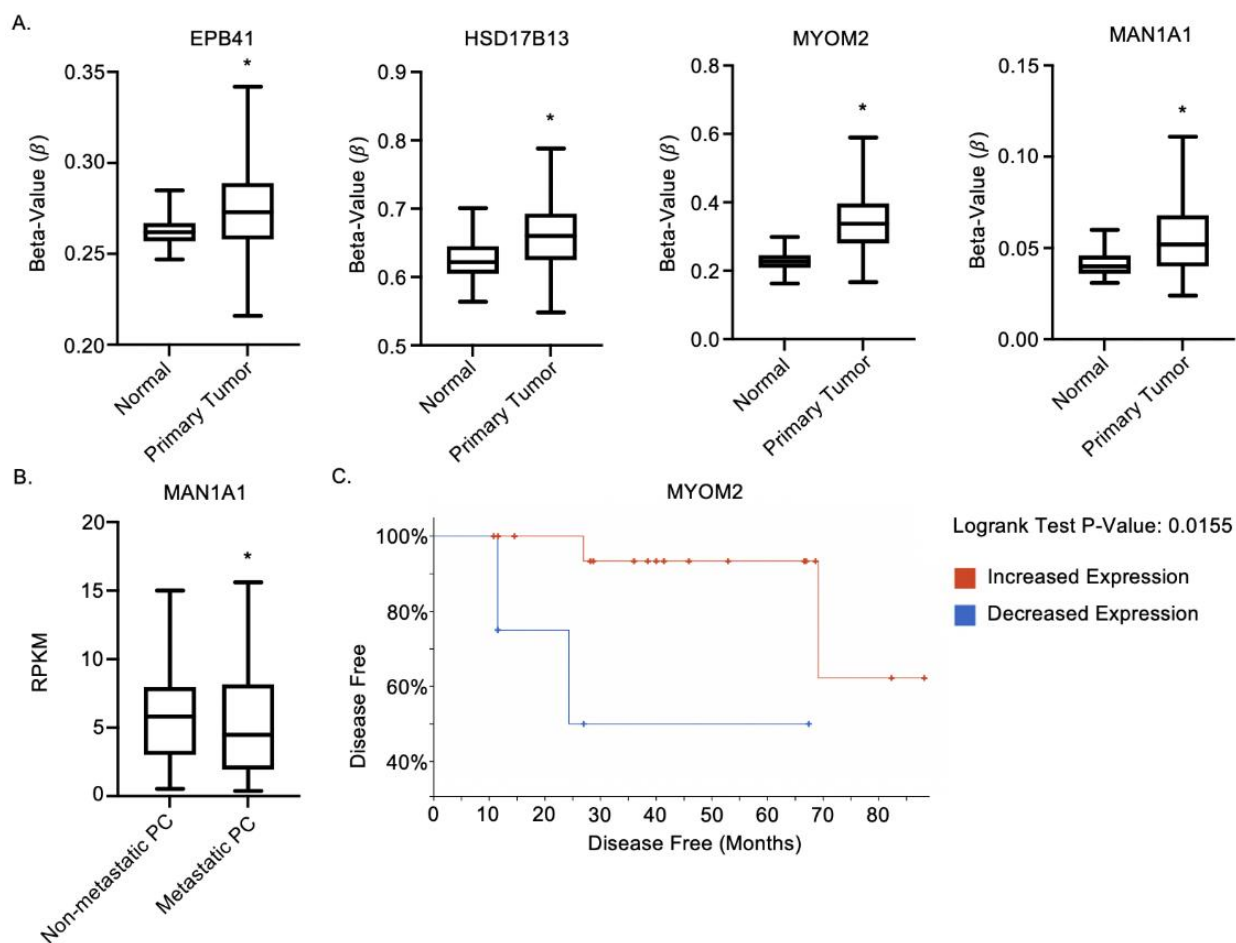


Figure 4-8. MAN1A1, EPB41, HSD17B13 and MYOM2 are altered in prostate cancer patients. (a,b) Ualcan analysis in prostate adenocarcinoma identified (a) 4 identified target genes (MAN1A1, EPB41, HSD17B13 and MYOM2) with increased promoter methylation in primary prostate cancer tumors (n = 502) compared to normal prostatic samples (n = 50) and (b) MAN1A1 RNA expression in metastatic prostate cancer (PC) (n = 42) vs. non-metastatic prostate cancer (n = 44). (c) cBioportal analysis of relationship between MYOM2 expression and progression free survival. * = significant difference between conditions.

4.4 Discussion

Prostate cancer is the most common cancer in American men and the second leading cause of cancer-related death¹. The majority of these deaths are associated with metastasis, a process involving the epithelial-to-mesenchymal (EMT) transition. Furthermore, growing evidence suggests that a p-EMT phenotype, whereby cells are able to simultaneously maintain both epithelial and mesenchymal characteristics, may lead to more aggressive disease than complete EMT¹⁴. Gaining a greater understanding of p-EMT may thus provide insights into the mechanisms of metastatic disease progression, which currently has no cure.

In the current study, we observed that inducible knockdown of Zeb1 in mesenchymal PC-3 cells resulted in a p-EMT phenotype including co-expression of epithelial and mesenchymal markers, a mixed epithelial/mesenchymal morphology, increased invasion and migration, and enhanced expression of p-EMT markers. We also observed a trend of increased CTC numbers in mice where p-EMT was induced after 9 weeks of tumor growth prior to Zeb1 knockdown. This suggests that induction of p-EMT in more progressed primary tumors may have a greater impact on CTC release than on early-stage primary tumors. Additionally, although not statistically significant we observed a trend towards greater incidence of macrometastases after early and midpoint p-EMT induction compared to p-EMT at a later stage mice, despite detecting less CTCs in these groups at endpoint. This potentially suggests that the CTCs produced by early and mid p-EMT induction may have a greater capacity for metastasis than late p-EMT induced mice. Additional studies are warranted in the future to further elucidate the temporal and biological impact of p-EMT on prostate cancer CTC generation and metastasis *in vivo*.

In addition to changes in gene and protein expression, the p-EMT phenotype is commonly associated with aberrant hypermethylation^{40,41}. The global de-methylating agent 5-azacytidine (5-aza) is FDA-approved for treating myelodysplastic syndrome and is currently in 44 phase III clinical trials for treating cancer patients ([ClinicalTrials.gov](https://clinicaltrials.gov); accessed on November 26, 2021), as well as 4 phase II clinical trials specifically for prostate cancer patients ([ClinicalTrials.gov](https://clinicaltrials.gov); accessed on November 26, 2021). When we treated our p-EMT prostate cancer cells with 5-aza, we observed a significant decrease in aggressive phenotype. Furthermore, our DNA methylation chip analysis revealed 10 potential markers for further investigation in association with p-EMT.

Our observations included increased DNA methylation of EPB41 and HSD17B13. EPB41 has been identified as a tumor suppressor in the molecular pathogenesis of meningiomas³³. HSD17B13 expression has also been shown to inhibit the progression and recurrence of hepatocellular carcinomas³⁷. Additionally, Ualcan online database analysis showed increased promoter methylation of both EPB41 and HSD17B13 in prostate cancer patients compared to healthy controls. Silencing of these genes due to increased DNA methylation could result in tumor progression and poor patient survival^{33,37}.

We also observed increased DNA methylation of MAN1A1 in Zeb1^{KD} cells, which correlated with decreased gene expression in prostate cancer patients when assessed on the UALCAN database. Reduced MAN1A1 expression has previously been associated with reduced survival in breast cancer patients³⁹. In our study, Ualcan online database analysis showed increased promoter methylation of MAN1A1 in prostate cancer patients compared to healthy controls and in metastatic prostate cancer patients compared to non-metastatic prostate cancer patients. This suggests that decreased expression of MAN1A1 may be associated with increased prostate cancer aggressiveness and could be a novel marker for identifying a p-EMT phenotype in patient tumors.

Lastly, we demonstrated increased DNA methylation of MYOM2. MYOM2 has been previously been observed to be downregulated in breast cancer patients, as determined by multiplex RT-qPCR³⁸. Our assessment using the cBioportal online database revealed that decreased MYOM2 expression is associated with significantly worse progression free survival in prostate cancer patients compared to those with high MYOM2 expression, suggesting that MYOM2 may be another potential marker for identifying aggressive prostate cancer.

In summary, in this study we developed a stable, inducible p-EMT prostate cancer model that provides the opportunity to investigate the aggressive p-EMT phenotype, a cell state that often occurs transiently *in vivo*. In addition, we have identified 4 potential biomarkers related to p-EMT for which decreased expression may be an indicator of metastatic disease and may warrant consideration for use in identifying patients who would benefit from 5-aza treatment to target hypermethylation. Currently, there is no cure for metastatic prostate cancer, however, early

detection and targeted treatment with agents that target hypermethylation may slow down the progression towards metastasis and improved patient outcomes.

4.5 Conclusions

In the current manuscript we created and characterized a stable inducible p-EMT cell line model by decreasing Zeb1 expression in mesenchymal PC-3 prostate cancer cells. This resulted in an increased aggressive phenotype compared to mesenchymal controls. We identified 10 potential p-EMT markers which had aberrant DNA methylation in these p-EMT cells which may be used as a screening panel for p-EMT patients in the future to allow for earlier detection of aggressive prostate cancer and/or potentially serve to identify patients who might benefit from 5-aza therapy.

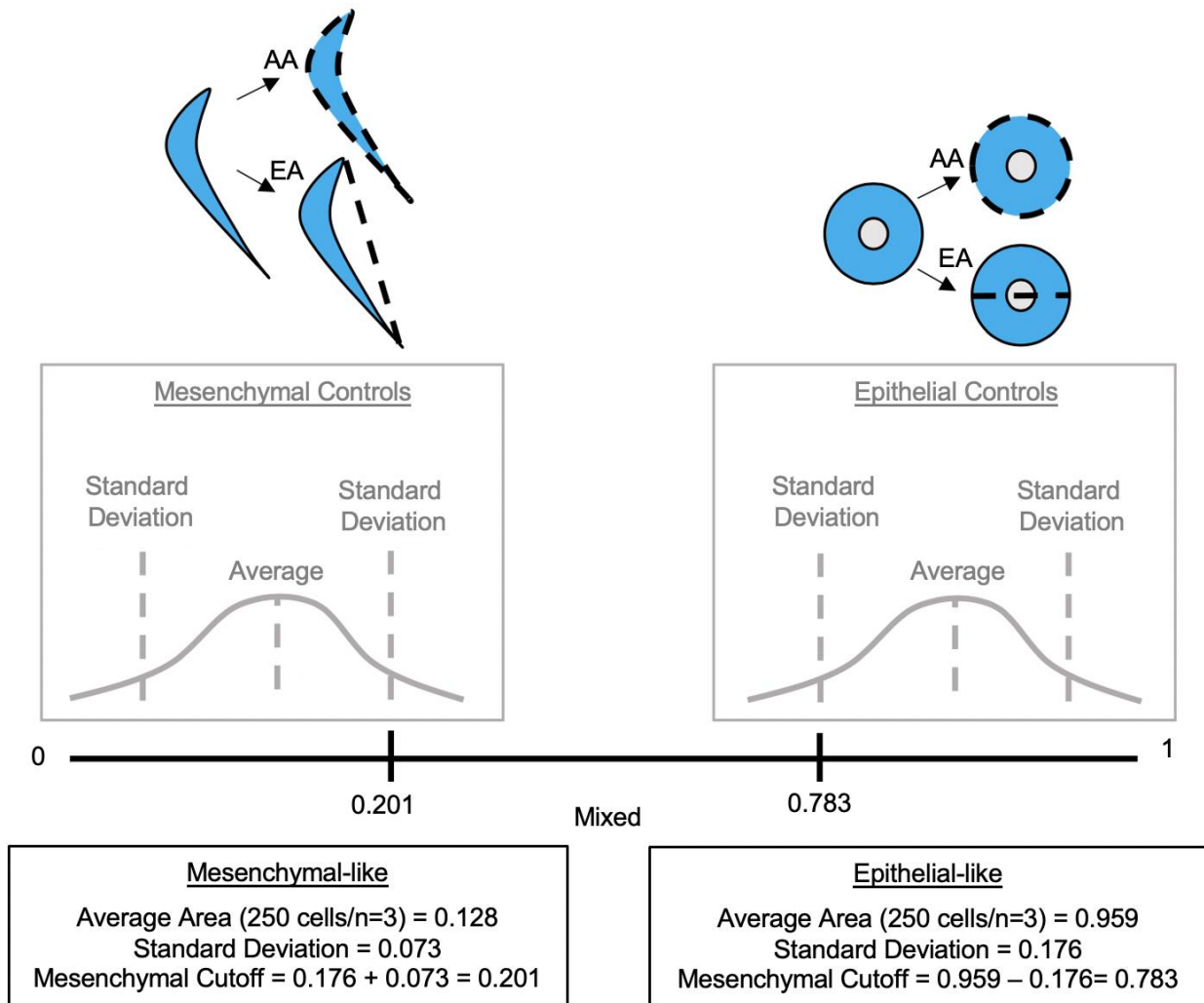
4.6 Supplemental Data – Chapter 4

Supplemental Table 4-1. Antibodies for Immunoblotting.

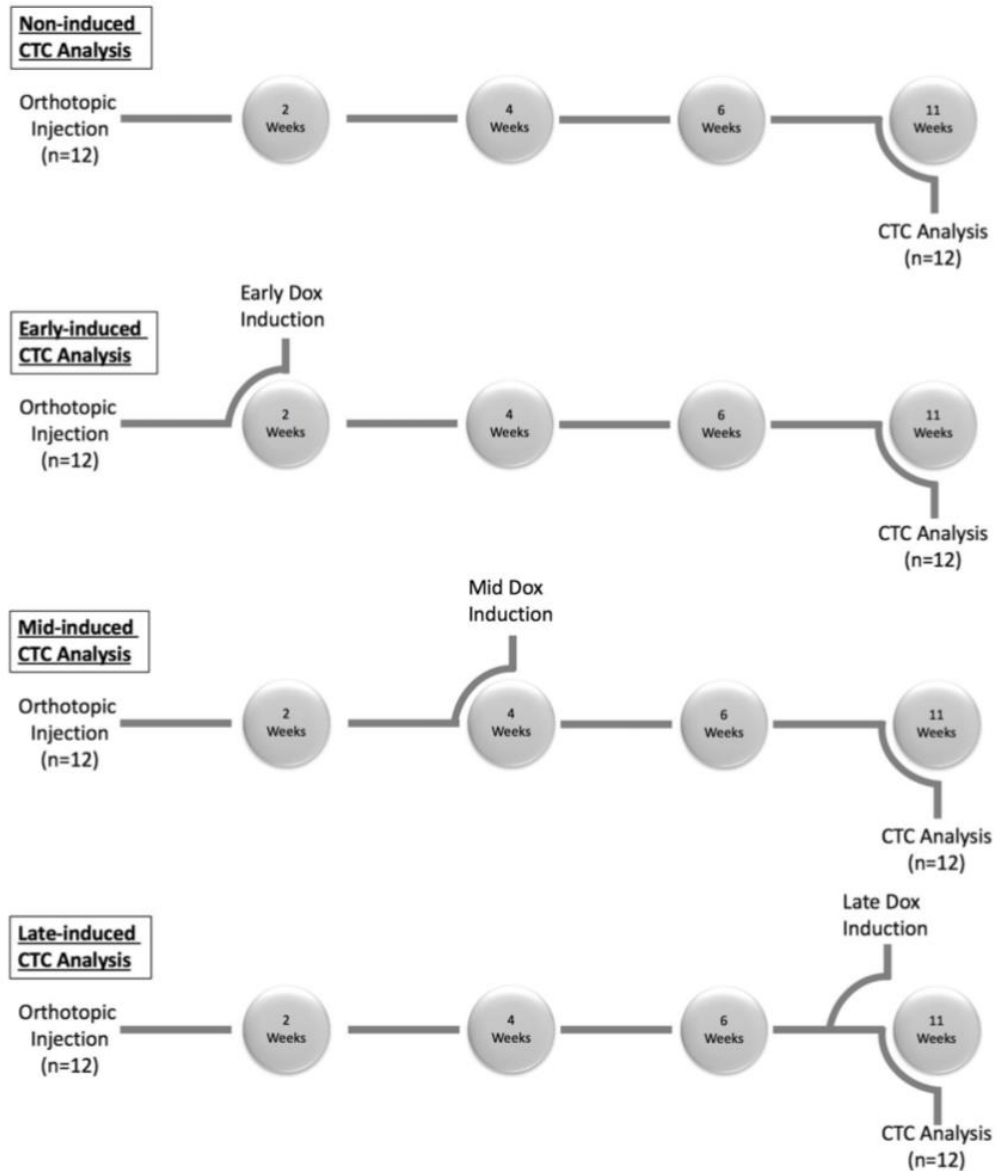
Target Protein	1° Host	kDa	1° Conditions (Overnight @ 4°C)	2° Conditions (1 hour @ room temperature)	Reduced?	Poly/Mono Clonal
Zeb1 (Cell Sig.- 3396)	Rabbit	200	1:500	1:1000	Yes	Mono (D80D3)
EpCAM (Abcam- ab32392)	Rabbit	39	1:1000	1:2000	Yes	Mono (E144)
E-Cadherin (BD Biosciences- 610181)	Mouse	120	1:2000	1:2000	Yes	Mono (36)
N-Cadherin (Abcam- ab76011)	Rabbit	100	1:1000	1:2000	Yes	Mono (EPR1791-4)
Vimentin (Millipore-MAB3400)	Mouse	60	1:1000	1:2000	Yes	Mono (V9)
P-Cadherin (Abcam- ab137729)	Rabbit	91	1:1000	1:2000	Yes	Poly
Integrin β4 (Abcam- ab29042)	Mouse	202	1:1000	1:1000	Yes	Mono (M126)
Actin (Sigma- A2006)	Rabbit	42	1:5000	1:5000	Yes	Poly

Supplemental Table 4-2. Forward and Reverse Primers used for RT-qPCR.

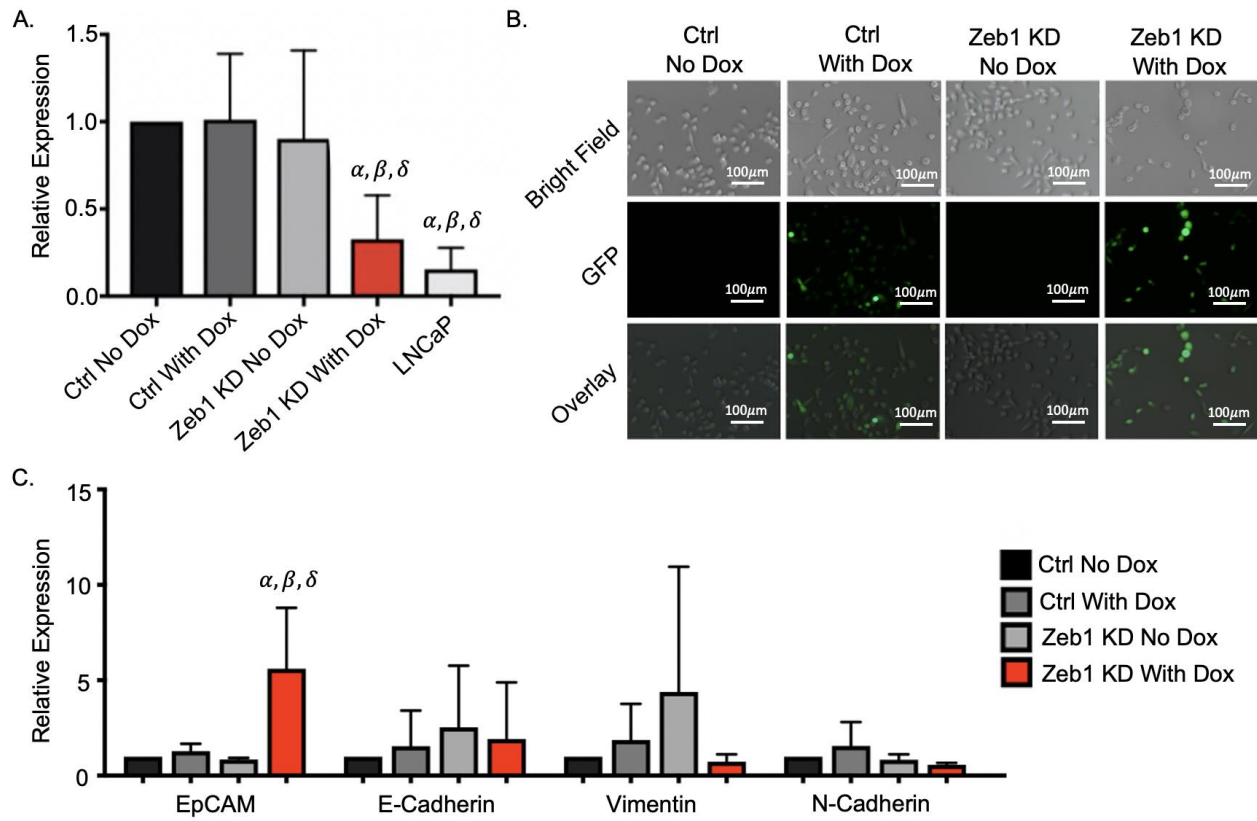
Target Gene	Forward Primer (5' → 3')	Reverse Primer (5' → 3')
Zeb1	AGCACTTGTCTTCTGTGTGATG	CAGGCTTCTCAGCTTCTGCT
EpCAM	CGACTTTTGCCGCAGCTCAGGA	GGGCCCCTTCAGGTTTTGCTCT
E-Cadherin	TGCTGATGCCCCCAATACCCA	GTGATTTCTGGCCCACGCCAA
N-Cadherin	TGACTCCAACGGGGACTGCACA	AGCTCAAGGACCCAGCAGTGGA
Vimentin	AACCAACGACAAAGCCCGCGTC	TTCCGGTTGGCAGCCTCAGAGA
P-Cadherin	AAGTGCTGCAGCCAAAGACAGA	AGGTAGACCCACCTCAATCATCCTC
Integrin β4	GCTTACACCTATTTCCCTGTC	GACCCAGTCCTCGTCTTCTG
GAPDH	TCCATGGCACCGTCAAGGCTGA	GCCAGCATCGCCCCACTTGATT



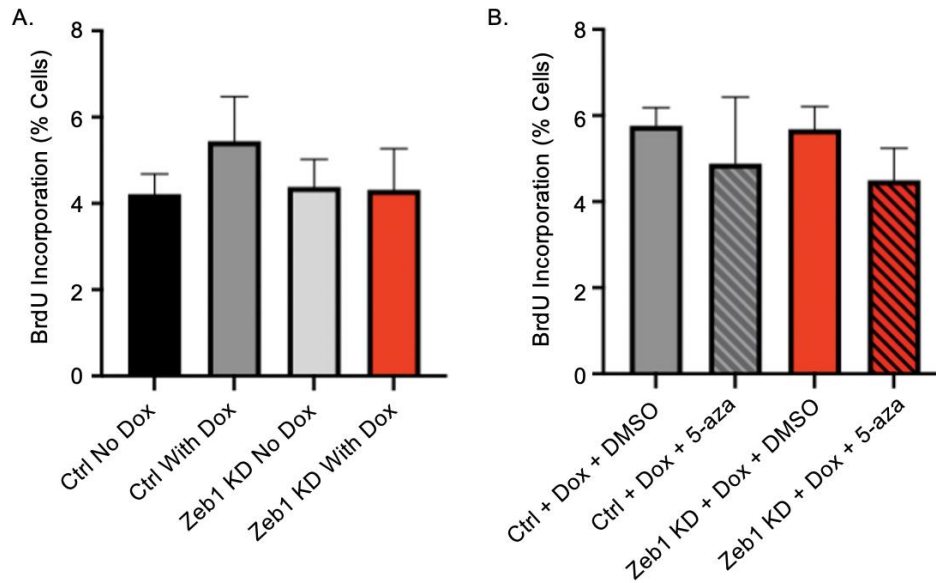
Supplemental Figure 4-1. Cell morphology assay calculations. Epithelial (MDA-MB-468 breast cancer cells) and mesenchymal (primary lung fibroblasts) control cells were assessed for cell shape (250 cells, n=3). The average was calculated and the “cut-off” points for a round (epithelial) cell and an elongated (mesenchymal) cell were calculated by subtracting/adding the standard deviation from/to the average. Zeb1KD and Ctrl cells were then analyzed for cell shape (250 cells, n=3). Any value within the mesenchymal “cut-off” (0-0.201) was considered mesenchymal-like, any value within the epithelial “cut-off” (0.783-1) was considered epithelial-like, and any value which fell in between (0.202-0.782) was considered mixed.



Supplemental Figure 4-2. Schematic of *in vivo* experimental design. Schematic of *in vivo* experimental design. Mice were orthotopically injected with 1×10^6 PC Zeb1KD (n=48) or PC-3 Ctrl cells (n=48). Dox chow was given at 2 (early), 4 (mid), or 9 (late) weeks, or not given Dox at all (n=12/group). Each group was sacrificed at 11 weeks or when mice succumbed to their disease. Blood was drawn 11 weeks and analyzed by the CellSearch® and VyCap. Tissues, primary tumors, and metastases were collected for further analysis.



Supplemental Figure 4-3. Zeb1 RNA can be inducibly knocked down in PC-3 human prostate cancer cells. Mesenchymal human PC-3 prostate cancer cells were engineered to knockdown expression of the master EMT regulator Zeb1 using the SMARTvector inducible lentiviral shRNA system (Dharmacon), which features Tet-on® induction of the target shRNA in the presence of Doxycycline (Dox). (a) RT-qPCR analysis of Zeb1 mRNA expression in the presence of absence of Dox in Zeb1^{KD} or Ctrl cells, or LNCaP cells. (b) Fluorescence microscopy of Zeb1^{KD} and Ctrl cells ± Dox. (c) RT-qPCR analysis of EpCAM, E-Cadherin, Vimentin, and N-Cadherin mRNA expression in Zeb1^{KD} or Ctrl cells ± Dox. Scale bars = 100 μ m. Data is presented as the mean \pm SEM (n=3). α = significantly different than PC-3 Ctrl no Dox. β = significantly different than Ctrl with Dox. δ = significantly different than Zeb1KD no Dox ($p \leq 0.05$).



Supplemental Figure 4-4. Knockdown of Zeb1 in PC-3 prostate cancer cells does not alter cell proliferation. Cells (1.6×10^4 /well) were seeded on 8-well chamber slides with or without Dox, DMSO, and/or 5 μ M 5-azacytidine (5-aza), a global demethylating agent. Cells were serum starved for 3 d and then treated with media containing fetal bovine serum albumin for 24 h. Cells were then treated with BrdU for 30 min and formalin fixed. Cells were incubated with a BrdU antibody overnight and visualized using 5 high-powered fields of view (FOV) using DAPI mounting media. **(a)** BrdU incorporation of Ctrl and Zeb1^{KD} cells \pm Dox. **(b)** BrdU incorporation of Ctrl and Zeb1^{KD} cells + Dox \pm DMSO or 5-aza (5 μ M). Data is presented as the mean/ \pm SEM (n=3).

4.7 References

1. Siegel RL, Miller KD, Jemal A. Cancer statistics, 2020. *CA Cancer J Clin.* 2020. doi:10.3322/caac.21590
2. Pantel K, Brakenhoff RH, Brandt B. Detection, clinical relevance and specific biological properties of disseminating tumour cells. *Nat Rev Cancer.* 2008. doi:10.1038/nrc2375
3. Fidler IJ. The pathogenesis of cancer metastasis: The “seed and soil” hypothesis revisited. *Nat Rev Cancer.* 2003;3(6):453-458. doi:10.1038/nrc1098
4. Kalluri R, Weinberg RA. The basics of epithelial-mesenchymal transition. *J Clin Invest.* 2009;119(6):1420-1428. doi:10.1172/JCI39104
5. Kano A. Tumor cell secretion of soluble factor(s) for specific immunosuppression. *Sci Rep.* 2015;5. doi:10.1038/srep08913
6. Weidner N, Semple JP, Welch WR, Folkman J. Tumor angiogenesis and metastasis--correlation in invasive breast carcinoma. *N Engl J Med.* 1991;324(1):1-8. doi:10.1056/NEJM199101033240101
7. Scott J, Kuhn P, Anderson ARA. Unifying metastasis-integrating intravasation, circulation and end-organ colonization. *Nat Rev Cancer.* 2012;12(7):445-446. doi:10.1038/nrc3287
8. Hou JM, Krebs M, Ward T, et al. Circulating tumor cells as a window on metastasis biology in lung cancer. *Am J Pathol.* 2011;178(3):989-996. doi:10.1016/j.ajpath.2010.12.003
9. Palstra RJ, Grosveld F. Transcription factor binding at enhancers: Shaping a genomic regulatory landscape in flux. *Front Genet.* 2012. doi:10.3389/fgene.2012.00195
10. Takeyama Y, Sato M, Horio M, et al. Knockdown of ZEB1, a master epithelial-to-mesenchymal transition (EMT) gene, suppresses anchorage-independent cell growth of lung cancer cells. *Cancer Lett.* 2010. doi:10.1016/j.canlet.2010.04.008
11. Graham TR, Yacoub R, Taliaferro-Smith L, et al. Reciprocal regulation of ZEB1 and AR in triple negative breast cancer cells. *Breast Cancer Res Treat.* 2010. doi:10.1007/s10549-009-0623-7
12. Jiang Y, Yan L, Xia L, et al. Zinc finger E-box– binding homeobox 1 (ZEB1) is required for neural differentiation of human embryonic stem cells. *J Biol Chem.* 2018. doi:10.1074/jbc.RA118.005498
13. Liao TT, Yang MH. Revisiting epithelial-mesenchymal transition in cancer metastasis: the connection between epithelial plasticity and stemness. *Mol Oncol.* 2017. doi:10.1002/1878-0261.12096
14. Jolly MK, Somarelli JA, Sheth M, et al. Hybrid epithelial/mesenchymal phenotypes promote metastasis and therapy resistance across carcinomas. *Pharmacol Ther.* 2019.

doi:10.1016/j.pharmthera.2018.09.007

15. Yu M, Bardia A, Wittner BS, et al. Circulating breast tumor cells exhibit dynamic changes in epithelial and mesenchymal composition. *Science* (80-). 2013. doi:10.1126/science.1228522
16. DeAngelis JT, Farrington WJ, Tollefsbol TO. An overview of epigenetic assays. *Mol Biotechnol*. 2008. doi:10.1007/s12033-007-9010-y
17. Kitagawa Y, Kyo S, Takakura M, et al. Demethylating reagent 5-azacytidine inhibits telomerase activity in human prostate cancer cells through transcriptional repression of hTERT. *Clin Cancer Res*. 2000;6(7):2868-2875.
18. Lowes LE, Goodale D, Xia Y, et al. Epithelial-to-mesenchymal transition leads to disease-stage differences in circulating tumor cell detection and metastasis in pre-clinical models of prostate cancer. *Oncotarget*. 2016. doi:10.18632/oncotarget.12682
19. Kitz J, Lowes L, Goodale D, Allan A. Circulating Tumor Cell Analysis in Preclinical Mouse Models of Metastasis. *Diagnostics*. 2018. doi:10.3390/diagnostics8020030
20. Bubendorf L, Schöpfer A, Wagner U, et al. Metastatic patterns of prostate cancer: An autopsy study of 1,589 patients. *Hum Pathol*. 2000;31(5):578-583. doi:10.1053/hp.2000.6698
21. Castle EP. Prostate cancer metastasis: Where does prostate cancer spread?
22. Goodale D, Phay C, Postenka CO, Keeney M, Allan AL. Characterization of tumor cell dissemination patterns in preclinical models of cancer metastasis using flow cytometry and laser scanning cytometry. *Cytom Part A*. 2009;75A(4):344-355. doi:10.1002/cyto.a.20657
23. Point SS. Infinium HD Methylation Assay Manual Workflow Checklist Convert DNA Create the BCD Plate Infinium HD Methylation Assay Manual Workflow Checklist Incubate DNA Fragment DNA. 2019;(November):1-5.
24. Kasper, Daniel Hansen, Martin, Aryee, Rafael, A. Irizarry, Andrew, E. Jaffe, Jovana, Maksimovic, E. Andres, Houseman, Jean-Philippe, Fortin, Tim, Triche, Shan, V. Andrews. Peter FH. <https://bioconductor.org/packages/release/bioc/html/minfi.html>.
25. Yuan, Tian, Tiffany, J Morris, Amy, P Webster, Zhen, Yang, Stephan, Beck, Andrew, Feber, Andrew ET. The Chip Analysis Methylation Pipeline.
26. Teschendorff AE, Marabita F, Lechner M, et al. A beta-mixture quantile normalization method for correcting probe design bias in Illumina Infinium 450 k DNA methylation data. *Bioinformatics*. 2013;29(2):189-196. doi:10.1093/bioinformatics/bts680
27. Ribeiro AS, Paredes J. P-Cadherin Linking Breast Cancer Stem Cells and Invasion: A Promising Marker to Identify an "Intermediate/Metastable" EMT State. *Front Oncol*. 2015. doi:10.3389/fonc.2014.00371

28. Bierie B, Pierce SE, Kroeger C, et al. Integrin- β 4 identifies cancer stem cell-enriched populations of partially mesenchymal carcinoma cells. *Proc Natl Acad Sci*. 2017. doi:10.1073/pnas.1618298114
29. Czibere A, Bruns I, Kröger N, et al. 5-Azacytidine for the treatment of patients with acute myeloid leukemia or myelodysplastic syndrome who relapse after allo-SCT: A retrospective analysis. *Bone Marrow Transplant*. 2010;45(5):872-876. doi:10.1038/bmt.2009.266
30. Cui J, Wang L, Ren X, Zhang Y, Zhang H. LRPPRC: A multifunctional protein involved in energy metabolism and human disease. *Front Physiol*. 2019;10(MAY):1-10. doi:10.3389/fphys.2019.00595
31. Agarwal R, Mori Y, Cheng Y, et al. Silencing of claudin-11 is associated with increased invasiveness of gastric cancer cells. *PLoS One*. 2009;4(11). doi:10.1371/journal.pone.0008002
32. Cheung KJ, Ewald AJ, Om Alblazi KM, et al. Perspectives in Cancer Research Molecular Insights into Cancer Invasion : Strategies for Prevention and Intervention. *Curr Oncol*. 2015. doi:10.1158/1078-0432.CCR-06-3045
33. Liu S, Liu J, Yu X, Shen T, Fu Q. Identification of a Two-Gene (PML-EPB41) Signature With Independent Prognostic Value in Osteosarcoma. *Front Oncol*. 2020;9(January):1-11. doi:10.3389/fonc.2019.01578
34. Yuan W, Ji J, Shu Y, et al. Downregulation of DAPK1 promotes the stemness of cancer stem cells and EMT process by activating ZEB1 in colorectal cancer. *J Mol Med*. 2019;97(1):89-102. doi:10.1007/s00109-018-1716-8
35. Vazquez A, Kulkarni D, Grochola LF, et al. A genetic variant in a PP2A regulatory subunit encoded by the PPP2R2B gene associates with altered breast cancer risk and recurrence. *Int J Cancer*. 2011;128(10):2335-2343. doi:10.1002/ijc.25582
36. Peng C, Zhang Z, Wu J, et al. A critical role for ZDHHC2 in metastasis and recurrence in human hepatocellular carcinoma. *Biomed Res Int*. 2014;2014. doi:10.1155/2014/832712
37. Chen J, Zhuo JY, Yang F, et al. 17-Beta-Hydroxysteroid Dehydrogenase 13 Inhibits the Progression and Recurrence of Hepatocellular Carcinoma. *Hepatobiliary Pancreat Dis Int*. 2018;17(3):220-226. doi:10.1016/j.hbpd.2018.04.006
38. Yamamoto F, Yamamoto M. Identification of genes that exhibit changes in expression on the 8p chromosomal arm by the Systematic Multiplex RT-PCR (SM RT-PCR) and DNA microarray hybridization methods. *Gene Expr*. 2008;14(4):217-227. doi:10.3727/105221608786883816
39. Legler K, Rosprim R, Karius T, et al. Reduced mannosidase MAN1A1 expression leads to aberrant N-glycosylation and impaired survival in breast cancer. *Br J Cancer*. 2018;118(6):847-856. doi:10.1038/bjc.2017.472

40. Tam WL, Weinberg RA. The epigenetics of epithelial-mesenchymal plasticity in cancer. *Nat Med*. 2013. doi:10.1038/nm.3336
41. Lu W, Kang Y. Epithelial-Mesenchymal Plasticity in Cancer Progression and Metastasis. *Dev Cell*. 2019. doi:10.1016/j.devcel.2019.04.010

Chapter 5

5 Overall Discussion

Prostate cancer is the second leading cause of cancer related deaths in American men, and the majority of these deaths occur as the result of metastasis^{1,2}. The process of metastasis is associated with an epithelial-to-mesenchymal transition (EMT) in cancer cells, leading to greater migratory and invasive capacity and enhanced resistance to therapy³⁻⁵. During metastasis and associated EMT, cancer cells are shed from the primary tumor and disseminate throughout the body as circulating tumor cells (CTCs) in the bloodstream^{3,6}. The presence and molecular characteristics of CTCs in patients has been correlated with increased metastatic disease, reduced survival, and therapy response/resistance^{7,8}. Assessment of CTCs therefore presents a unique opportunity to study cancer progression and treatment effectiveness from a simple blood test⁹. However, outstanding questions regarding the effectiveness of CTC capture regardless of EMT phenotype and limited application for downstream analysis due to CTC heterogeneity has resulted in hesitation in the clinical adoption of CTCs as a biomarker for directing patient care^{3,10}. This thesis aimed to gain a greater understanding of the functional role of EMT in CTC generation, detection, and metastatic behavior by converging technology development/validation, clinical studies, and pre-clinical investigations of CTCs and EMT. In the future, this knowledge could lead to increased accessibility of liquid CTC biopsies for prostate cancer patients of any disease stage and/or EMT status and allow for a greater number of patients to benefit from a personalized medicine approach to combating disease progression and improving outcomes.

5.1 Summary of Key Experimental Findings

1. Using novel CTC capture and enumeration approaches developed in this thesis, the Parsortix® and VyCap CTC technologies are valuable for EMT-independent clinical and preclinical blood sample analysis.
2. In addition to EMT-independent capture and enumeration of CTCs, small sample RNA isolation and analysis techniques developed in this thesis demonstrate that CTCs can be harvested from clinical and preclinical blood samples with Parsortix® and VyCap and used for downstream molecular analysis.

3. In metastatic prostate cancer patients at different disease progression stages along the spectrum of hormone-sensitive to castrate-resistant, CTC enumeration is similar between CellSearch® and Parsortix®.
4. HyCEAD molecular analysis of prostate cancer CTCs identified 19 genes whose differential expression among metastatic prostate cancer patient cohorts may contribute to disease progression. Of these, 13 genes were validated through UALCAN TCGA analysis to be associated with prostate cancer, metastasis, and/or decreased overall survival.
5. Decreased expression of the EMT-inducing transcription factor Zeb1 in mesenchymal PC-3 prostate cancer cells results in an aggressive partial EMT (p-EMT) phenotype including co-expression of epithelial and mesenchymal markers, a mixed epithelial/mesenchymal morphology, increased invasion and migration, and enhanced expression of p-EMT markers.
6. Treatment of p-EMT prostate cancer cells with the global de-methylating drug 5-azacytidine (5-aza) mitigates the observed aggressive phenotype. DNA methylation chip analysis revealed 10 potential targets for identifying and/or targeting p-EMT prostate cancer in the future.
7. Analysis of clinical data through The Cancer Genome Atlas (TCGA) demonstrates that 4 of these genes (EPB41, HSD17B13, MYOM2, and MAN1A1) have differential methylation in prostate cancer and are associated with disease progression and metastatic disease.

5.2 Implications of Experimental Findings

5.2.1 Parsortix® and VyCap technologies are valuable for EMT-independent capture, enumeration and analysis of CTCs in clinical and pre-clinical blood samples

The CellSearch® is currently the only FDA-approved technology for enumerating CTCs in the clinical management setting¹¹. However, CellSearch® only captures CTCs which express EpCAM (epithelial cell adhesion molecule) and in previous studies, was unable to detect CTCs in approximately 30% of patients with various cancers who had widespread metastatic disease^{11,12}. This is potentially due to the loss of EpCAM expression and the concomitant gain of mesenchymal

marker expression associated with EMT and metastasis¹³⁻¹⁶. Based on this, we developed and validated novel protocols for isolating, enumerating, and analyzing CTCs regardless of EMT phenotype for both clinical (human) and pre-clinical (mouse) studies. For clinical studies in patients, human breast or prostate cancer CTCs in human blood can be successfully isolated using Parsortix® and identified/enumerated based on expression of the epithelial marker EpCAM and/or the mesenchymal marker N-Cadherin¹⁷. This allows for capture of CTCs in patient samples regardless of epithelial and/or mesenchymal marker expression and provides an improvement over CellSearch®. Although the Parsortix® is not yet FDA-approved, its potential clinical validity is supported by a CE mark in Europe and a number of promising clinical studies ([Clinicaltrials.gov](https://clinicaltrials.gov); accessed on December 1, 2021), and this is a key advantage of this platform. However, the main limitation of the Parsortix® is the time it takes to process a single sample; approximately seven hours to separate, stain, harvest, and clean the instrument in preparation for the next sample. While this is somewhat manageable in the clinical trials setting, it is less than optimal for pre-clinical studies, and thus we assessed the VyCap platform as an alternative. For pre-clinical studies in xenograft mouse models, we demonstrated that human prostate and breast cancer CTCs spiked into mouse blood can be successfully isolated using VyCap and identified/enumerated based on their unique expression of human leukocyte antigen (HLA)¹⁷. This allows for high-throughput analysis of CTCs regardless of EMT phenotype in pre-clinical xenograft mouse studies.

In addition to the reliance on EpCAM expression for CTC isolation, another disadvantage of the FDA- and Health Canada-approved CellSearch® is the limited ability for CTC harvesting and downstream molecular analysis of CTCs¹¹. This is problematic as there is a growing need for accurate, real-time assessment of disease evolution and progression and how molecular characteristics may influence the probability of metastasis, relapse, and/or response to treatment¹⁸. Additionally, a complex set of biological processes must occur for cancer cells to metastasize, which generates considerable heterogeneity after primary diagnosis¹⁹. Therefore, treatment decisions based on molecular characteristics of the primary tumor may be inaccurate as these characteristics may not represent the molecular changes that occur during disease progression and development of metastasis¹⁹⁻²¹. We developed and validated a small sample RNA isolation and analysis protocol for downstream CTC analysis using either the Parsortix® for clinical human samples or the VyCap for pre-clinical mouse samples¹⁷. The ability to assess gene expression in real-time during disease progression has the potential to allow early identification of molecular

changes driving metastatic disease without invasive biopsies. Combined with our validated CTC enumeration protocols, this will allow researchers to capture and analyze CTCs regardless of EMT phenotype and assess for biological markers to aid in advancing the understanding of EMT, metastasis, and CTC generation.

5.2.2 Use of Parsortix® and HyCEAD for analysis of CTCs in prostate cancer patients

Due to the reliance of the epithelial marker EpCAM to isolate CTCs, adoption of CTC analysis has been slow to move into clinical practice because of uncertainties about the relationship between EMT and CTCs and the corresponding potential for false negative results in metastatic cancer patients¹¹. Our development and validation of an EMT-independent CTC enumeration protocol for Parsortix® was driven by this unmet need, and in Chapter 3 we compared CTC capture and enumeration between Parsortix® and CellSearch® in metastatic prostate cancer patients at different stages of disease progression from hormone-sensitive, bone-only metastasis to fully progressed castrate-resistant disease. We originally hypothesized that as cancer progressed, we would observe trends of reduced CTC capture using the epithelial-based CellSearch® and increased capture using the EMT-independent Parsortix®. However, our results demonstrated that there was no significant difference in CTC enumeration between the two platforms regardless of patient cohort. This highlights that Parsortix® is able to capture and enumerate CTCs just as effectively as CellSearch® (considered the clinical “gold standard”), further validating that Parsortix® is a good alternative for CTC enumeration in clinical trials where there is interest in harvesting CTCs for downstream analysis. In addition, our results suggest that the EpCAM selection step of the CellSearch® protocol enables reliable detection of CTCs with a mesenchymal or hybrid epithelial/mesenchymal phenotype, thus supporting the continued adoption of CTC evaluation into clinical practice for prostate cancer patients.

As mentioned above, a significant limitation of the CellSearch® is the inability to harvest CTCs for downstream molecular analysis¹¹. This unmet need has driven the development of molecular analysis technology for downstream analysis of CTCs harvested from Parsortix®. This technology assesses RNA from harvested CTCs via Hybrid Capture Extension and Detection (HyCEAD) mRNA analysis, multiplex amplification, and chemiluminescent detection of up to 100 genes using a single flow through chip²². After harvesting CTCs from 28 of our clinical prostate cancer

patient samples, we assessed mRNA expression of 155 genes and found altered expression in 119 genes. Of these, we identified 19 biologically relevant genes that gained or lost expression through the progressive metastatic patient cohorts. The loss of expression of 3 of these genes or the increased expression of 16 of these genes has been described in the literature as being associated with increased tumor progression²³⁻⁴². Further investigation using the TCGA database revealed that 11 of these 19 genes had significantly differential expression in normal tissue compared to prostate cancer tissue, 7 of the 19 genes had significantly differential expression in metastatic prostate cancer compared to primary tumors, and 1 out of 19 was associated with decreased overall survival in prostate cancer patients. Together, the HyCEAD analysis in our clinical study provides a strong foundation for future work aimed at developing a novel prostate cancer panel for characterizing metastatic progression in prostate cancer patients using CTCs. These biomarkers may identify patients' metastatic progression earlier than previously possible and without invasive biopsies, thus providing physicians with critical information to guide treatment and ultimately improve patient outcomes.

5.2.3 Reduced Zeb1 expression in prostate cancer cells leads to an aggressive partial-EMT phenotype associated with altered global methylation patterns

To further investigate the relationship between EMT and metastasis, we knocked down the expression of the EMT-inducing transcription factor Zeb1 in mesenchymal PC-3 prostate cancer cells^{43,44}. We originally hypothesized that this would lead to a mesenchymal-to-epithelial transition (MET) and subsequent decreased cell aggressiveness. Unexpectedly, we instead observed an increase in cell aggressiveness upon Zeb1 knockdown (Zeb1^{KD}) associated with co-expression of epithelial and mesenchymal markers, a mixed epithelial/mesenchymal cell morphology, and enhanced migration and invasion compared to control PC-3 cells. Upon continued investigation, we revised our hypothesis and investigated the possibility that knockdown of Zeb1 in PC-3 cells leads to a partial-EMT phenotype. Cells displaying p-EMT retain attributes from both epithelial and mesenchymal cells^{14,45} and have enhanced ability for migration, stemness, tumor progression, and CTC generation^{3,46,47}. Due to their high tumorigenic potential, p-EMT cells have been associated with poorer patient prognosis compared to cells with complete EMT or MET⁴⁷. Our development of a stable p-EMT cell line allowed for *in vitro* characterization, and paves the way for future *in vivo* analysis of p-EMT (typically a plastic/transient state)⁴⁷ and its

relationship with CTC generation, metastasis, and capture. Additionally, we were able to mitigate the aggressive nature of our p-EMT prostate cancer cells by treatment with the global demethylating drug 5-azacytidine (5-aza)⁴⁸. Currently, 5-aza is used to treat acute myeloid leukemia and myelodysplastic syndrome, but is also in phase 2 and 3 trials for treating many cancers including prostate cancer⁴⁹. Thus, we have identified 5-aza as a promising therapy for treating aggressive p-EMT cancers in the future which may reduce disease progression and enhance overall survival for prostate cancer patients.

The p-EMT phenotype is commonly associated with aberrant hypermethylation of DNA^{50,51}. This is consistent with the results of our studies, which demonstrated that treatment with 5-aza leads to decreased migration and invasion in p-EMT prostate cancer cells. Global methylation analysis using an Infinium MethylationEPIC array revealed 10 genes in Zeb1^{KD} cells (versus controls) whose DNA hypermethylation and subsequent reversal in the presence of 5-aza treatment suggest that they may contribute to increased cancer aggressiveness. Of these, 6 of 10 do not have established differential methylation in prostate cancer patients, while 4 of 10 genes do have established differential methylation in prostate cancer patients as assessed via TCGA data. This includes a correlation between MYOM2 hypermethylation and metastatic prostate cancer, and a correlation between decreased MAN1A1 expression and decreased progression free survival in prostate cancer patients. Notably, while all 10 of these genes have been individually described in the literature as contributing to cancer progression when silenced⁵²⁻⁶¹, to the best of our knowledge our study provides the first evidence that these 10 genes may provide a basis for developing a novel p-EMT gene panel or signature for prostate cancer. This may provide a framework to enhance prognostic and/or therapeutic options for aggressive prostate cancer in the future by identifying new p-EMT biomarkers to classify patients who may benefit from combination treatment with the clinically relevant inhibitor 5-azacitadine.

5.3 Possible Limitations of the Thesis Work

The data presented throughout this thesis represents novel findings related to the role of EMT in CTC technology development and CTC/metastasis biology in both the pre-clinical and clinical settings. Although these findings provide significant contributions to the fields of CTC analysis and prostate cancer, there are some limitations related to this work which are discussed in detail below.

In Chapter 2, we developed two novel EMT-independent approaches for analyzing CTCs and compared their CTC capture/enumeration capabilities relative to the Health Canada and FDA-cleared CellSearch®. Due to the small amount of blood available from mouse pre-clinical *in vivo* studies, the CellSearch® CTC enumeration protocol had to be modified because the smaller volume was not compatible with the automated immunomagnetic CellSearch® Autoprep system normally used in the clinical protocol³. It was apparent even at baseline recovery of pre-stained cells that the mouse CellSearch® CTC enumeration protocol was inferior to the VyCap mouse CTC enumeration protocol regardless of EMT phenotype¹⁷. This may be due to the manual immuno-magnetic separation and transfer step to the CellSearch® MagNest™ cartridge for analysis using the CellSearch® Analyzer. During this step, it is possible to lose a significant number of CTCs which do not stay in the magnet but are instead discarded as waste. However, one significant advantage of using the CellSearch® for analyzing samples is the automated image capture of the CellSearch® Analyzer, which not only allows for multiple users to assess for and confirm the presence of CTCs but allows for long-term data storage of all CTCs captured by CellSearch® for future re-analysis if necessary. While our developed protocol for mouse CTC analysis using VyCap allows for image capture of individual CTCs, it does not include automated, whole chip imaging to allow for multi-user CTC enumeration or data storage. However, VyCap is compatible with ACCEPT, an open-source CTC image analysis program which can automatically identify CTCs based on different parameters using image analysis algorithms⁶². This could allow user identification of CTCs with the same benefits of the CellSearch®. Lastly, in order to maintain the capacity for high user-specific customization, which is not typically associated with clinically validated and approved tests, the manufacturers of VyCap are not planning to seek FDA- or Health Canada-approval. While this ultimately hinders the clinical utility of this platform, it does allow for diverse use in the pre-clinical setting which can be customized for many different research applications.

In Chapter 3, we compared the EMT-independent Parsortix® analysis protocol developed in Chapter 2 with the CellSearch® for CTC analysis in metastatic prostate cancer patients at different disease progression stages along the spectrum of hormone-sensitive to castrate-resistant. When we designed the study, we expected to see significantly enhanced capture of CTCs by the Parsortix® as disease progressed. However, our findings instead revealed no significant differences in capture

between patient cohorts. One possible reason that we did not obtain the expected results is due to the pilot nature of the study and the resulting small sample size of each prostate cancer cohort ($n = 9-10$ patients each). Due to the heterogeneity of CTC number in each cohort, it is possible that an increase in sample size would provide a better understanding of how disease progression affects CTC generation as well as CTC capture and enumeration using CellSearch® versus Parsortix®. Having completed the small sample pilot study, a power analysis could determine the optimal sample size for each cohort for a follow-up study in the future. Additionally, our novel EMT-independent CTC enumeration protocol for Parsortix® depends on the expression of either (1) the epithelial marker EpCAM, and/or (2) the mesenchymal marker N-Cadherin¹⁷. EpCAM has been identified as a marker for carcinoma due to its high expression on rapidly proliferating tumors of epithelial origin⁶³, while an increase in N-Cadherin expression has been shown to be associated with EMT and increased cancer invasion and metastasis⁶⁴. While N-Cadherin is an established mesenchymal marker, a loss of N-Cadherin has been reported in some metastatic and poorly differentiated cancers including invasive ductal carcinoma, melanoma, lung adenocarcinoma and others⁶⁵. Thus, it is possible that even using a combination of epithelial (EpCAM), and mesenchymal (N-Cadherin) markers may still miss some mesenchymal CTCs which do not have expression of either marker. Additionally, there is some expression of N-Cadherin on blood cell components such as including basophils, neutrophils, mucosal-associated invariant T (MAIT) cells, and natural killer (NK) cells⁶⁶. However these blood cell components also have expression of CD45⁶⁷ which would preclude them as being positively identified as CTCs¹⁷. Additionally, similar to VyCap, our Parsortix® CTC enumeration protocol does not include automated image capture for multiple users to analyze potential positive CTCs or for long-term data storage for re-analysis of CTCs. Unlike VyCap, Parsortix® does not have any available software for users who are interested in automated image capture, which is a disadvantage. Lastly, although Parsortix® has the CE mark in Europe, it is not currently approved for any clinical use in Canada or the United States. These are two significant potential drawbacks to using Parsortix® for CTC enumeration and must be considered when deciding which CTC platform is optimal for a clinical research study.

In Chapter 3 we also harvested CTCs, isolated RNA, and carried out downstream molecular analysis of CTCs using HyCEAD²². While HyCEAD analysis has significant benefits over traditional multiplex technologies such as ability to analyze a much greater number of genes of interest and the capacity to capture RNA from a single CTC²², the current inability to customize a

mRNA analysis panel is a significant drawback to using this technology. This hinders the ability to tailor the analysis to a specific research question and instead relies on a bank of pre-selected targets by ANGLE plc. While many of these pre-selected targets were of significant relevance to this thesis work, this may not always be the case for future research. However, HyCEAD mRNA analysis is an emerging technique being developed by ANGLE plc and after further verification researchers may be able to request specific targets to be integrated into the existing HyCEAD panels, which would be very impactful for future research. Additionally, the design of our study involved pooling all CTCs harvested from either the Parsortix® or VyCap prior to isolating RNA, which preclude single-cell analysis of individual CTCs¹⁷. While it was not feasible for this thesis, future research should focus on single-cell CTC analysis due to the heterogeneity that exists among CTCs^{68,69}. Overall, pooling of CTCs could confound interpretation of the clinical relevance of the molecular findings due to vastly different marker expression and different metastatic potentials of CTCs subpopulations⁷⁰.

Lastly, Chapter 4 focused on experimental studies of partial-EMT in prostate cancer models. These studies consisted of mainly *in vitro* work focused on a loss of function (LOF) of transcription factor Zeb1 in mesenchymal human prostate cancer cells, which may not accurately recapitulate cell behavior during *in vivo* metastasis. Although we completed a large *in vivo* study to add to this body of work, we only observed trends rather than significant differences between groups. It is possible that the shRNA construct was not induced as successfully by the doxycycline administration *in vivo* as it was *in vitro*, resulting in a lack of expected inhibition of Zeb1. We are currently investigating the success of the induction by assessing the levels of Zeb1 in the primary tumor via immunohistochemistry, as suboptimal Zeb1^{KD} induction *in vivo* could limit our ability to properly investigate the role of p-EMT in systemic metastasis and CTC generation. Optimizing the *in vivo* induction of Zeb1 knockdown and repeating the pre-clinical animal studies will add significance to our study as it will introduce a biological component which is not possible to replicate with *in vitro* work alone. Secondly, due to the large size of Zeb1 (200 kDa)⁷¹, only LOF experiments were conducted using an inducible Zeb1 shRNA lentivirus. It would be difficult, but not impossible, to conduct a gain of function experiment with Zeb1 overexpression, and this complementary data would help to solidify the research put forth in this thesis. Lastly, this work was completed with only one mesenchymal prostate cancer cell line (PC-3), which may not accurately reflect the heterogeneity of prostate cancer in patients^{72,73}. In addition, cultured cell

lines can be genetically and phenotypically unstable and can accumulate mutations over time, and thus are not considered “normal” cells⁷⁴. As such, conducting *in vitro* and *in vivo* work with only one cell line limits the potential application of the research to prostate cancer patients. Future replication of this work in additional cell lines such as, DU145 ([ATCC HTB-81](#)), PC3-emt ([ATCC CLR-3471](#)) and/or patient derived prostate cancer cells will add greater clinical significance to this p-EMT work⁷⁵.

5.4 Future Directions

The work presented in this thesis will have significant impact on CTC enumeration as it relates to EMT. However, results obtained throughout this research have created some questions which will need to be addressed in future studies.

As discussed above, one potential reason that we were unable to observe a significant difference in CTC capture in our clinical study could be due to the heterogeneity in CTC numbers and our small sample size (n = 9-10 per cohort). Increasing the sample size of this study may help to identify small differences that exist when enumerating using CellSearch® versus Parsortix®. Additionally, this clinical trial involved three distinct cohorts of patients with different metastatic characteristics and CTC sampling at a single point in time. This meant that it was somewhat difficult to assess differences between the groups, as these could be due to patient and metastatic variability that could impact CTC release regardless of EMT phenotype. To address this, the design of future studies could incorporate serial CTC sampling in each patient as their disease progresses to help elucidate how CTC generation, capture, and molecular characteristics evolve over time in individual patients.

Another future direction for this work will be to expand on the RNA analysis completed on captured CTCs. In the future, HyCEAD technology may be able to accommodate customized panels for RNA analysis, although this is not currently available. For pooled CTCs, down to a single CTC, NanoString technology can allow for mRNA and miRNA analysis of over 800 sequences, and researchers can design custom codesets for specific pathways of interest⁷⁶. This would greatly increase the impact of the RNA analysis completed on our pooled CTCs. However, ideally, CTC analysis would be completed at the single-cell level on individual CTCs for maximal impact, and both Parsortix® and VyCap have the capacity to isolate single CTCs with additional

technical components added to their base platform^{17,77-79}. Parsortix® recently announced that combined use of their platform with the micromanipulator CellCelector™ from Automated Lab Solutions (Jena, Germany) will enable single CTCs to be analyzed^{78,79}. Additionally, VyCap's Puncher technology combines silicone microchips, fluorescence imaging, and a punching method to isolate and transfer single cells into microtubes for downstream analysis and even live cell culture and propagation of CTCs⁷⁷. Both of these single CTC isolation technologies would allow for downstream single CTC analysis which could be completed using HyCEAD, NanoString, or even whole genome sequencing^{22,76,80}. This would allow us to assess CTC heterogeneity and add tremendous clinical value for understanding EMT and marker expression during the metastatic process.

This work developed and assessed a novel p-EMT cell line which is stable *in vitro* and can be used to assess many questions regarding the process of EMT and how it relates to CTC biology. However, as alluded to in the previous section, there are additional experiments that can be completed to increase the impact of this work. Beyond adding additional cell lines and gain of function approaches, the most important future work will be *in vivo* experiments. These experiments will add a biological component to the research which is unable to be replicated with *in vitro* work. Once successful induction of the lentivirus is optimized and subsequent Zeb1^{KD} can be obtained *in vivo*, studies can be conducted to assess how p-EMT effects CTC generation, detection, and enumeration through various stages of disease progression in a mouse model. These mice could also be treated with 5-azacytidine to assess how global de-methylation alters tumor burden, CTC generation, and overall survival^{81,82}. Successful completion of these pre-clinical *in vivo* studies may then warrant a subsequent clinical trial for patients with aggressive p-EMT prostate cancer to receive 5-aza treatment.

Lastly, our methylation data was assessed for differential methylation among known genes whose silencing has been associated with cancer progression⁸³. Re-evaluating our methylation data by assessing different parameters may reveal more p-EMT markers to add to our potential biomarker panel. Additionally, all our identified EMT, p-EMT, methylation, and HyCEAD markers could be combined to create a Signature-score (S-Score)⁸⁴. S-scores can be used to quantify the expression pattern of tumor samples from previously identified gene signature sets⁸⁴. The successful creation of an S-Score will allow researchers to focus on known biological functions which manifest a

phenotype⁸⁵, in this case a p-EMT phenotype, which can be used to identify patients with aggressive cancers.

5.5 Final Conclusions

The work presented in this thesis added significant contributions to the field of CTC research especially as it relates to EMT and p-EMT. From these studies, future researchers will be able to capture CTCs from mouse or human samples independent of EMT status and complete downstream RNA analysis. Ultimately, we provided support for the continued use of CellSearch® in the clinical setting and provided parameters for when Parsortix® and HyCEAD may aid in clinical research, with potential application as a personalized medicine tool in the future. Additionally, we provided insights into how the p-EMT phenotype changes cell marker expression, phenotype, and cell aggressiveness and completed preliminary experiments to provide support for implementation of an investigational cancer drug, 5-azacitidine. Lastly, we identified novel p-EMT and metastatic markers which can be combined with EMT-independent CTC enumeration protocols and downstream RNA analysis to identify prostate cancer patients who would benefit from 5-aza treatment. This could have enormous clinical impact in the future by classifying prostate cancer patients with aggressive p-EMT cancers through a simple blood test and providing them with an appropriate treatment which may improve progression free and overall survival.

5.6 References

1. Mehlen P, Puisieux A. Metastasis: A question of life or death. *Nat Rev Cancer*. 2006;6(6):449-458. doi:10.1038/nrc1886
2. Siegel RL, Miller KD, Jemal A. Cancer statistics, 2020. *CA Cancer J Clin*. 2020. doi:10.3322/caac.21590
3. Lowes LE, Goodale D, Xia Y, et al. Epithelial-to-mesenchymal transition leads to disease-stage differences in circulating tumor cell detection and metastasis in pre-clinical models of prostate cancer. *Oncotarget*. 2016. doi:10.18632/oncotarget.12682
4. Cancer P. Ablin, R. J. & Mason, M. D. in *Metastasis of Prostate Cancer (Mason, 1) 1-405 (Springer Netherlands, 2007)*. <http://link.springer.com/10.1007/978-1-4020-5847-9>.
5. Ashrafizadeh M, Zarrabi A, Hushmandi K, et al. Association of the Epithelial-Mesenchymal Transition (EMT) with Cisplatin Resistance. *Int J Mol Sci*. 2020;21(11). doi:10.3390/ijms21114002
6. Andree KC, van Dalum G, Terstappen LWMM. Challenges in circulating tumor cell detection by the CellSearch system. *Mol Oncol*. 2016;10(3):395-407. doi:10.1016/j.molonc.2015.12.002
7. Lee SJ, Lee J, Kim ST, et al. Circulating tumor cells are predictive of poor response to chemotherapy in metastatic gastric cancer. *Int J Biol Markers*. 2015;30(4):e382-e386. doi:10.5301/ijbm.5000151
8. Qiao Y-Y, Lin K-X, Zhang Z, et al. Monitoring disease progression and treatment efficacy with circulating tumor cells in esophageal squamous cell carcinoma: A case report. *World J Gastroenterol*. 2015;21(25):7921-7928. doi:10.3748/wjg.v21.i25.7921
9. Ried K, Eng P, Sali A. Screening for Circulating Tumour Cells Allows Early Detection of Cancer and Monitoring of Treatment Effectiveness: An Observational Study. 2017;18:2275-2285. doi:10.22034/APJCP.2017.18.8.2275
10. Sharma S, Zhuang R, Long M, et al. Circulating Tumor Cell Isolation, Culture, and Downstream Molecular Analysis. *Biotechnol Adv*. 2018;36(4):1063-1078.
11. Alunni-Fabbroni M, Sandri MT. Circulating tumour cells in clinical practice: Methods of detection and possible characterization. *Methods*. 2010;50(4):289-297. doi:10.1016/j.ymeth.2010.01.027
12. Allard WJ, Matera J, Miller MC, et al. Tumor cells circulate in the peripheral blood of all major carcinomas but not in healthy subjects or patients with nonmalignant diseases. *Clin Cancer Res*. 2004;10(20):6897-6904. doi:10.1158/1078-0432.CCR-04-0378

13. Mittal V. Epithelial Mesenchymal Transition in Tumor Metastasis. *Annu Rev Pathol Mech Dis*. 2018. doi:10.1146/annurev-pathol-020117-043854
14. Kalluri R, Weinberg RA. The basics of epithelial-mesenchymal transition. *J Clin Invest*. 2009;119(6):1420-1428. doi:10.1172/JCI39104
15. Jolly MK. Implications of the Hybrid Epithelial/Mesenchymal Phenotype in Metastasis. *Front Oncol*. 2015;5. doi:10.3389/fonc.2015.00155
16. Gorges TM, Tinhofer I, Drosch M, et al. Circulating tumour cells escape from EpCAM-based detection due to epithelial-to-mesenchymal transition. *BMC Cancer*. 2012;12. doi:10.1186/1471-2407-12-178
17. Kitz J, Lowes L, Goodale D, Allan A. Circulating Tumor Cell Analysis in Preclinical Mouse Models of Metastasis. *Diagnostics*. 2018. doi:10.3390/diagnostics8020030
18. Batth IS, Mitra A, Rood S, Kopetz S, Menter D, Li S. CTC analysis: an update on technological progress. *Transl Res*. 2019;212:14-25. doi:10.1016/j.trsl.2019.07.003
19. Chandran UR, Ma C, Dhir R, et al. Gene expression profiles of prostate cancer reveal involvement of multiple molecular pathways in the metastatic process. *BMC Cancer*. 2007;7:1-21. doi:10.1186/1471-2407-7-64
20. Eysenck LG. A history of prostate cancer treatment - Denmeade - 2002 - *Nat Rev Cancer*. 2002;2(May).
21. Portera CA, Berman RS, Ellis LM. Molecular determinants of colon cancer metastasis. *Surg Oncol*. 1998;7(3-4):183-195. doi:10.1016/S0960-7404(99)00020-1
22. Englert D, Kolesnikova M, Zaman N, et al. Multiplex gene expression using the HyCEAD assay in CTCs isolated with the Parsortix™ system Analytical Sensitivity and Dynamic Range HyCEAD Process and Probe Design for CTCs Reproducibility of Expression Measurements. :72.
23. Gurel B, Ali TZ, Montgomery EA, et al. NKX3.1 as a marker of prostatic origin in metastatic tumors. *Am J Surg Pathol*. 2010;34(8):1097-1105. doi:10.1097/PAS.0b013e3181e6cbf3
24. Nakajima H, Koizumi K. Family with sequence similarity 107: A family of stress responsive small proteins with diverse functions in cancer and the nervous system (Review). *Biomed reports*. 2014;2(3):321-325. doi:10.3892/br.2014.243
25. Arafteh R, Samuels Y. PIK3CA in cancer: The past 30 years. *Semin Cancer Biol*. 2019;59:36-49. doi:https://doi.org/10.1016/j.semcancer.2019.02.002
26. García Z, Kumar A, Marqués M, Cortés I, Carrera AC. Phosphoinositide 3-kinase controls early and late events in mammalian cell division. *EMBO J*. 2006;25(4):655-661. doi:10.1038/sj.emboj.7600967

27. Yu Z, Wang Y, Jiang Y, et al. NID2 can serve as a potential prognosis prediction biomarker and promotes the invasion and migration of gastric cancer. *Pathol - Res Pract.* 2019;215(10):152553. doi:<https://doi.org/10.1016/j.prp.2019.152553>
28. Ratajska M, Matusiak M, Kuzniacka A, et al. Cancer predisposing BARD1 mutations affect exon skipping and are associated with overexpression of specific BARD1 isoforms. *Oncol Rep.* 2015;34(5):2609-2617. doi:10.3892/or.2015.4235
29. Sugie S, Mukai S, Yamasaki K, Kamibeppu T, Tsukino H, Kamoto T. Significant Association of Caveolin-1 and Caveolin-2 with Prostate Cancer Progression. *Cancer Genomics Proteomics.* 2015;12(6):391-396.
30. Jiang X, Zhang C, Qi S, et al. Elevated expression of ZNF217 promotes prostate cancer growth by restraining ferroportin-conducted iron egress. *Oncotarget.* 2016;7(51):84893-84906. doi:10.18632/oncotarget.12753
31. Nordby Y, Andersen S, Richardsen E, et al. Stromal expression of VEGF-A and VEGFR-2 in prostate tissue is associated with biochemical and clinical recurrence after radical prostatectomy. *Prostate.* 2015;75(15):1682-1693. doi:10.1002/pros.23048
32. Johnson SAS, Lin JJ, Walkey CJ, Leathers MP, Coarfa C, Johnson DL. Elevated TATA-binding protein expression drives vascular endothelial growth factor expression in colon cancer. *Oncotarget.* 2017;8(30):48832-48845. doi:10.18632/oncotarget.16384
33. Ray D, Epstein DM. Tumorigenic de-differentiation: the alternative splicing way. *Mol & Cell Oncol.* 2020;7(6):1809959. doi:10.1080/23723556.2020.1809959
34. Kim KY, Yoon M, Cho Y, et al. Targeting metastatic breast cancer with peptide epitopes derived from autocatalytic loop of Prss14/ST14 membrane serine protease and with monoclonal antibodies. *J Exp Clin Cancer Res.* 2019;38(1):363. doi:10.1186/s13046-019-1373-y
35. Su X, Liu N, Wu W, et al. Comprehensive analysis of prognostic value and immune infiltration of kindlin family members in non-small cell lung cancer. *BMC Med Genomics.* 2021;14(1):119. doi:10.1186/s12920-021-00967-2
36. Schaefer-Klein JL, Murphy SJ, Johnson SH, Vasmatazis G, Kovtun I V. Topoisomerase 2 Alpha Cooperates with Androgen Receptor to Contribute to Prostate Cancer Progression. *PLoS One.* 2015;10(11):1-17. doi:10.1371/journal.pone.0142327
37. Adamo P, Ladomery MR. The oncogene ERG: A key factor in prostate cancer. *Oncogene.* 2016;35(4):403-414. doi:10.1038/onc.2015.109
38. Lee C, Fernandez KJ, Alexandrou S, et al. Cyclin E2 promotes whole genome doubling in breast cancer. *Cancers (Basel).* 2020;12(8):1-19. doi:10.3390/cancers12082268
39. Subramani R, Lopez-Valdez R, Salcido A, et al. Growth hormone receptor inhibition decreases the growth and metastasis of pancreatic ductal adenocarcinoma. *Exp Mol Med.*

- 2014;46(10):1-11. doi:10.1038/emm.2014.61
40. Liu H, Zhang Z, Zhen P, Zhou M. High Expression of VSTM2L Induced Resistance to Chemoradiotherapy in Rectal Cancer through Downstream IL-4 Signaling. *J Immunol Res.* 2021;2021. doi:10.1155/2021/6657012
 41. Zhang L, Jia G, Shi B, Ge G, Duan H, Yang Y. PRSS8 is Downregulated and Suppresses Tumour Growth and Metastases in Hepatocellular Carcinoma. *Cell Physiol Biochem.* 2016;40(3-4):757-769. doi:10.1159/000453136
 42. Li W, Li S, Yang J, Cui C, Yu M, Zhang Y. ITGBL1 promotes EMT, invasion and migration by activating NF- κ B signaling pathway in prostate cancer. *Onco Targets Ther.* 2019;12:3753-3763. doi:10.2147/OTT.S200082
 43. Zhang Y, Xu L, Li A, Han X. The roles of ZEB1 in tumorigenic progression and epigenetic modifications. *Biomed Pharmacother.* 2019;110(November 2018):400-408. doi:10.1016/j.biopha.2018.11.112
 44. Bery F, Figiel S, Kouba S, et al. Hypoxia promotes prostate cancer aggressiveness by upregulating EMT-activator Zeb1 and SK3 channel expression. *Int J Mol Sci.* 2020;21(13):1-10. doi:10.3390/ijms21134786
 45. Saitoh M. JB special review-cellular plasticity in epithelial homeostasis and diseases: Involvement of partial EMT in cancer progression. *J Biochem.* 2018;164(4):257-264. doi:10.1093/jb/mvy047
 46. Chao Y, Wu Q, Acquafondata M, Dhir R, Wells A. Partial mesenchymal to epithelial reverting transition in breast and prostate cancer metastases. *Cancer Microenviron.* 2012;5(1):19-28. doi:10.1007/s12307-011-0085-4
 47. Sinha D, Saha P, Samanta A, Bishayee A. Emerging concepts of hybrid epithelial-to-mesenchymal transition in cancer progression. *Biomolecules.* 2020;10(11):1-22. doi:10.3390/biom10111561
 48. Zhou Y, Hu Z. Genome-wide demethylation by 5-aza-2'-deoxycytidine alters the cell fate of stem/progenitor cells. *Stem cell Rev reports.* 2015;11(1):87-95. doi:10.1007/s12015-014-9542-z
 49. Czibere A, Bruns I, Kröger N, et al. 5-Azacytidine for the treatment of patients with acute myeloid leukemia or myelodysplastic syndrome who relapse after allo-SCT: A retrospective analysis. *Bone Marrow Transplant.* 2010;45(5):872-876. doi:10.1038/bmt.2009.266
 50. Tam WL, Weinberg RA. The epigenetics of epithelial-mesenchymal plasticity in cancer. *Nat Med.* 2013. doi:10.1038/nm.3336
 51. Lu W, Kang Y. Epithelial-Mesenchymal Plasticity in Cancer Progression and Metastasis. *Dev Cell.* 2019. doi:10.1016/j.devcel.2019.04.010

52. Cui J, Wang L, Ren X, Zhang Y, Zhang H. LRPPRC: A multifunctional protein involved in energy metabolism and human disease. *Front Physiol.* 2019;10(MAY):1-10. doi:10.3389/fphys.2019.00595
53. Agarwal R, Mori Y, Cheng Y, et al. Silencing of claudin-11 is associated with increased invasiveness of gastric cancer cells. *PLoS One.* 2009;4(11). doi:10.1371/journal.pone.0008002
54. Cheung KJ, Ewald AJ, Om Alblazi KM, et al. Perspectives in Cancer Research Molecular Insights into Cancer Invasion : Strategies for Prevention and Intervention. *Curr Oncol.* 2015. doi:10.1158/1078-0432.CCR-06-3045
55. Liu S, Liu J, Yu X, Shen T, Fu Q. Identification of a Two-Gene (PML-EPB41) Signature With Independent Prognostic Value in Osteosarcoma. *Front Oncol.* 2020;9(January):1-11. doi:10.3389/fonc.2019.01578
56. Yuan W, Ji J, Shu Y, et al. Downregulation of DAPK1 promotes the stemness of cancer stem cells and EMT process by activating ZEB1 in colorectal cancer. *J Mol Med.* 2019;97(1):89-102. doi:10.1007/s00109-018-1716-8
57. Vazquez A, Kulkarni D, Grochola LF, et al. A genetic variant in a PP2A regulatory subunit encoded by the PPP2R2B gene associates with altered breast cancer risk and recurrence. *Int J Cancer.* 2011;128(10):2335-2343. doi:10.1002/ijc.25582
58. Peng C, Zhang Z, Wu J, et al. A critical role for ZDHHC2 in metastasis and recurrence in human hepatocellular carcinoma. *Biomed Res Int.* 2014;2014. doi:10.1155/2014/832712
59. Chen J, Zhuo JY, Yang F, et al. 17-Beta-Hydroxysteroid Dehydrogenase 13 Inhibits the Progression and Recurrence of Hepatocellular Carcinoma. *Hepatobiliary Pancreat Dis Int.* 2018;17(3):220-226. doi:10.1016/j.hbpd.2018.04.006
60. Yamamoto F, Yamamoto M. Identification of genes that exhibit changes in expression on the 8p chromosomal arm by the Systematic Multiplex RT-PCR (SM RT-PCR) and DNA microarray hybridization methods. *Gene Expr.* 2008;14(4):217-227. doi:10.3727/105221608786883816
61. Legler K, Rosprim R, Karius T, et al. Reduced mannosidase MAN1A1 expression leads to aberrant N-glycosylation and impaired survival in breast cancer. *Br J Cancer.* 2018;118(6):847-856. doi:10.1038/bjc.2017.472
62. Segeren H, Andree KC, Oomens L, Westendorp B. Collection of cells for single-cell RNA sequencing using high-resolution fluorescence microscopy | Elsevier Enhanced Reader. 2021:1-16. <https://emea.mitsubishielectric.com/ar/products-solutions/factory-automation/index.html>.
63. Trzpis M, McLaughlin PMJ, De Leij LMFH, Harmsen MC. Epithelial cell adhesion molecule: More than a carcinoma marker and adhesion molecule. *Am J Pathol.* 2007;171(2):386-395. doi:10.2353/ajpath.2007.070152

64. Loh CY, Chai JY, Tang TF, et al. *The E-Cadherin and N-Cadherin Switch in Epithelial-to-Mesenchymal Transition: Signaling, Therapeutic Implications, and Challenges*. Vol 8.; 2019. doi:10.3390/cells8101118
65. CBioPortal. Metastatic Solid Tumors. https://www.cbioportal.org/results/mutations?cancer_study_list=metastatic_solid_tumors_mich_2017&Z_SCORE_THRESHOLD=2.0&RPPA_SCORE_THRESHOLD=2.0&profileFilter=mutations%2Cfusion&case_set_id=metastatic_solid_tumors_mich_2017_sequenced&gene_list=CDH2&geneset. Published 2021.
66. Atlas P. The Human Protein Atlas- CDH2. <https://www.proteinatlas.org/ENSG00000170558-CDH2/blood>. Published 2021.
67. Atlas P. The Human Protein Atlas- PTPRC. <https://www.proteinatlas.org/ENSG00000081237-PTPRC/blood>. Published 2021.
68. Conteduca V, Ku S, Fernandez L, et al. Circulating tumor cell heterogeneity in neuroendocrine prostate cancer by single cell copy number analysis. *npj Precis Oncol*. 2021;1-8. doi:10.1038/s41698-021-00211-1
69. Yu T, Wang C, Xie M, et al. Biomedicine & Pharmacotherapy Heterogeneity of CTC contributes to the organotropism of breast cancer. *Biomed Pharmacother*. 2021;137(January):111314. doi:10.1016/j.biopha.2021.111314
70. Lim S Bin, Lim CT, Lim WT. Single-cell analysis of circulating tumor cells: Why heterogeneity matters. *Cancers (Basel)*. 2019;11(10):1-22. doi:10.3390/cancers11101595
71. Hanrahan K, O'Neill A, Prencipe M, et al. The role of epithelial-mesenchymal transition drivers ZEB1 and ZEB2 in mediating docetaxel-resistant prostate cancer. *Mol Oncol*. 2017;11(3):251-265. doi:10.1002/1878-0261.12030
72. Segeritz C-P, Vallier L. Cell Culture: Growing Cells as Model Systems In Vitro. *Basic Sci Methods Clin Res*. 2017:151-172. doi:10.1016/B978-0-12-803077-6.00009-6
73. Chen S, Zhu G, Yang Y, et al. Single-cell analysis reveals transcriptomic remodellings in distinct cell types that contribute to human prostate cancer progression. *Nat Cell Biol*. 2021;23(1):87-98. doi:10.1038/s41556-020-00613-6
74. Geraghty RJ, Capes-Davis A, Davis JM, et al. Guidelines for the use of cell lines in biomedical research. *Br J Cancer*. 2014;111(6):1021-1046. doi:10.1038/bjc.2014.166
75. Puca L, Bareja R, Prandi D, et al. Patient derived organoids to model rare prostate cancer phenotypes. *Nat Commun*. 2018;9(1):2404. doi:10.1038/s41467-018-04495-z
76. Core GR. NanoString Applications.
77. Stevens M, Oomens L, Broekmaat J, et al. VyCAP's puncher technology for single cell identification, isolation, and analysis. *Cytom Part A*. 2018. doi:10.1002/cyto.a.23631

78. Medical N. DCCNet demonstrates use of Parsortix system for single cell CTC analysis. News Medical Life Sciences.
79. Ladurner M, Wieser M, Eigentler A, et al. Validation of cell-free rna and circulating tumor cells for molecular marker analysis in metastatic prostate cancer. *Biomedicines*. 2021;9(8):1-18. doi:10.3390/biomedicines9081004
80. Xu J, Liao K, Yang X, Wu C, Wu W, Han S. Using single-cell sequencing technology to detect circulating tumor cells in solid tumors. *Mol Cancer*. 2021;20(1):1-17. doi:10.1186/s12943-021-01392-w
81. Müller F, Cunningham T, Stookey S, et al. 5-Azacytidine prevents relapse and produces long-term complete remissions in leukemia xenografts treated with Moxetumomab pasudotox. *Proc Natl Acad Sci*. 2018;115(8):E1867 LP-E1875. doi:10.1073/pnas.1714512115
82. Gailhouste L, Liew LC, Hatada I, Nakagama H, Ochiya T. Epigenetic reprogramming using 5-azacytidine promotes an anti-cancer response in pancreatic adenocarcinoma cells. *Cell Death Dis*. 2018;9(5):468. doi:10.1038/s41419-018-0487-z
83. Kitz J, Goodale D, Postenka C, Lowes LE, Allan AL. EMT-independent detection of circulating tumor cells in human blood samples and pre-clinical mouse models of metastasis. *Clin Exp Metastasis*. 2021;38(1):97-108. doi:10.1007/s10585-020-10070-y
84. Hsiao T-H, Harry Chen H-I, Lu J-Y, et al. Utilizing signature-score to identify oncogenic pathways of cholangiocarcinoma. *Transl Cancer Res*. 2013;2(1):6-17. doi:10.3978/j.issn.2218-676X.2012.12.04.Utilizing
85. Chen Hlh, Hsiao TH, Chen Y, Keller C. S-score: A novel scoring method of gene signatures for molecular classification. *Proc - IEEE Int Work Genomic Signal Process Stat*. 2011:154-157. doi:10.1109/gensips.2011.6169468

Appendices

Appendix 1. Research Ethics Board approval for project ID: 109759 “Dynamic influence of the epithelial-to-mesenchymal transition (EMT) on circulating tumor cell (CTC) generation, phenotype, and disease progression in prostate cancer”.



Date: 9 September 2021

To: Dr. Alison Allan

Project ID: 109759

Study Title: Dynamic influence of the epithelial-to-mesenchymal transition (EMT) on circulating tumor cell (CTC) generation, phenotype, and disease progression in prostate cancer.

Application Type: Continuing Ethics Review (CER) Form

Review Type: Delegated

REB Meeting Date: 07/Sept/2021

Date Approval Issued: 09/Sep/2021

REB Approval Expiry Date: 05/Oct/2022

Dear Dr. Alison Allan,

The Western University Research Ethics Board has reviewed the application. This study, including all currently approved documents, has been re-approved until the expiry date noted above.

REB members involved in the research project do not participate in the review, discussion or decision.

Western University REB operates in compliance with, and is constituted in accordance with, the requirements of the Tri-Council Policy Statement: Ethical Conduct for Research Involving Humans (TCPS 2); the International Conference on Harmonisation Good Clinical Practice Consolidated Guideline (ICH GCP); Part C, Division 5 of the Food and Drug Regulations; Part 4 of the Natural Health Products Regulations; Part 3 of the Medical Devices Regulations and the provisions of the Ontario Personal Health Information Protection Act (PHIPA 2004) and its applicable regulations. The REB is registered with the U.S. Department of Health & Human Services under the IRB registration number IRB 00000940.

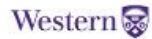
Please do not hesitate to contact us if you have any questions.

Sincerely,

The Office of Human Research Ethics

Note: This correspondence includes an electronic signature (validation and approval via an online system that is compliant with all regulations).

Appendix 2. Animal Care Committee Approval for 2020-124 “Circulating tumor cells (CTCs) in prostate cancer”.



AUP Number: 2020-124

PI Name: Allan, Alison

AUP Title: Circulating tumor cells (CTCs) in prostate cancer.

Approval Date: 01/01/2021

Official Notice of Animal Care Committee (ACC) Approval:

Your new Animal Use Protocol (AUP) 2020-124:1: entitled " Circulating tumor cells (CTCs) in prostate cancer."

has been APPROVED by the Animal Care Committee of the University Council on Animal Care. This approval, although valid for up to four years, is subject to annual Protocol Renewal.

Prior to commencing animal work, please review your AUP with your research team to ensure full understanding by everyone listed within this AUP.

As per your declaration within this approved AUP, you are obligated to ensure that:

1) Animals used in this research project will be cared for in alignment with:

a) Western's Senate MAPPs 7.12, 7.10, and 7.15

http://www.uwo.ca/univsec/policies_procedures/research.html

b) University Council on Animal Care Policies and related Animal Care Committee procedures

http://uwo.ca/research/services/animalethics/animal_care_and_use_policies.htm

2) As per UCAC's Animal Use Protocols Policy,

a) this AUP accurately represents intended animal use;

b) external approvals associated with this AUP, including permits and scientific/departmental peer approvals, are complete and accurate;

c) any divergence from this AUP will not be undertaken until the related Protocol Modification is approved by the ACC; and

d) AUP form submissions - Annual Protocol Renewals and Full AUP Renewals - will be submitted and attended to within timeframes outlined by the ACC.

e)

http://uwo.ca/research/services/animalethics/animal_use_protocols.html

3) As per MAPP 7.10 all individuals listed within this AUP as having any hands-on animal contact will

a) be made familiar with and have direct access to this AUP;

b) complete all required CCAC mandatory training (training@uwo.ca); and

c) be overseen by me to ensure appropriate care and use of animals.

4) As per MAPP 7.15,

a) Practice will align with approved AUP elements;

b) Unrestricted access to all animal areas will be given to ACVS Veterinarians and ACC Leaders;

c) UCAC policies and related ACC procedures will be followed, including but not limited to:

- i) Research Animal Procurement
- ii) Animal Care and Use Records
- iii) Sick Animal Response
- iv) Continuing Care Visits

5) As per institutional OH&S policies, all individuals listed within this AUP who will be using or potentially exposed to hazardous materials will have completed in advance the appropriate institutional OH&S training, facility-level training, and reviewed related (M)SDS Sheets,
<http://www.uwo.ca/hr/learning/required/index.html>

Submitted by: Copeman, Laura
on behalf of the Animal Care Committee
University Council on Animal Care

Dr. Timothy Regnault,
Animal Care Committee Chair

The University of Western Ontario

Animal Care Committee / University Council on Animal Care

London, Ontario Canada N6A 5C1

519-661-2111 x 88792 Fax 519-661-2028

[auspc@uwo.ca] auspc@uwo.ca

<http://www.uwo.ca/research/services/animalethics/index.html>

Curriculum Vitae

Name: Jenna Kitz

Post-secondary Education and Degrees: University of Guelph
Guelph, Ontario, Canada
2012-2016 B.Sc. (Hons)

The University of Western Ontario
London, Ontario, Canada
2016-2021 Ph.D

Honours and Awards: OVC Graduate Stipend Support Scholarship (Declined)
2016

Lawson Internal Research Fund Scholarship
2016-2017

Ontario Graduate Scholarship
2018-2019, 2019-2020, 2020-2021

CaRTT Strategic Training Program Competition
2018

ACB Travel Award
2019, 2021

CIHR Travel Award
2019

Related Work Experience Teaching Assistantships
The University of Western Ontario
2017, 2019, 2020, 2021

4th Year Thesis Mentor
The University of Western Ontario
2018, 2019

Research Assistant
Victoria Hospital
2019-2021

Guest Lecturer
The University of Western Ontario
2020, 2021

Extracurriculars

Society of Graduate Students
ACB Student Representative
The University of Western Ontario
2016-2017

Graduate Education Council (GEC)
Schulich Student Representative
The University of Western Ontario
2017-2018

GEC Subcommittee on Program Review
Student Representative
The University of Western Ontario
2017-2018

Victoria Hospital
Peri-operative Waiting Room Volunteer
Victoria Hospital
2017-2020

Biochemistry Program Review
Student Representative on Review Committee
The University of Western Ontario
2018

Let's Talk Science
Classroom Outreach Volunteer
The University of Western Ontario
2018-2020

Senate
Graduate Student Representative
The University of Western Ontario
2019-2021

ACB Students' Council
Co-Chair
The University of Western Ontario
2020-2021

Schulich Graduate Student Council
ACB Student Representative
The University of Western Ontario
2020-2021

Nominating Committee
 Senate Graduate Representative
 The University of Western Ontario
 2020-2021

ACB Mentor/Mentee Program
 Founder
 The University of Western Ontario
 2021

Publications:

Kitz, J., Lefebvre, C., Carlos, J., Lowes, L., Allan, A.L. Reduced Zeb1 expression in prostate cancer cells leads to an aggressive p-EMT phenotype associated with altered global methylation patterns. *International Journal of Molecular Sciences*. 2021. 22(12840), 1-16.

Kitz, J., Goodale, D., Postenka, C., Lowes, L.E., Allan, A.L. EMT independent detection of circulating tumor cells in pre-clinical mouse and human whole blood samples. *Clinical and Experimental Metastasis*. 2021. 38:97-109.

Kitz, J., Lowes LE, Goodale D, and Allan, A.L. Circulating tumor cell analysis in preclinical models of cancer metastasis. *Diagnostics*. 2018. 8(2), 30.

Watson, K., Jones, R., Bruce, A., Nersesian, S., **Kitz, J.**, Moorehead, R. Re-expression of miR-200c Suppresses Proliferation, Colony Formation and In Vivo Tumor Growth of Murine Claudin-Low Mammary Tumor Cells. *Oncotarget*. 2017. 8:23727-49.

Conference Abstracts/Talks

Kitz, J., Lowes, L.E., Allan, A.L. “The influence of the epithelial-to-mesenchymal transition of prostate cancer circulating tumor cells effects detection and enumeration by the CellSearch System®”. ACB Research Day. Poster Presentation. University of Western Ontario. Oct. 2017.

Kitz, J., Lowes, L.E., Allan, A.L. “The influence of the epithelial-to-mesenchymal transition of prostate cancer circulating tumor cells effects detection and enumeration by the CellSearch System®”. Canadian Cancer Research Conference. Poster Presentation. Vancouver, Canada. Nov. 2017.

Kitz, J., Lowes, L.E., Allan, A.L. “Epithelial-to-mesenchymal transition of prostate cancer circulating tumor cells effects detection and enumeration by the CellSearch System®”. Oncology Research and Education Day. Poster presentation. London, Ontario. June 2017.

Kitz, J., Lowes, L.E., Goodale, D., Allan, A.L. “The influence of the epithelial-to-mesenchymal transition on circulating tumor cell generation, phenotype, and metastasis in prostate cancer”. ACB Research Day. Oral presentation. University of Western Ontario, Canada. Oct. 2018.

Kitz, J., Lowes, L.E., Goodale, D., Allan, A.L. “The role of the epithelial-to-mesenchymal transition of prostate cancer circulating tumor cells on metastasis and detection by the CellSearch System®”. Oncology Research and Education Day. Poster Presentation. London, Ontario. June 2018.

Kitz, J., Lowes, L.E., Carlos, J., Goodale, D., Allan, A.L. The role of the epithelial-to-mesenchymal transition of prostate cancer circulating tumor cells on metastasis and detection by the CellSearch System. ACB Research Day. Poster Presentation. University of Western Ontario. October 2019.

Kitz, J., Lowes, L.E., Carlos, J., Goodale, D., Allan, A.L. The influence of the epithelial-to-mesenchymal transition and detection of circulating tumor cells in pre-clinical models of prostate cancer, Advances in Circulating Tumor Cells. Poster presentation. Corfu, Greece. Oct. 2019.

Kitz, J., Lowes, L.E., Carlos, J., Goodale, D., Allan, A.L. The role of the epithelial-to-mesenchymal transition of prostate cancer circulating tumor cells on metastasis and detection by the CellSearch System. Oncology Research and Education Day. Poster Presentation. London, Ont. Canada. June 2019.

Kitz, J., Goodale, D., Lowes, L.E., Carlos, J., Allan, A.L. Importance of epithelial-to-mesenchymal transition and partial EMT in prostate circulating tumor cells (CTC) and metastasis. Canadian Student Health Research Forum. Poster Presentation. Winnipeg, Canada. June 2020 (Virtual).

Kitz, J., Lowes, L.E., Carlos, J., Allan, A.L. Importance of epithelial-to-mesenchymal transition (EMT) and partial EMT (p-EMT) in prostate circulating tumor cells (CTC) and metastasis. Oncology Research and Education Day. London, Canada. June 2021 (Virtual).

Kitz, J., Lowes, L.E., Carlos, J., and Allan, A.L. The role of epithelial-to-mesenchymal transition on circulating tumor cell generation phenotype and metastasis in prostate cancer. Advances in Circulating Tumor Cells. Kalamata, Greece. September 2021 (Abstract accepted and published, unable to attend meeting due to COVID-19).